PRECIPITATION EMBRITTLEMENT STUDIES IN VACUUM MELTED IRON-CHROMIUM ALLOYS.

Thesis by

William Vale Wright Jr.

In Partial Fulfillment of the Requirements

For the Degree of

Doctor of Philosophy

California Institute of Technology

Pasadena, California

1955

ACKNOWLEDGEMENTS

The author wishes to express his sincere gratitude and appreciation to Professor Pol Duwez for his inspiration, encouragement, and guidance during the progress of this thesis; to Professor D.S. Clark for his valuable criticism of this thesis; to Dr. A.J. Lena of the Allegheny-Ludlum Corporation and Mr. H.E. Martens of the Jet Propulsion Laboratory for their helpful discussions and ideas; to Mrs. C. Lathbury of Pacific Semiconductors, Incorporated for invaluable assistance in metallographic specimen preparation and preparation of figures; to Miss Rosemarie Stampfel for typing the manuscript; and to the National Science Foundation, Hughes Aircraft Company, Pacific Semiconductors, Incorporated, and the California Institute of Technology for their support of this work.

The vacuum melted iron-chromium alloys used in this study were provided by the Jet Propulsion Laboratory of the California Institute of Technology through the courtesy of Professor Duwez.

ABSTRACT

This thesis presents the results of an experimental study on the nature of precipitation embrittlement (475°C embrittlement) in iron-chromium alloys. Electrical resistance, hardness, tension properties, and microstructure were studied using 19, 25, 34, 42, and 49 per cent chromium-iron vacuum melted alloys.

Precipitation embrittlement was found to occur from 450°C to about 540°C with the rate of embrittlement increasing with temperature. Maximum embrittlement occurs near 500°C. Increasing the chromium content from 19 to 49 per cent increases the rate and magnitude of precipitation embrittlement. An activation energy of 60,000 cal/mol was established for the process.

Precipitation embrittlement was found to be analogous to precipitation hardening in alloys where the formation of a coherent precipitate is responsible for property changes in the alloy. A chromium rich body centered cubic ferrite with slightly larger lattice parameter than the iron rich matrix is proposed as the non-equilibrium coherent precipitate which eventually decomposes to form gross sigma phase.

TABLE OF CONTENTS

I. INTRODUCTION

Historical Survey.

Embrittlement of high chromium ferritic stainless steels has long been significant in petroleum and chemical industries. These stainless steels are very oxidation resistant when the chromium content is in excess of 20 per cent (1),* and are used in many applications involving high temperature oxidation resistance.

When equipment made of such steel has been used for a long period of time at temperatures near 475°C, and then cooled to room temperature, an extremely brittle condition results. Ordinary maintainance operations caused failure of the embrittled material. In early reports of this phenomenon the material was described as resembling glass in fragility and brittleness. For many years intensive research studies have been made in an attempt to determine the cause of this embrittlement in high chromium stainless steels.

Since this embrittlement phenomenon was first noticed in alloys held at or near 475°C for long periods of time, and since the cause of embrittlement was not known, the phenomenon was named 475°C embrittlement. This name has been retained throughout the literature treating this subject. However, the embrittlement is now known to occur over a range of temperature, and is believed to be caused by precipitation of a second phase. Therefore, in this thesis the name precipitation embrittlement will be used to describe the phenomenon heretofore called 475°C embrittlement.

---

* Numbers in parentheses refer to the bibliography at the end of this thesis.

An early revue of this work was given by Becket in 1938 (2), from which some interesting conclusions were drawn. Becket recognized that precipitation embrittlement "is probably caused by precipitation, although the nature of the precipitate is unknown". Becket reported precipitation embrittlement in high purity vacuum melted iron-chromium alloys, thus establishing the phenomenon as being inherent to the iron-chromium alloy system. Microscopic sigma phase was not observed for alloys with chromium content less than 35 per cent, or with aging temperatures below 600°C. A series of experiments measuring hardness as a function of aging temperature from 300 to 900°C for 60 hours aging had shown a marked hardness peak at 475°C in all alloys from 21 per cent chromium to 58 per cent chromium; in addition, a large hardness increase occurred at chromium compositions of 45 and 49 per cent from 600 to 800°C associated with sigma phase formation. Becket noted that failure in precipitation embrittled alloys is transcrystalline while sigma phase first forms in the grain boundaries. He concluded that precipitation embrittlement is independent of sigma phase formation.

The iron-chromium phase diagram which has been accepted as the best establishment of sigma phase boundaries using pure iron-chromium alloys is that of Cook and Jones (3) shown in Fig. 1. Sigma boundaries were not determined below 600°C, but the sigma + alpha boundary was shown at approximately 25 per cent chromium at 600°C. Cook and Jones aged their specimens for a maximum of 1440 hours and considered that equilibrium had been obtained in that time. Subsequent investigations by Heger (4), Shortsleeve and Nicholson (5), and Link and Marshall (6)

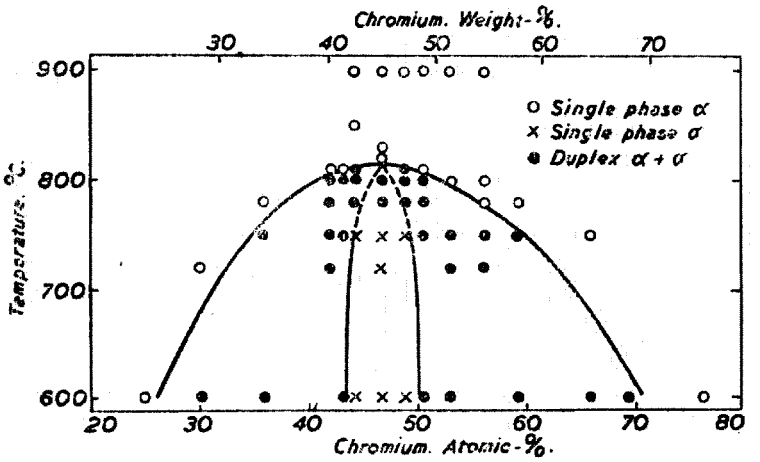

—Iron-Chromium Phase Diagram over the Range 25–76% Chromium.

Fig. 1. Portion of iron-chromium phase diagram by Cook and Jones (3).

have indicated equilibrium may not be obtained after aging for many thousands of hours at 600 to 850°C and the $\alpha + \sigma$ boundary may be extended to lesser chromium content than that shown by Cook and Jones. Shortsleeve and Nicholson have shown that silicon and manganese impurities shift the $\alpha + \sigma$ boundary to lower chromium content while carbon impurities shift it to higher chromium content.

Newell (7) added some new data in 1946. Using a 27 per cent chromium commerical alloy, Type 446, he has shown the kinetics of tensile property changes with 475°C aging, where tensile strength increased up to 108 hours aging, and elongation decreased rapidly in the first 36 hours of aging. Newell reported Neumann bands due to lattice strains and broadening of back reflection X-ray lines after 13,000 hours aging at 475°C. He found no change in X-ray powder patterns with 475°C aging of 27 per cent chromium-iron alloys, but found sigma phase lines appearing after 1000 hours at 540°C.

Heger (8) published a thorough review of precipitation embrittlement of ferritic iron-chromium alloys in 1951. Heger has shown that sigma phase will form at 475°C in alloys with chromium content as low as 17 per cent when the specimens are severely cold worked and aged for several thousand hours. Otherwise no identifiable structural changes have been associated with precipitation embrittlement. On the basis of his observations and the work of Bandel and Tofaute (9), Heger suggested that precipitation embrittlement is analogous to precipitation hardening in aluminum-copper alloys and may involve the reaction: alpha iron → transition phase → sigma phase, where the transition phase is coherent

with the alpha iron structure and causes large coherency stresses. Heger also noted that precipitates of nitrides, phosphides and carbides are formed when commerical alloys with these impurities are aged at 475°C.

Lena and Hawkes (10) published the latest work on precipitation embrittlement in 1954. With data on a high purity 28 per cent chromium vacuum melted alloy, and a commerical type 31.6 per cent chromium alloy, Lena concluded that,

> "(1) High purity Fe-Cr alloys exhibit little tendency to embrittle when aged at 475°C unless strained prior to aging. (2) 475°C embrittlement of commercial Fe-Cr alloys is not simply due to a grain boundary precipitate as evidenced by the large increase in hardness of single crystals after aging at 475°C. (3) It is postulated that the embrittlement of Fe-Cr alloys after aging for short times at 475°C is caused by the accelerated formation of an intermediate stage in the formation of sigma phase under the influence of lattice strains. In pure alloys the straining must be applied by external deformation, whereas commercial alloys are strained prior to embrittlement by the precipitation of a nitride phase. The intermediate stage is believed to consist of the formation of the chromium ferrite reported by Fisher, Dullis, and Carroll."

Fisher, Dullis, and Carroll (11) aged commercial type alloys of about 27 per cent chromium content for 10,000 to 34,000 hours at 485°C. They dissolved the matrix of these alloys in an alcohol solution of picric acid and hydrochloric acid. The residue was a body centered cubic chromium rich precipitate (80 per cent chromium) with lattice parameter, a, equal to 2.878 Å. When specimens of this material were severely cold worked before aging, sigma phase was extracted from the embrittled material. Fisher, Dullis, and Carroll have proposed that precipitation embrittlement is due to the formation of the chromium rich coherent precipitate.

Statement of Problem.

The present study was undertaken to determine new information concerning the kinetics and mechanism of precipitation embrittlement in pure iron-chromium alloys and to support or disprove existing theories, or propose a new theory for precipitation embrittlement.

Experimental Methods.

Vacuum melted alloys of nominal composition 19, 25, 34, 42 and 49 per cent chromium were purchased from Vacuum Metals Corporation and used for all experiments in this study.

Previous studies of precipitation embrittlement have shown or indicated: (1) precipitation embrittlement occurs in pure iron-chromium alloys and must be considered inherent to the iron-chromium system. (2) 475°C embrittlement involves precipitation of a second phase in the alpha solid solution matrix. (3) The embrittlement is associated with sigma phase formation, but is not due to direct precipitation of gross sigma phase.

The experimental methods chosen for this study are (1) strain aging experiments in 25 per cent chromium-iron alloys to show evidence of precipitation of a second phase and the effect of strain on the rate of embrittlement; (2) electrical resistance isothermal aging experiments to establish the kinetics of precipitation embrittlement in 25 per cent chromium-iron alloys; (3) isothermal aging experiments with 19, 25, 34, 42 and 49 per cent chromium-iron alloys using a temperature gradient

furnace and measuring hardness; and (4) metallographic and X-ray studies to determine the nature of the precipitate and the relation of sigma phase to precipitation embrittlement. Each experimental method and its result are discussed in detail in separate sections which follow.

II. MATERIALS, SPECIMEN PREPARATION, AND HEAT TREATMENT PROCEDURE.

The iron-chromium alloys used in this study were vacuum cast by the Vacuum Metals Corporation. The analysis of these alloys, Table 1, was provided by the Vacuum Metals Corporation. The alloys were received as 0.5 in. diameter round bars. Each alloy was annealed and homogenized for 0.5 hours at 1090°C and water quenched before use in these experiments.

TABLE 1

Analysis of Alloys Prepared by the Vacuum Metals Corporation

Nominal Per cent Cr	Per cent Cr	Per cent C	Per cent O_2	Per cent N_2
19	19.36	0.0017	0.021	0.00003
25	25.48	0.016	0.034	0.00028
34	33.75	0.0036	0.062	0.00051
42	41.58	0.0077	0.086	0.0015
49	48.91	0.0064	0.102	0.0017

The microtension specimens, Section III, were prepared by slicing some of the 0.5 in. bar stock into four radial sections, machining these radial sections into 0.125 in. round bars, and then machining the microtension specimens from the 0.125 in. bar stock on a jeweler's lathe. The electrical resistance specimens, Section IV, were prepared by centerless grinding 0.100 in. diameter cylinders 2.0 in. long from the 0.125 in. bar stock described above. The specimens to be treated in the gradient

furnace, Section V, were prepared by cold rolling 0.5 in. bar stock into 0.040 in. square wire. The microtension specimens, electrical resistance specimens, and one gradient furnace specimen were annealed for 0.5 hours at 1000°C after their preparation.

All specimens used in this study were sealed in Vycor tubing in 5.10^{-5} mm Hg vacuum before heat treatment in order to prevent nitrogen or oxygen contamination during heat treatment.

Furnaces for isothermal aging heat treatment of electrical resistance specimens and strain aging specimens were controlled in temperature by the following technique. Large copper blocks were placed in the furnaces for specimen holders. A chromel-alumel control thermocouple connected to a Leeds and Northrup Micromax Controller was placed between each copper block and its furnace heating element. Thermal inertia in the copper blocks stabilized the core temperature of these copper blocks to $\pm$ 2°C, although the control thermocouple temperature might vary $\pm$ 5°C or more. The core temperature was measured with a separate chromel-alumel thermocouple placed in the core of the copper blocks. Chromel-alumel cold junction thermocouples were placed in crushed ice baths. Thermocouple voltage was measured by a Leeds and Northrup Portable Precision Potentiometer, Model 8662. The measurement error of the potentiometer is $\pm$ 0.05 mv(12) which corresponds to $\pm$ 1°C at 500°C for chromel-alumel thermocouples (13). The cold junction ice bath used crushed ice in a Dewar flask with the cold junction thermocouple enclosed in a 1/8th inch diameter protection tube filled with oil. The cold junction temperature is estimated to be accurate within $\pm$ 0.5°C.

The hot junction thermocouple was enclosed in a 1/8th inch diameter hole drilled near the center of the copper furnace block and was in contact with the copper furnace block. Temperature errors between the furnace block and hot junction thermocouple due to radiation or conduction are estimated to be less than $\pm$ 0.5°C. All chromel-alumel thermocouple material used for cold junctions and hot junctions in these experiments was taken from the same spools of chromel and alumel wire. Thus, the error in relative temperature measurements indicated by these thermocouples due to thermocouple calibration was probably $\pm$ 0.5°C, although the absolute temperature may be in much larger error. There is also a possible error due to temperature difference between the potential connections of the potentiometer, since only a single cold junction was used, and this error is estimated to be less than $\pm$ 1°C. The total relative temperature measurement error is then estimated to be $\pm$ 3.5°C.

III. STRAIN AGING EXPERIMENTS

Methods and Procedures.

Strain aging experiments with 25 per cent chromium-iron alloys were performed to provide evidence of precipitation of a second phase, to show the effects of embrittlement on static tension properties of this alloy, and to show the effect of strain on the kinetics of precipitation embrittlement.

Tension tests were performed on a Chevenard Microtension machine (Type Mi34-NR113), because the available amount of vacuum melted 25 per cent chromium-iron alloy was limited. A typical microtension specimen with 1.5 millimeter diameter gage section and 7.5 millimeter gage length is shown in Fig. 2. All tension tests were made at room temperature, 25°C.

A series of specimens was aged one-half hour to 534 hours at 490°C after annealing and then tested. Another series of specimens was strained in tension to a permanent deformation of from 2 per cent elongation to 6 per cent elongation before aging. These specimens were then aged for times of one-half hour to 1022 hours at 490°C and retested. A few specimens were aged and retested over several cycles of strain plus aging. One specimen was strained, aged for 24 hours at 490°C, tested, annealed for one-half hour at 700°C and retested to show the effect of 700°C aging on removing the embrittlement acquired at 490°C.

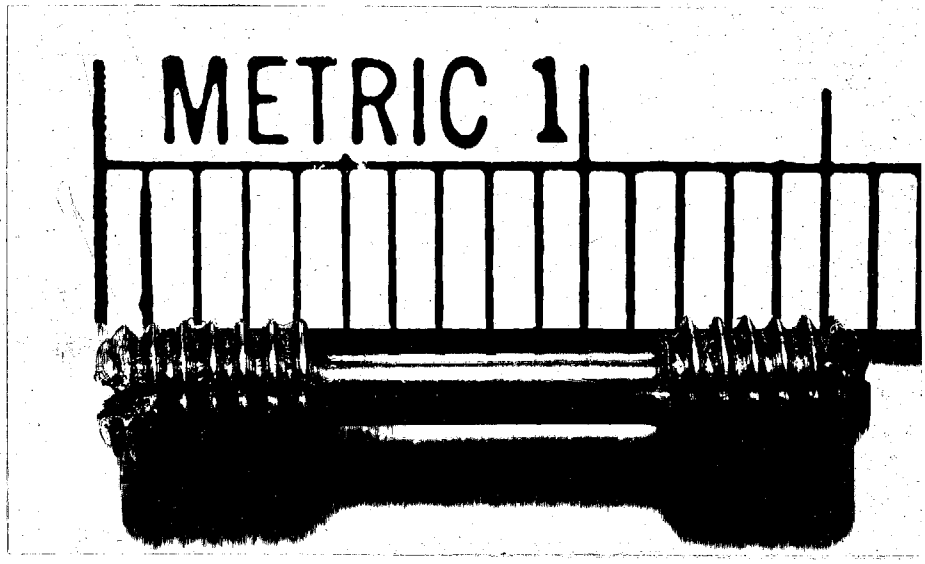

Fig. 2. Microtension Specimen.

Results.

Some typical stress-strain curves, are shown in Figs. 3 to 8. Fig. 3 shows the stress-strain curve for an annealed 25 per cent chromium-iron specimen which was strained to 2.5 per cent elongation, then partially unloaded, and then reloaded without heat treatment between tests. The reloaded stress-strain curve is an extension of the original stress-strain curve as if the loading cycle had not been interrupted. Fig. 4 shows the effect of aging at 475°C for 2.5 hours and 4.5 hours between loading cycles. Note that the 0.2 per cent offset yield strength is not only raised from 47,500 psi to 62,000 psi and 70,000 psi, but a yield point similar to that found in mild steel appears. Fig. 5 shows a similar effect where the specimen was aged 170 hours at 490°C, and the yield strength was raised from 41,000 psi to 105,000 psi. Fig. 6 shows the effect of strain aging for 24 hours at 490°C followed by 0.5 hours at 700°C. Strain aging at 490°C increased the yield strength from 40,000 psi to 63,500 psi, but 0.5 hours at 700°C reduced the yield strength to 26,800 psi, although the mild steel type of yield was retained. Fig. 7 shows a stress-strain curve obtained with an annealed specimen aged at 490°C without previous strain. The absence of a mild steel type yield point is notable. Fig. 8 illustrates one of a series of specimens aged at 490°C after approximately 4 per cent initial elongation, and the yield point is quite apparent. The yield strength increases and the ductility decreases with continued aging in both initially annealed and initially strained specimens. These results are summarized in Table 2. Embrittlement is shown to occur by the decrease in specimen elongation after aging at 490°C. Elongation is decreased to zero per cent after sufficient aging at 490°C.

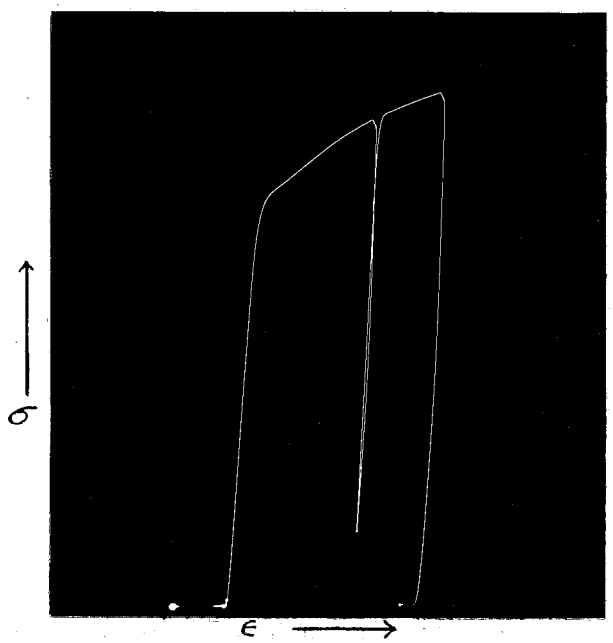

Fig. 3. Annealed 25 per cent chromium-iron stress-strain curve. Initial loading, a. Reloading, b.

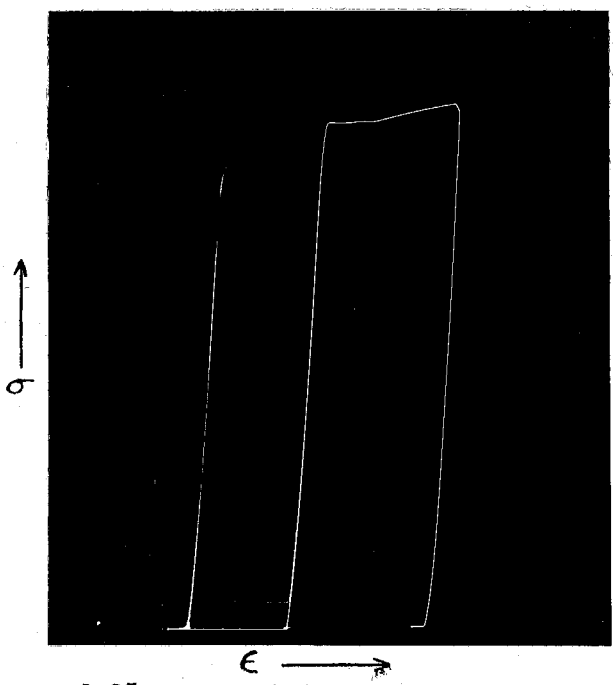

Fig. 4. Strain aged 25 per cent iron-chromium specimen, 2.5 hours and 4.5 hours at 475°C. Initial loading, a. Reloading without aging, b. Reloading after 2.5 hours at 475°C, c. Reloading after 4.5 hours at 475°C, d.

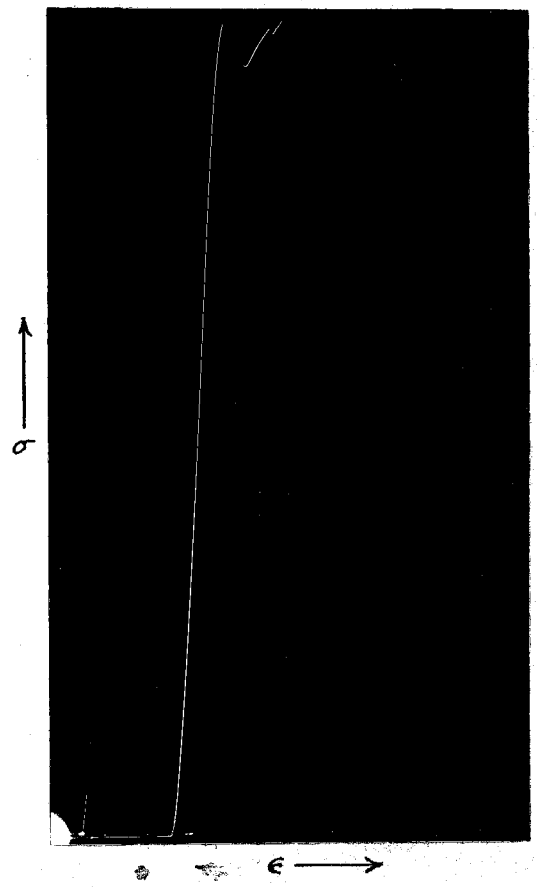

Fig. 5. 25 per cent chromium-iron strain aged 170 hours at 490°C. Initial loading, a. Reloading after 170 hours at 490°C, b.

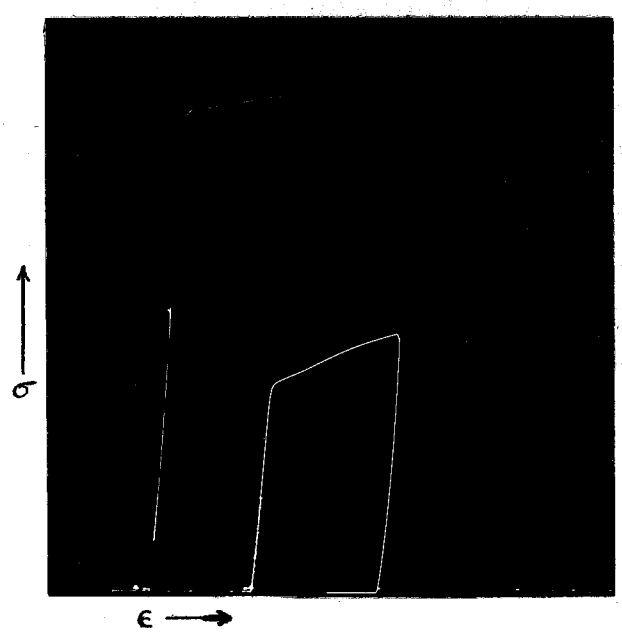

Fig. 6. 25 per cent chromium-iron strain aged and annealed 0.5 hours at 700°C. Initial loading, a. Reloading after 24 hours at 490°C, b. Reloading after 0.5 hours at 700°C, c.

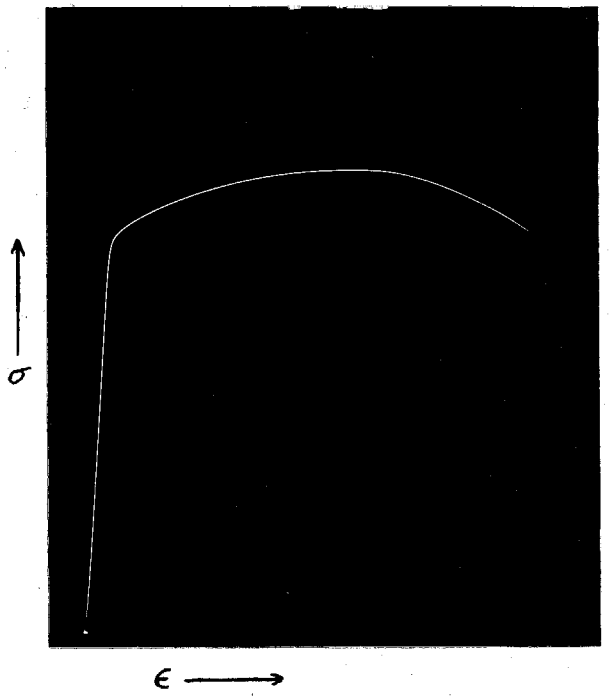

Fig. 7. 25 per cent chromium-iron annealed and aged 4 hours at 490°C.

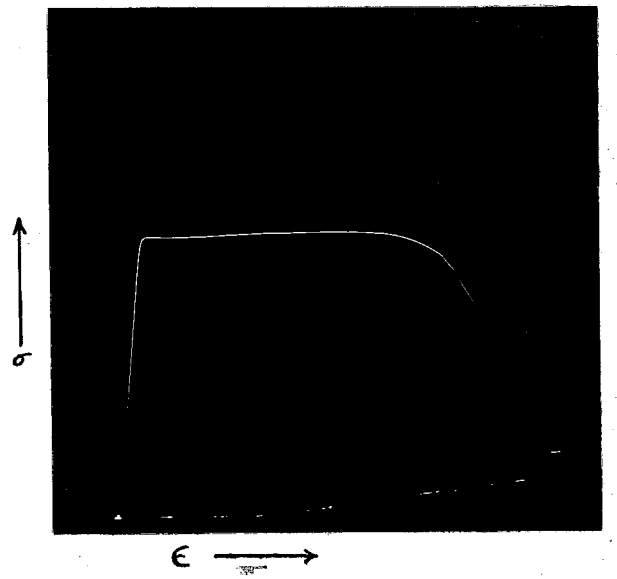

Fig. 8. 25 per cent chromium-iron elongated 4 per cent in tension and aged 1 hour at 490°C.

TABLE 2

Results of Microtension Tests.

Initial strain per cent	Time at temperature	Temperature °C	yield strength	ultimate strength	elongation per cent	gage section dia. mm	gage length mm
0	0	490	59,000	63,500	6	1.57	7.0
0	0	490	60,500	67,000	8	1.37	7.0
0	0.5	490	55,000	65,100	12	1.27	8.0
0	1	490	56,500	64,000	8	1.48	6.0
0	1	490	57,000	64,500	5	1.27	8.0
0	2	490	49,500	53,800	1.9	1.43	7.5
0	4	490	56,600	68,500	12	1.45	7.5
0	5	490	63,500	77,600	10	1.34	8.0
0	16	490	51,000	59,000	1.6	1.49	7.1
0	25	490	47,000	47,000	0	1.34	8.0
0	65	490	53,500	53,500	1	1.45	7.5
0	160	490	83,800	88,000	2.5	1.12	8.0
0	534	490	65,000	65,000	0	1.45	7.5
4	0	490	66,800	74,500	1	1.32	7.5
4	1	490	65,500	65,500	8.7	1.15	7.5
4	11.2	490	74,000	74,000	6.7	1.36	7.5
4	110.5	490	80,500	80,500	6.7	1.23	7.5
4	418	490	107,000	107,000	0.3	1.37	7.5
4	1022	490	94,000	94,000	0	1.26	7.5
4	2.5	475	62,000	---	---	1.50	7.5
4	4.5	475	70,000	---	---	1.50	7.5
3	170	475	105,000	105,000	0	1.48	7.5
2	0.5	700	26,800	---	---	1.47	7.5

Interpretation of Results.

A limited discussion of the strain aging experimental results is appropriate here, although supporting metallographic work described in Section VI will add to an integrated discussion in Section VI.

The strain aging experiments have established that embrittlement occurs in a vacuum melted iron-chromium alloy when it is aged at 490°C, and that there is a strain aging effect. Such a strain aging effect has usually been associated with the formation of a second phase(14). Plastic strain prior to aging accelerates the embrittlement, increases the yield strength for a given aging time, and tends to hold ductility at a higher level for a given yield strength or aging time. Plastic deformation prior to aging changes the shape of stress-strain curves obtained after aging, particularly in that a mild steel type of yield point is developed. Some of these effects may be related to interstitial impurities in the 25 per cent chromium-iron alloy.

Some interesting studies on this vacuum melted 25 per cent chromium-iron alloy have been conducted by Martens at the Jet Propulsion Laboratory (15), and these studies substantiate the embrittlement effect in this alloy when aged at 475°C.

Martens used annealed 0.25 in. by 0.25 in. by 1 in. Izod impact specimens with a 0.050 in. 45° groove, and aged them at 475°C. Martens made impact tests with a 100 in. pound Izod machine. Vickers hardness was measured on a Tukon tester. The results of this experiment are summarized in Table 3.

Martens' work shows that impact energy decreases with increasing aging time while hardness increases, correlating well with the static tension tests described above.

TABLE 3

Impact Data On 25 Per Cent Chromium-Iron Vacuum Cast Alloy Specimens*

Temperature	Time	Impact Energy In. Lb.	10kg Vickers Hardness Number
as quenched		100	187
475°C	25 hr.	86-100	194-205
475°C	40 hrs.	60-78	201-206
475°C	56 hrs.	39-51	199-203
475°C	72 hrs.	35-37	207-209
475°C	120 hrs.	29-33	215-221
475°C	240 hrs.	24-30	225-235

* See Martens (15).

IV. ELECTRICAL RESISTANCE EXPERIMENTS

Methods and Procedure.

Electrical resistance measurements were made with a Leeds and Northrup Type 4340 Students Kelvin double bridge. The specimens were 25 per cent chromium-iron alloy, 0.100 in. diameter, 2 in. long, centerless ground rods; specimen fabrication is described in section II. The specimen holder had pointed steel potential contacts 1 in. apart. A specimen and the specimen holder are shown in Fig. 9.

Since this experiment is designed to show a change in electrical resistance as a function of aging treatments, relative errors in resistance measurements are important. The primary sources of relative error are 1) errors inherent to the Kelvin bridge, 2) thermoelectric effects, 3) geometry of the specimen and specimen holder, 4) temperature of the specimen, and 5) surface condition of the specimen.

Errors inherent to the Kelvin bridge depend on several factors. The bridge in perfect condition has an accuracy of $\pm$ 0.7 per cent (16). The surface condition of the main slidewire and of decade contacts will affect this accuracy somewhat, but surface conditions of the bridge used in this experiment were not apparently varied during the experiment. Inherent Kelvin bridge error with respect to relative changes in electrical resistance are estimated to be at maximum $\pm$ 1.0 per cent.

Thermoelectric sources of error were eliminated by reversing the direction of bridge current on two separate balancing operations.

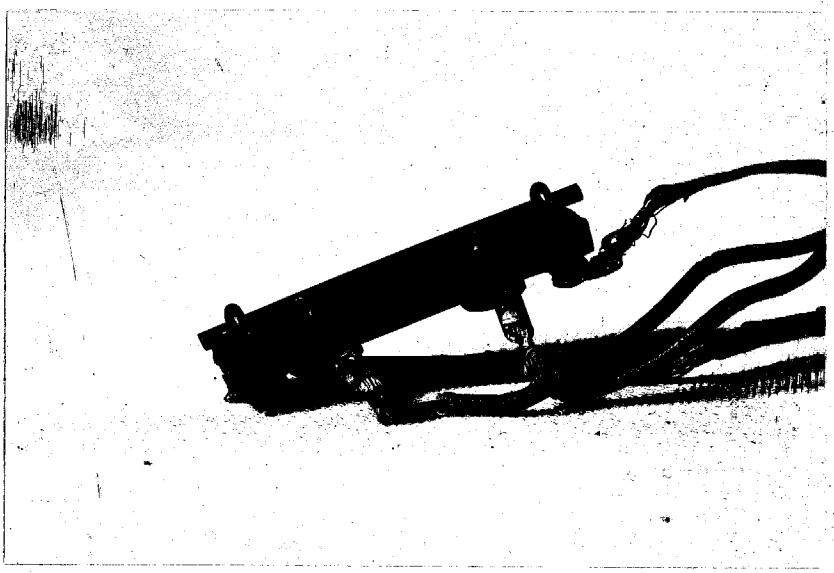

Fig. 9. Electrical resistance specimen in the specimen holder.

In this experiment the null point was found to be independent of current direction within ± 0.5 micro ohm.

The specimens were cylindrical to at least ± 0.0001 in. and the dimensions of a specimen were not observed to change during aging. Thus, the specimen diameter was constant to a fraction of 0.1 per cent. The length of specimen over which resistance was measured depended on the spacing of the pointed steel potential leads. The position of these leads was fixed in the specimen holder and could change during the course of the experiment only by deformation and wear of the points. The maximum amount of such change is estimated to be 0.005 in. which would introduce a resistance error of 0.5 per cent.

Specimen temperature was controlled by a constant temperature circulating oil bath with temperature observed to be 311.5 ± 0.1°K consistently, and by a Dewar flask liquid nitrogen bath estimated to be 77.4 ± 0.5°K. The corresponding error in resistance is estimated to be less than ± 0.1 per cent.

The effect of specimen surface condition cannot be treated quantitatively. The Kelvin bridge is designed to eliminate contact potential and resistance effects; however, if one potential lead is in good contact with the specimen while the other has a contact resistance comparable to circuit impedances of the bridge arm, large errors can occur. The pointed steel contacts were designed to puncture surface films and minimize contact resistance. Further, the specimens were carefully cleaned in acetone and sealed in vacuum before heat treatment to minimize formation of surface films. Nevertheless, surface films did form in some cases after many hours of

aging in the 500°C range. It was occasionally necessary to clean the specimen by pickling in a hot solution of 10 per cent hydrochloric acid and 10 per cent sulfuric acid. The specimen dimensions were checked before and after pickling. Electrical resistance was also measured before and after pickling treatments. Usually no dimensional or resistance changes were noted after the pickling treatment, and corrections were carried through the experiment when changes did occur.

Total experimental errors in the electrical resistance experiments are estimated to be ± 2 per cent. Reproducibility checks were made by measuring some specimens several times and was found to be ± 0.7 per cent.

The electrical resistance specimens were annealed for 30 minutes at 1090°C and water quenched after centerless grinding. Initial resistance of each specimen was measured at 77.4°K and 311.5°K. The specimens were aged isothermally in constant temperature furnaces described in Section II. A given specimen was aged 0.2, 0.4, 0.8, 1.6, ... , 2000 hours at one temperature, i.e., the aging time was doubled at each increment. Electrical resistance at 77.4°K and 311.5°K was measured after each aging increment, thus giving electrical resistance vs. log time data.

Specimens 1, 2, 3, and 4 were strained in tension to 0.67, 2.0, 3.3, and 10 per cent elongation respectively before isothermal heat treatment. Specimens 5 to 12 were not strained after annealing.

Results, 460°C to 525°C.

The results of these isothermal aging experiments for temperatures of 460°C, 475°C, 490°C and 525°C are shown in Figs. 10

to 15. Figs. 10, 11, 13, 15 are plots of electrical resistance vs. log time for annealed specimens aged at temperatures of 460°C, 475°C, 490°C, and 525°C, respectively. Fig. 12 shows the effect of plastic deformation on aging at 475°C, and Fig. 14 shows the effect of plastic deformation on aging at 490°C.

Results are plotted with the resistance scale for room temperature measurements at the right and for liquid nitrogen temperature measurements at the left. The liquid nitrogen temperature resistance unit scale and room temperature resistance unit scale are equal but have different zero suppression so that both curves can be shown on one graph.

Aging at 460°C, Fig. 10, produces a 55 μohm decrease in electrical resistance measured at 311.5°K after 8 hours aging followed by a 25 μohm increase after 500 hours aging, and decreasing again after 1000 and 2000 hours aging. Resistance measured at liquid nitrogen temperature decreases 20 μohm after 2 hours aging then increases steadily 200 μohm after 2000 hours at 460°C.

After aging a 25 per cent chromium-iron specimen at 475°C, Fig. 11, electrical resistance measured at 311.5°K decreases 55 μohms in 8 hours followed by a 55 μohm increase in 1000 hours, and decreases again after 2000 hours aging. Electrical resistance measured at 77.4°K decreases 7 μohms in 0.8 hours, then increases steadily 250 μohms after 2000 hours at 475°C.

After 490°C aging, Fig. 13, electrical resistance measured at 311.5°K decreases, shows a small anomalous increase at 2 hours, and decreases 37 μohms after 8 hours aging, then increases 75 μohms

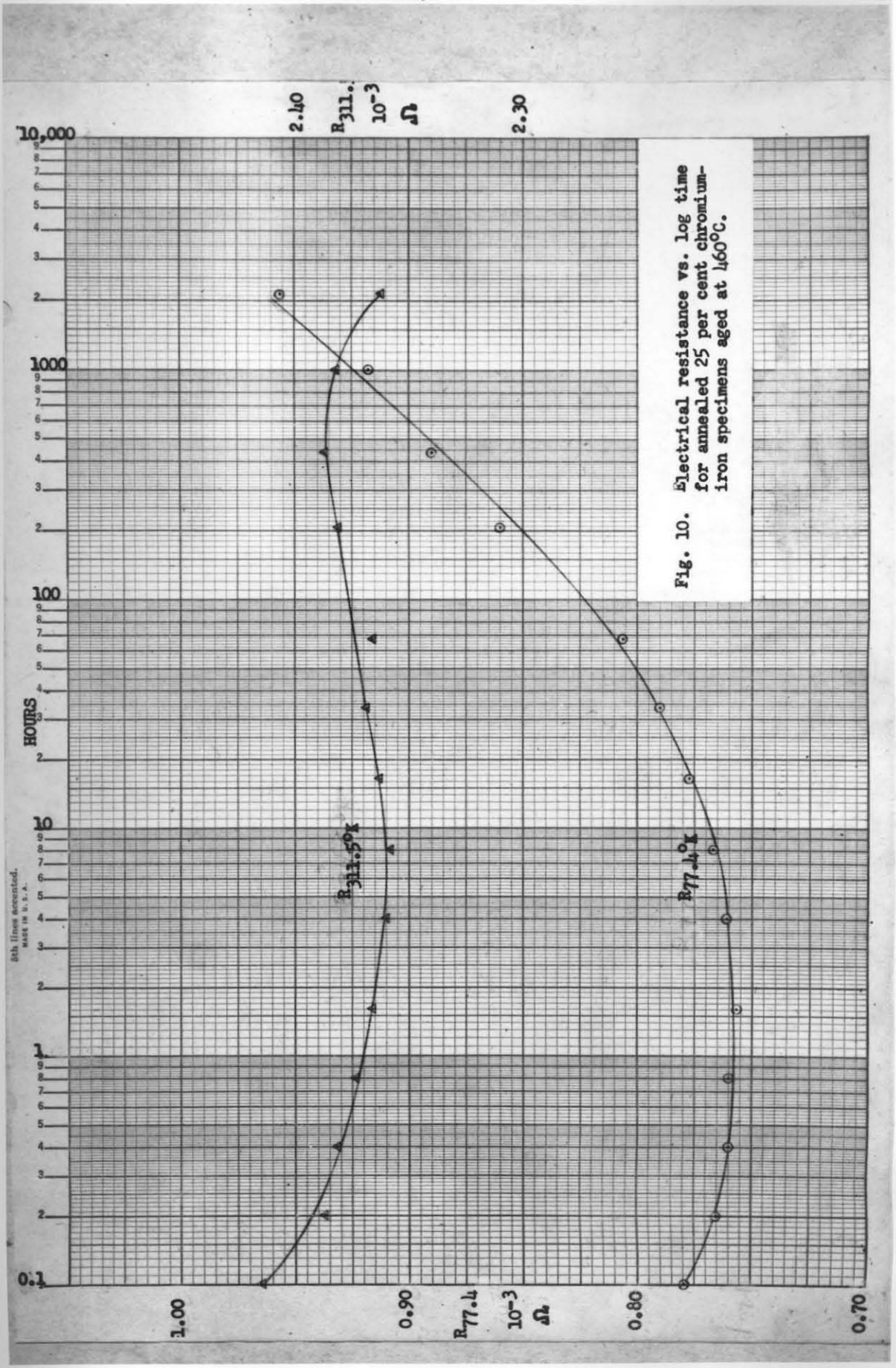

Fig. 10. Electrical resistance vs. log time for annealed 25 per cent chromium-iron specimens aged at 460°C.

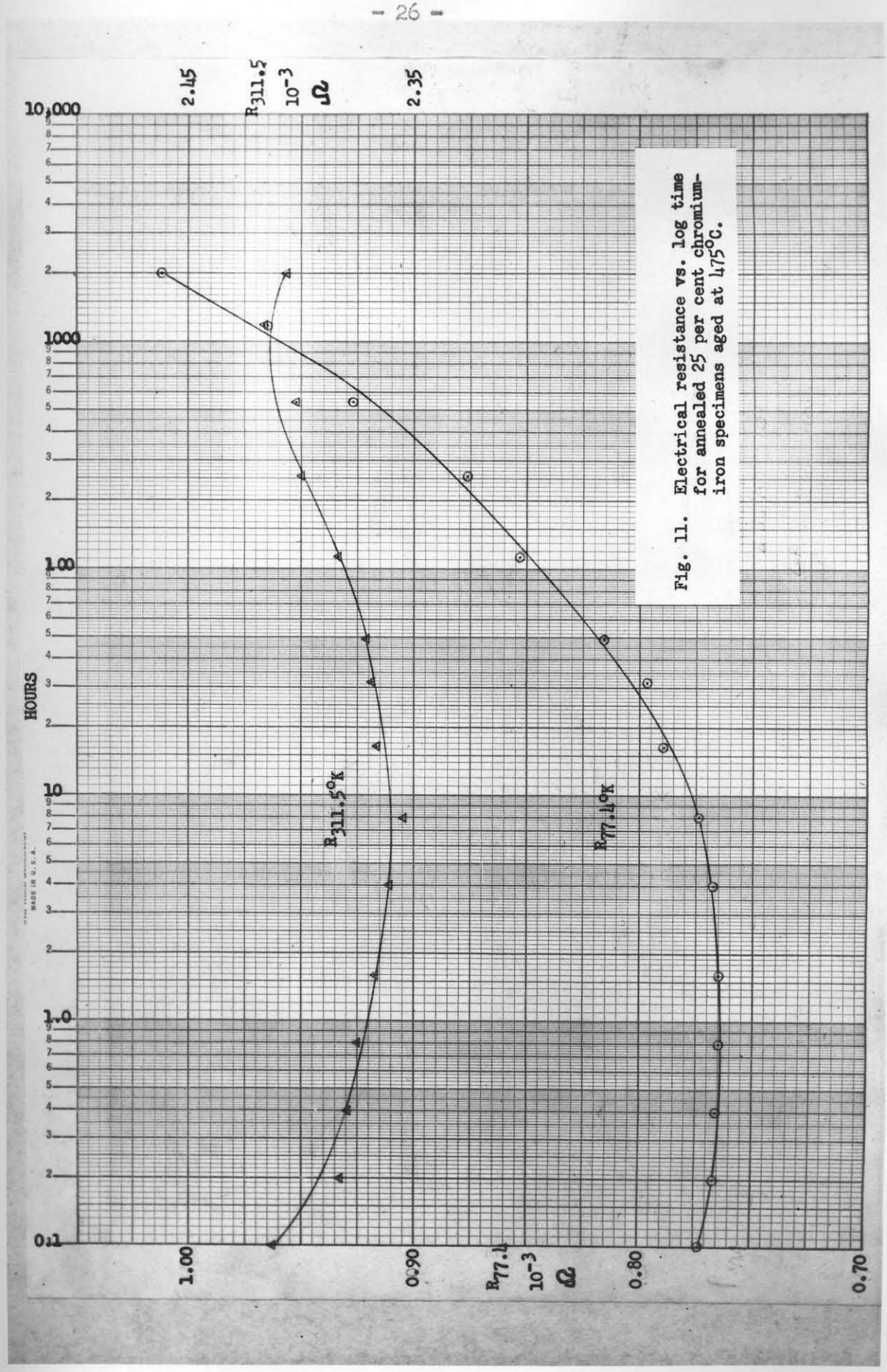

Fig. 11. Electrical resistance vs. log time for annealed 25 per cent chromium-iron specimens aged at 475°C.

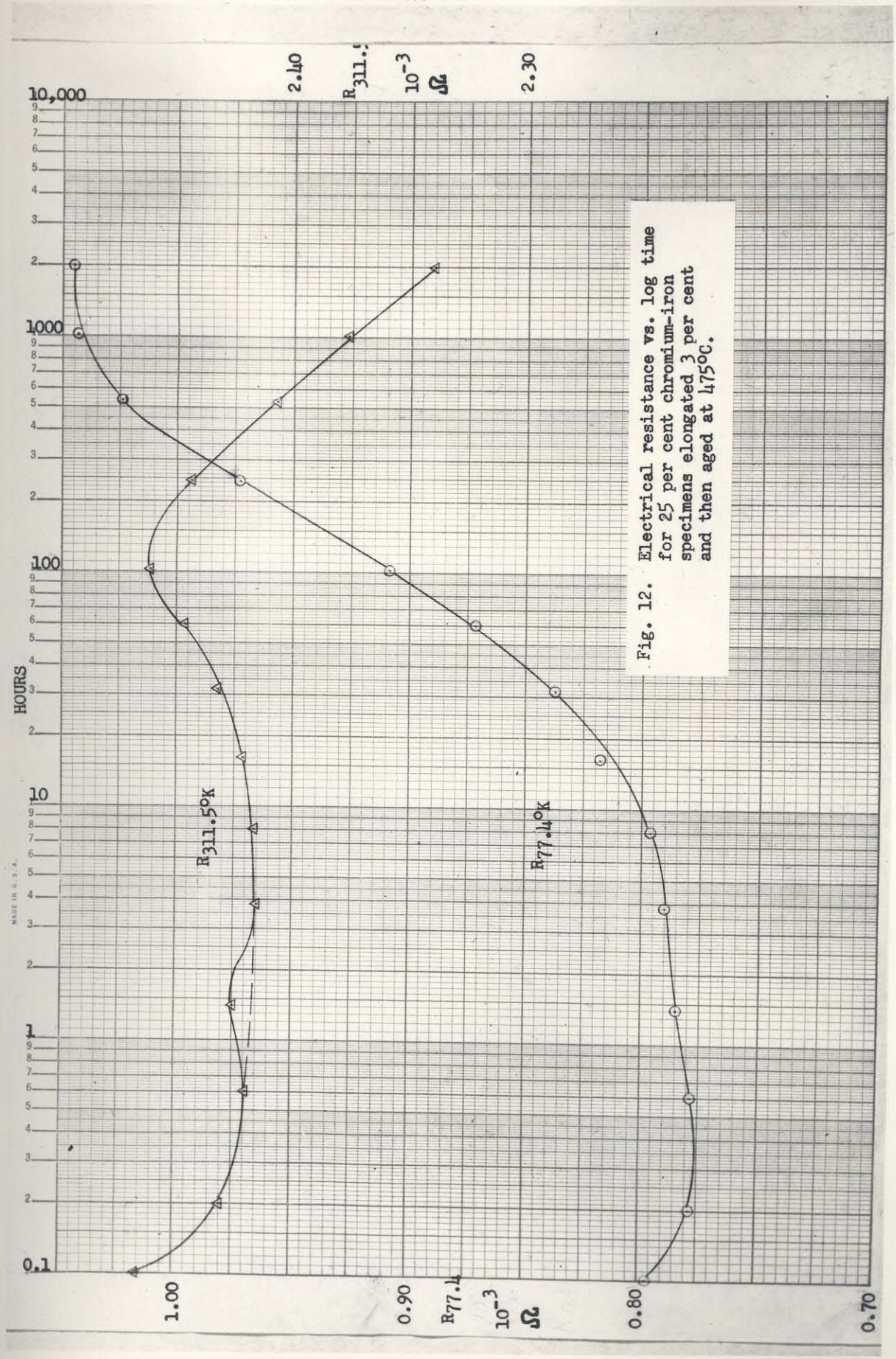

Fig. 12. Electrical resistance vs. log time for 25 per cent chromium-iron specimens elongated 3 per cent and then aged at 475°C.

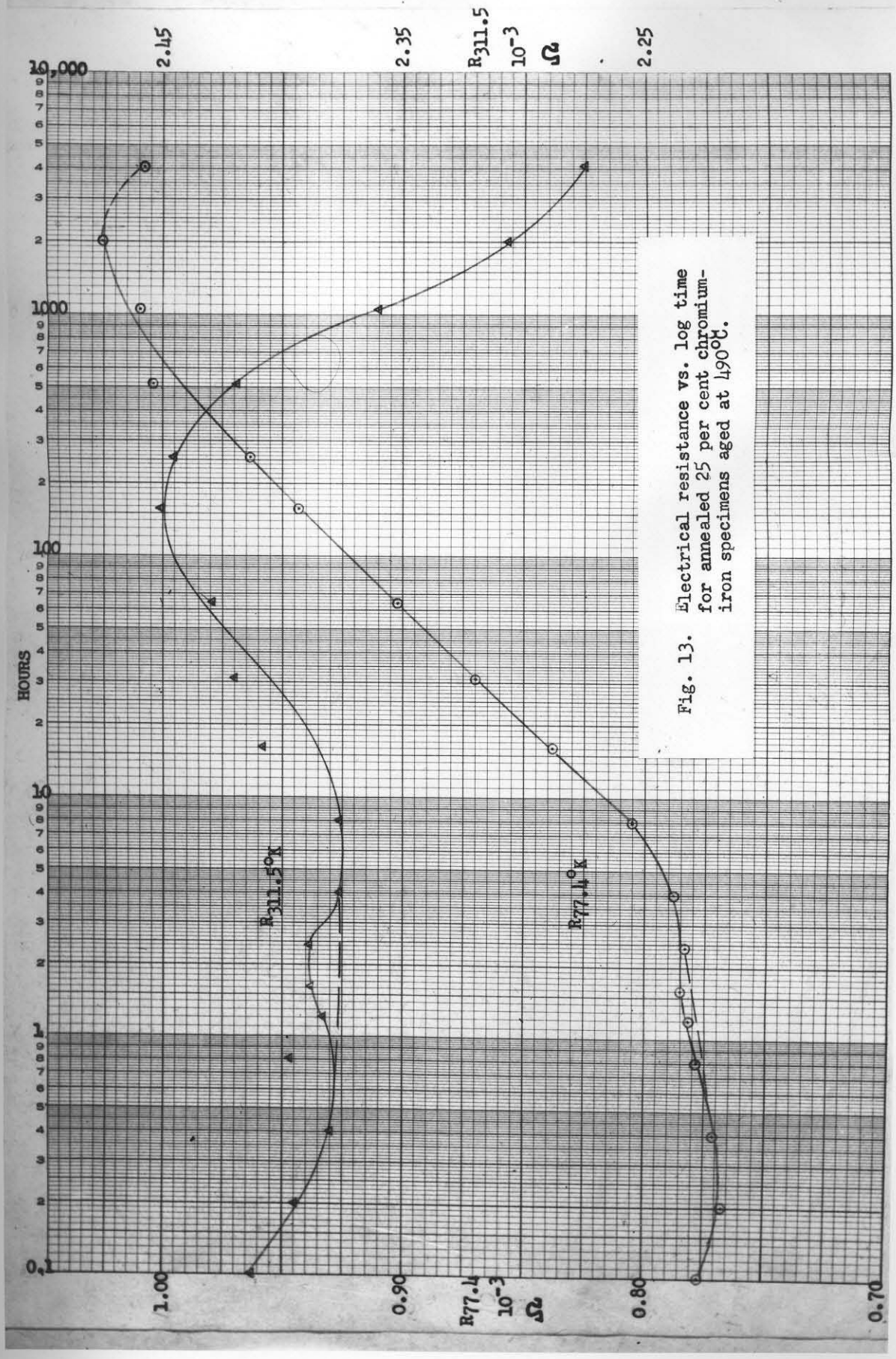

Fig. 13. Electrical resistance vs. log time for annealed 25 per cent chromium-iron specimens aged at 490°C.

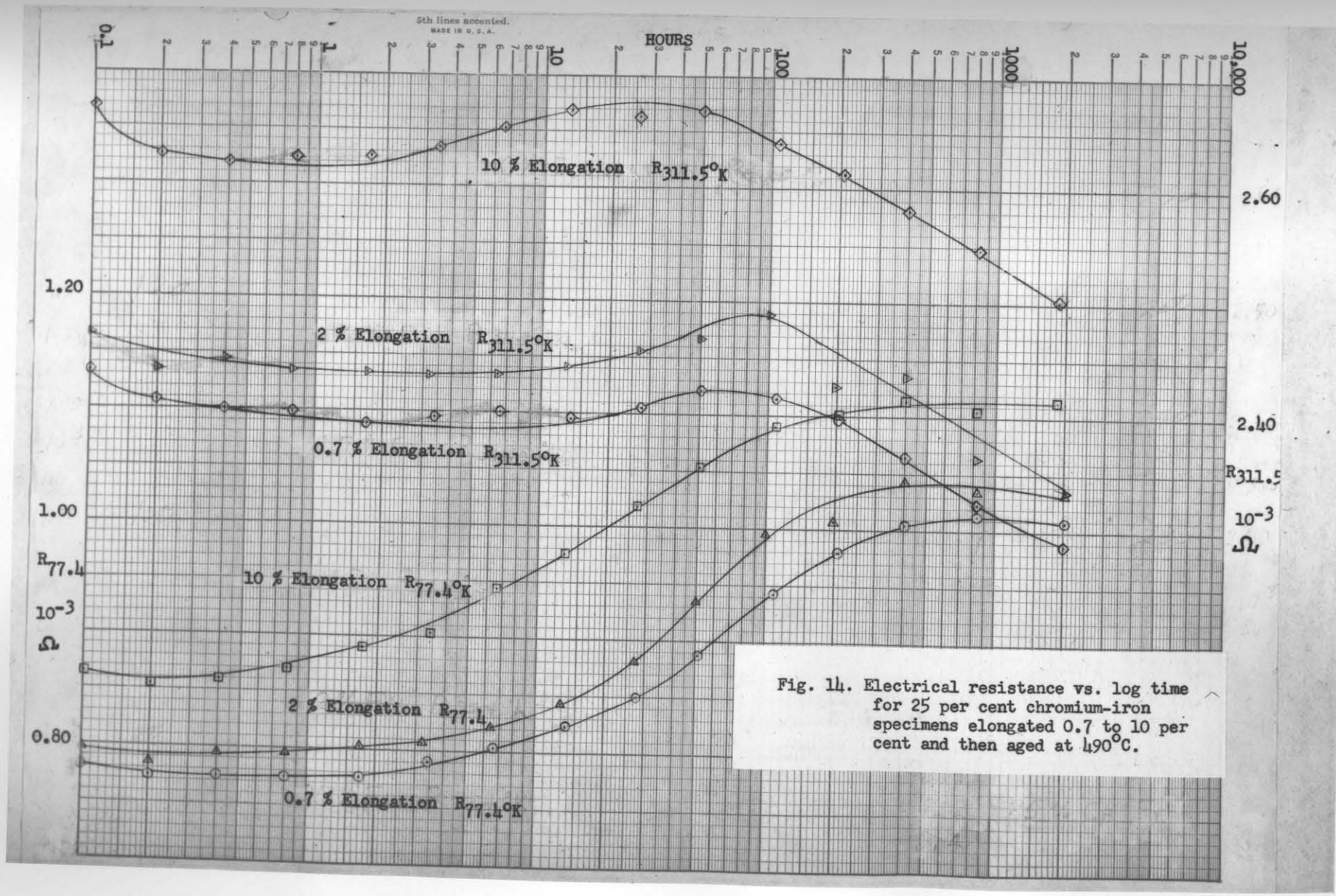

Fig. 14. Electrical resistance vs. log time for 25 per cent chromium-iron specimens elongated 0.7 to 10 per cent and then aged at 490°C.

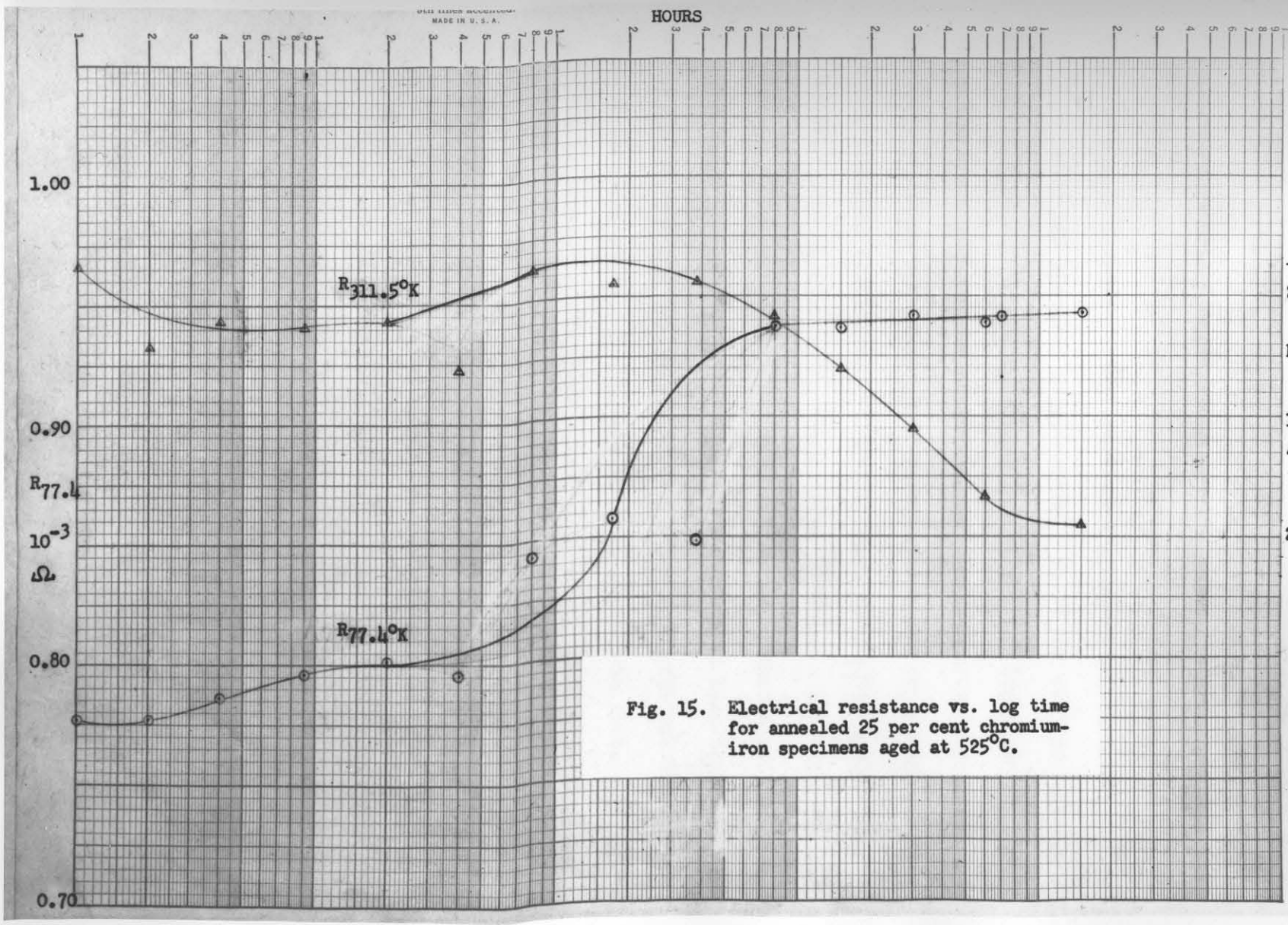

Fig. 15. Electrical resistance vs. log time for annealed 25 per cent chromium-iron specimens aged at 525°C.

in 150 hours, and finally decreases 175 μohms after 4000 hours. Electrical resistance measured at 77.4°K decreases slightly after 0.2 hours, increases slightly to a plateau after 2 hours, then steadily increases 250 μohms after 2000 hours at 490°C. There is an indication of a resistance decrease after 4000 hours aging at 490°C.

When the specimen is elongated 1 to 10 per cent in tension before aging at 490°C, the resulting resistance vs. log time curves (Fig. 14) are similar in shape to the 490°C aging curves for an initially annealed specimen. Cold work has several important effects, however. Maximum electrical resistance measured at room temperature is attained with shorter aging times, e.g. in 3 hours with 10 per cent elongation compared to 150 hours with the annealed specimen. The total changes in resistance are equal to or somewhat less than the corresponding changes in the annealed specimen. Electrical resistance changes measured at 77.4°K follow a pattern similar to those of the annealed specimens, but again time to reach maximum resistance increase is shortened. A maximum increase of 265 μohms was observed at 400 hours in the specimen elongated 10 per cent, corresponding to 265 μohms at 400 hours in the specimen elongated 2 per cent, 235 μohms at 840 hours in the specimen elongated 0.7 per cent, and 250 μohms at 2000 hours in the annealed specimen. Thus cold work seems to accelerate the aging process without affecting the maximum change in resistance and without modifying the basic shape of the aging curves. It is interesting to note that change in resistance due to 10 per cent elongation is 258 μohms measured at 311.5°K compared to 93 μohms for the same specimen measured at 77.4°K. This behavior violates

Mattheissen's rule for dilute solid solutions that change in resistance due to structure change is independent of temperature. Similarly, the resistance change during aging of the specimens described above is quite different at liquid nitrogen temperature than at room temperature. This will be discussed in more detail later. The relative change in resistance ($\Delta R/R$) due to cold work is more nearly the same at room temperature and at liquid nitrogen temperature than the total change in resistance as shown in Table 4.

The results of aging an annealed 25 per cent chromium-iron resistance specimen at 525°C are shown in Fig. 15. Electrical resistance measured at 311.5°K decreases 40 μohms in 4 hours aging with a slight increase at 2 hours, increases 40 μohms after 10 hours, and finally decreases 110 μohms after 1500 hours aging at 525°C. Resistance measured at 77.4°K increases 25 μohms to a plateau in 2 hours aging, rises to 60 μohms after 20 hours, followed by an additional 80 μohms increase at 80 hours, and a very slight increase from 80 to 1500 hours aging.

Interpretation of Results, 460°C to 525°C.

The effects obtained after aging annealed 25 per cent chromium-iron specimens between 460 and 525°C show several consistent features. Electrical resistance measured at 311.5°K decreases approximately 50 μohms in 8 hours aging at 460°C, 475°C, and 490°C, and in 4 hours at 525°C. There is an anomalous resistance increase superimposed on this decrease, resulting in a resistance peak in 2 hours aging at 490°C and 525°C. This effect is shown most strongly in the 490°C

TABLE 4

The Effect of Cold Work on the Electrical Resistance of 25 Per cent Chromium-Iron Specimens.

Per cent Elongation	$\Delta R_{77.4^\circ K}$ μohms	$\Delta R_{311.5^\circ K}$ μohms	$(\frac{\Delta R}{R})_{77.4^\circ K}$ per cent	$(\frac{\Delta R}{R})_{311.5^\circ K}$ per cent
0.7	5	15	0.65	0.62
2	21	51	2.7	2.1
3.3	21	59	2.7	2.4
10	88	258	11.3	10.8

aging curves, Fig. 13. This anomalous increase of resistance could reasonably be associated with interstitial impurity effects such as those caused by nitrogen, oxygen, and carbon. Lena (10) reports a similar electrical resistance increase which peaks in about 1 hour at 475°C due to lattice strain associated with nitride precipitation.

The general decrease in electrical resistance measured at 311.5°K occurring in the first 8 hours of aging (4 hours at 525°C) may be interpreted as a result of chromium depletion from the matrix solid solution and beginning of local ordered domains or nuclei. Alexander and Hanson (17) and Fink and Smith (18) have pointed out that such a process would be expected to decrease resistance. After this initial decrease, electrical resistance measured at 311.5°K increases 25 μohms in 500 hours at 460°C, 55 μohms in 1000 hours at 475°C, 75 μohms in 150 hours at 490°C, and 40 μohms in 10 hours at 525°C. The rate and magnitude of this increase of resistance seem highly temperature sensitive. This increase in resistance may be attributed to lattice strain associated with the formation of second phase nuclei which are coherent with the lattice of the matrix and slightly different in size. This explanation for an increase of electrical resistance accompanying precipitation hardening reactions was suggested by Mehl and Jetter (19), and the effect of a coherent second phase is discussed by A.H. Geisler (20). The same author discusses the effect of the amount of disregistry between precipitate and matrix on aging kinetics (21). He points out that in systems where disregistry between matrix and precipitate is small, e.g. in aluminum-silver and copper-nickel-cobalt, the increase of electrical

resistance is small and does not become apparent until after a moderate degree of solid solution decomposition has occurred, and this increase in resistance is not recovered until late in the aging process. With alloys where matrix precipitate disregistry is large, e.g. aluminum-zinc or copper-beryllium, loss of coherency takes place early before gross solid solution decomposition has occurred, and the resistance increase starts initially instead of following an initial decrease. Geisler (21) illustrates these effects diagramatically in Fig. 16.

The room temperature aging curves of a 25 per cent chromium-iron alloy aged between 460°C and 525°C seem definitely to resemble the aluminum-silver type of curve illustrated above, suggesting the formation of a coherent precipitate having little disregistry with the alpha matrix.

The increase in resistance discussed above is followed by a continuous decrease in electrical resistance measured at 311.5°K after longer aging times. This continuous decrease in electrical resistance may be interpreted as the result of solid solution depletion effects becoming dominant in the process. This phase of the aging process would be expected to occur after sufficient aging time according to Geisler [(21) and Fig. 16]. The time of reaching maximum electrical resistance measured at 311.5°K decreases with increasing temperature from 460° to 525°C.

The aging curves obtained by measuring the electrical resistance of the aged specimens at 77.4°K are quite different from the aging curves obtained by measuring the electrical resistance of the aged specimens at 311.5°K. Emphasis should be placed on the fact

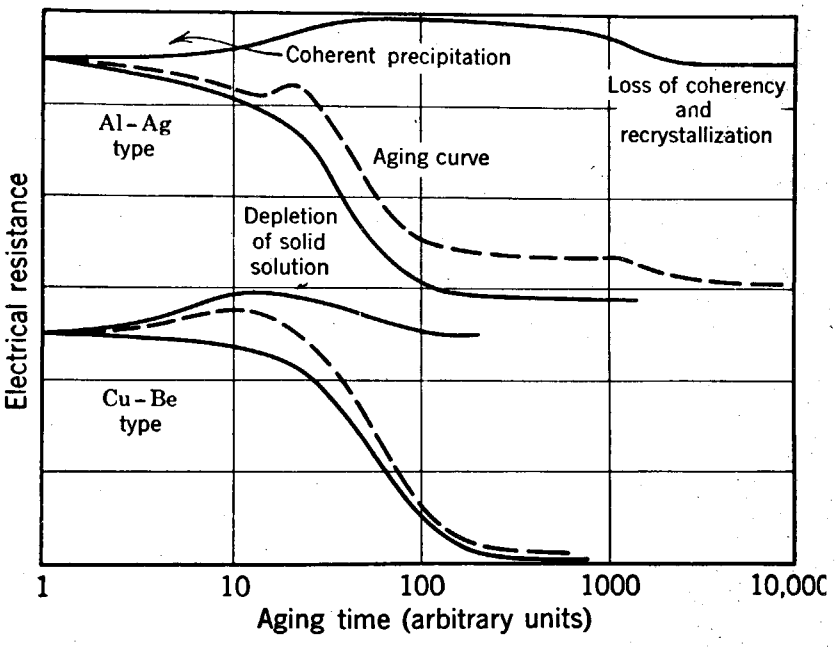

Fig. 16. Effect of lattice disregistry on aging kinetics, from Geisler (21).

that the observed structural changes took place at an aging temperature much above the temperature at which resistance was measured. Electrical resistance measurements were made at least twice at 77.4°K and twice at 311.5°K for points plotted on the aging curves. No structural changes have been observed either at room temperature or liquid nitrogen temperature regardless of the order in which the resistance measurements were made, and regardless of the time these specimens were stored at room temperature before their resistance was measured. If any structural changes occurred between room temperature and liquid nitrogen temperature they must have been completely reversible in very short times, i.e. martensite type shear reactions, which have never been observed in the iron-chromium alloy system. The differences between aging curves obtained by measuring resistance at room temperature and at liquid nitrogen temperature must then be explained on the basis of the difference in measurement temperature and the fact that the electrical resistance of a given metallic structure is highly temperature dependent. An interpretation of resistance changes measured at 77.4°K after aging 25 per cent chromium iron specimens at 460, 475, 490, and 525°C follows.

An initial decrease in resistance of 23 μohms in 2 hours at 460°C, 7 μohms in 1 hour at 475°C, and 10 μohms in 0.2 hours at 490°C occurs, while no decrease occurs at 525°C. Following the initial decrease aging at 460°C shows a steady increase of 200 μohms in 2000 hours. Similarly, there is a steady increase in electrical resistance measured at 77.4°K with aging at 475°C of 250 μohms in 2000 hours. After aging at 490°C, electrical resistance increases to a plateau in

1.5 hours, then increases 250 μohms steadily in 2000 hours. The electrical resistance data measured at 77.4°K with specimens aged at 525°C is difficult to interpret, Fig. 15. The resistance increases 25 μohms to a plateau for a period from 8 to 38 hours, then increases again 80 μohms to a plateau for a period from 80 to 1500 hours.

The initial decrease in resistance may be interpreted as solid solution depletion and formation of nuclei as in the case of room temperature resistance effects. This initial decrease is smaller with 490°C aging than with lower temperature aging because of the superimposed nitride precipitation which strains the lattice. The initial decrease in electrical resistance is lost with 525°C aging because precipitate coherency with the matrix is lost much earlier than with 490°C aging or lower temperature aging. There is a steady rise following the initial decrease in electrical resistance measured at 77.4°K, which continues after 2000 hours at 460°C or 475°C, which may not continue after 2000 hours at 490°C, and which does not continue after 80 hours at 525°C. Taking the time for one-half of the total resistance changes which occur with aging at 525°C and 490°C, and assuming the total change at 460°C and 475°C would with sufficient aging time equal that at 490°C, then taking the estimated half time for aging at 460°C and 475°C the results shown in Table 5 are obtained.

It is clear that the precipitation embrittlement process does not look the same when studied by electrical resistance measured at 77.4°K, as it does when studied by electrical resistance measured at 311.5°K. This is most obvious in the 490°C aging curves, Fig. 13.

TABLE 5

The Relation of Temperature and Aging Rate

Aging Temperature °C	Time for 1/2 Total 77.4°K Resistance Change hours
460	520
475	265
490	55
525	15

Since the unit scales for resistance measured at 311.5°K and resistance measured at 77.4°K are equal, it is shown that there is a 50 per cent larger total change in electrical resistance measured at 77.4°K than in electrical resistance measured at 311.5°K. Further, the total change in resistance measured at 77.4°K is an increase, while the change in resistance measured at 311.5°K is a decrease. Thus, Mattheissen's rule does not agree in magnitude, or in sign with results observed in this case.

Concerning the effect of cold work on aging at 490°C (Fig. 14) it is clear that cold work markedly affects the rate of reaction, but does not influence the shape of the aging curves, that is, cold work does not alter the basic aging process but does affect the rate of aging. It is also apparent that little or no recovery of electrical resistance due to cold working occurs with 490°C aging. This result, is consistent with results described in Section IV. The effect of cold work on aging rates at 490°C is summarized below.

Per cent Elongation	Time to Reach Maximum Resistance Measured at 311.5°K	Time to Reach Half Resistance Change Measured at 77.4°K
0	150 hours	55 hours
0.7	60	55
2	85	44
10	25	17

The time to reach one-half the total resistance change measured at 77.4°K is plotted against per cent elongation in Fig. 17.

Electrical resistance vs. log time is plotted for a specimen elongated 3.3 per cent and aged at 475°C in Fig. 12. An anomalous increase in resistance in the first hour indicates an interstitial precipitate. This anomalous increase is not present in the annealed specimen aged at 475°C, Fig. 11. The effect of cold work on the time to reach one-half the total resistance change in specimens aged at 475°C is plotted in Fig. 17. Cold work seems to have been more effective in accelerating aging at 475°C than at 490°C as indicated by the steeper slope of the 475°C line in Fig. 17.

An attempt to explain the behavior described above will be highly qualitative, since no quantitative theory exists relating electrical resistance to microstructure in a two phase age hardenable alloy system. Further, Mattheissen's rule applies to dilute solid solutions, whereas the 25 per cent chromium-iron alloy is a concentrated solid solution.

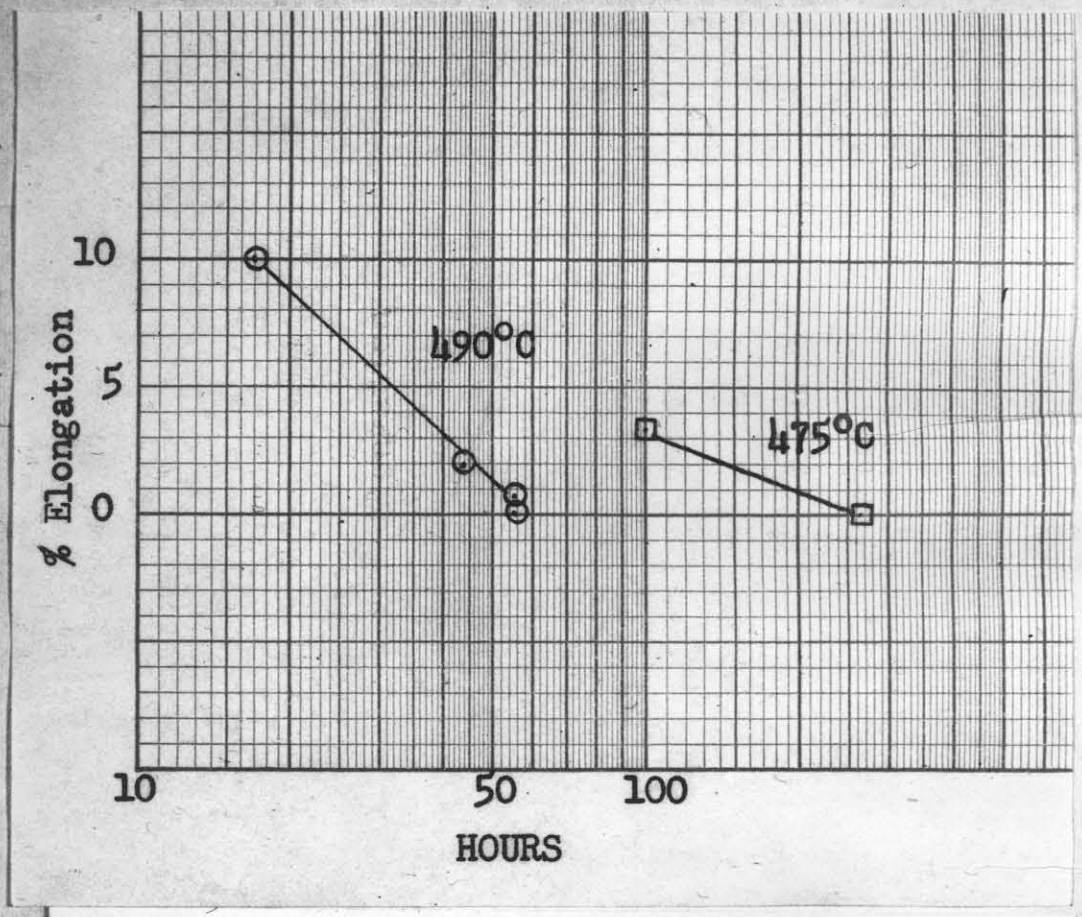

Fig. 17. The effect of cold work on the time to reach one-half the total resistance change measured at 77.4°K with specimens aged at 490°C and at 475°C.

As discussed above, the behavior of electrical resistance measured at 311.5°K can be explained separately on the basis of solid solution depletion and the formation of a coherent precipitate with little lattice disregistry. Similarly, the behavior of electrical resistance measured at 77.4°K can be explained separately on the same basis, with an initial decrease due to solid solution depletion and local nucleation followed by a steady increase due to lattice strain caused by a coherent precipitate formation and growth. However, solid solution depletion effects are never observed to dominate lattice strain effects when resistance measurements are made at 77.4°K. Even in the 525°C aging curves, Fig. 15, maximum resistance is maintained over a large part of the aging period without an ultimate decrease in resistance. Referring again to Fig. 16, it is apparent that the aging curves obtained by measuring electrical resistance at 77.4°K resemble that portion of the theoretical aging curve due to coherent precipitate strain, rather than that portion due to solid solution depletion.

One may hypothesize that lattice strain and coherent precipitate with the magnitude and distribution occurring in this alloy and with these aging conditions provide more electron scattering at 77.4°K than impurity atoms in the matrix lattice provide, particularly since the matrix lattice is not a dilute solid solution of chromium in iron. Conversely, electron scattering at 311.5°K with a much shorter electron mean free path may be more sensitive to solid solution depletion than to coherent precipitate scattering, thus 311.5°K aging curves reach a resistance peak and decrease long before 77.4°K

aging curves reach a resistance peak. This idea may be developed further with regard to the effect of cold work on 311.5°K resistance and 77.4°K resistance.

Cold working presumably strains the lattice uniformly, thus producing a strain on a sub-micro scale of smaller order than nuclei spacing, i.e. dislocation density is high compared to nuclei density. This would predict a larger electrical resistance effect due to cold working on resistance measured at 311.5°K, than on resistance measured at 77.4°K, and this is indeed observed to be the case.

The resistance behavior at 77.4°K as related to resistance behavior at 311.5°K can then be explained on the basis that electron scattering at 77.4°K is more effective from scattering centers with much larger spacing than the scattering centers responsible for resistance effects at 311.5°K.

This observed liquid nitrogen temperature behavior is a strong argument for the existence of a coherent precipitate with little lattice disregistry, since electrical resistance measured at 77.4°K continues to increase even after solid solution depletion effects are apparent in electrical resistance measured at 311.5°K. Thus, the coherent precipitate will continue to grow while maintaining lattice coherency during advanced portions of the aging cycle.

When studying temperature dependent kinetic processes, it is interesting to plot log τ vs. 1/T, where τ is a characteristic time for the reaction at temperature T°K. If the process reaction rate is proportional to $e^{-Q/RT}$, a straight line can be drawn through the points of a log τ vs. 1/T plot, and the slope of the line is Q/R,

thus determining Q, an activation energy for the process. The time to reach maximum electrical resistance measured at 311.5°K, and the time to reach one-half the total change in electrical resistance measured at 77.4°K were chosen as characteristic times for the reaction. In the case of cold worked specimens, activation energy was obtained for specimens elongated 3.3 per cent and then aged at 475°C and 490°C. The data for 3.3 per cent elongation and 490°C aging was taken from Fig. 17 where the effect of cold work on aging kinetics is plotted against per cent elongation.

Activation energy data is plotted in Fig. 18. Electrical resistance data measured at 311.5°K gives an activation energy of 58,000 cal/mol, while electrical resistance data measured at 77.4°K gives an activation energy of 68,000 cal/mol. Both sets of data represent the same aging process, although they may represent two different phases of this process. Furthermore, errors in activation energy data taken in such a limited temperature range are large, and choosing appropriate times for equivalent stages in the process is difficult. Estimated errors are indicated in Fig. 18. The data is best interpreted as indicating an activation energy of 63,000 ± 10,000 cal/mol for the precipitation embrittlement process in annealed 25 per cent chromium-iron specimens.

The activation energy determined for the cold worked specimens is 58,000 cal/mol (Fig. 18), indicating 3.3 per cent elongation does not change the activation energy for precipitation embrittlement within the experimental error.

Results, 550°C to 600°C.

Resistance aging curves for aging temperatures of 550°C, 575°C, and 600°C are shown in Figs. 19, 20, and 21, respectively. Electrical resistance measured at 311.5°K has a very rapid decrease of 27 μohms in less than 0.2 hour at 550°C, remains practically constant (slight increase) for 50 hours aging, then decreases 20 μohms in 2000 hours. Electrical resistance measured at 77.4°K increases 25 μohms in 2 hours, decreases slightly at 25 hours, increases 30 μohms very rapidly at 50 hours, then may decrease slightly with further aging at 550°C, with very scattered data occurring after 50 hours aging.

Aging annealed 25 per cent chromium-iron specimens at 575°C produces a steady decrease of 55 μohms in electrical resistance measured at 311.5°K after 2000 hours. Electrical resistance measured at 77.4°K increases slightly with a peak at 0.2 hour, then decreases steadily 22 μohms at 25 hours aging, a sharp 12 μohms increase occurs at 25 hours followed by a general decrease in resistance.

Aging at 600°C shows a 50 μohm decrease in resistance measured at 311.5°K in 1 hour, followed by small fluctuations about a constant value. Electrical resistance measured at 77.4°K shows a 25 μohm decrease in 0.2 hour followed by fluctuations about an essentially constant value.

Interpretation of Results, 550°C to 600°C.

There is no consistent electrical resistance effect at aging temperatures of 550 to 600°C in 25 per cent chromium-iron which can be related to precipitation embrittlement. Most observed effects can be

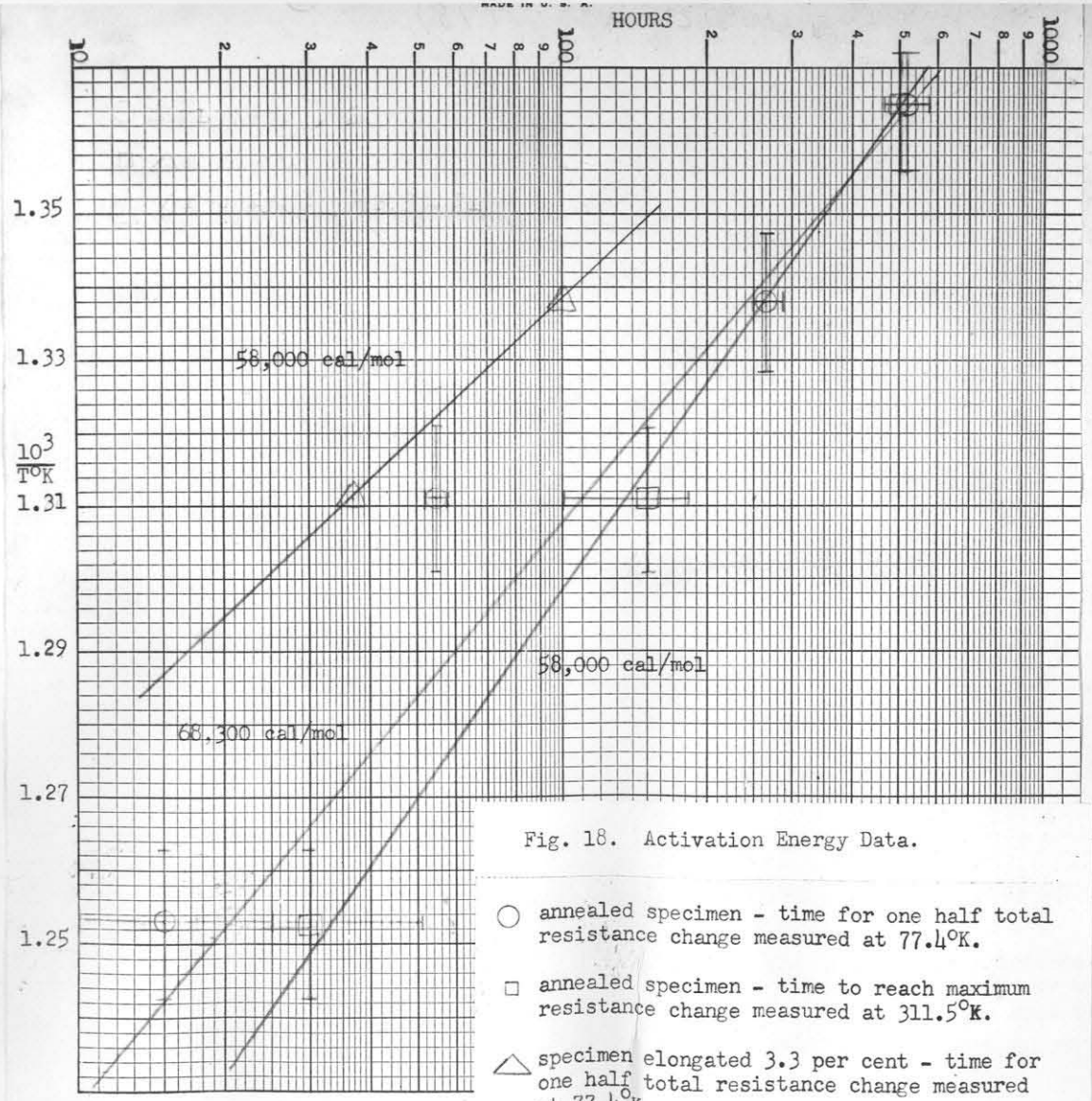

Fig. 18. Activation Energy Data.

○ annealed specimen - time for one half total resistance change measured at 77.4°K.

□ annealed specimen - time to reach maximum resistance change measured at 311.5°K.

△ specimen elongated 3.3 per cent - time for one half total resistance change measured at 77.4°K.

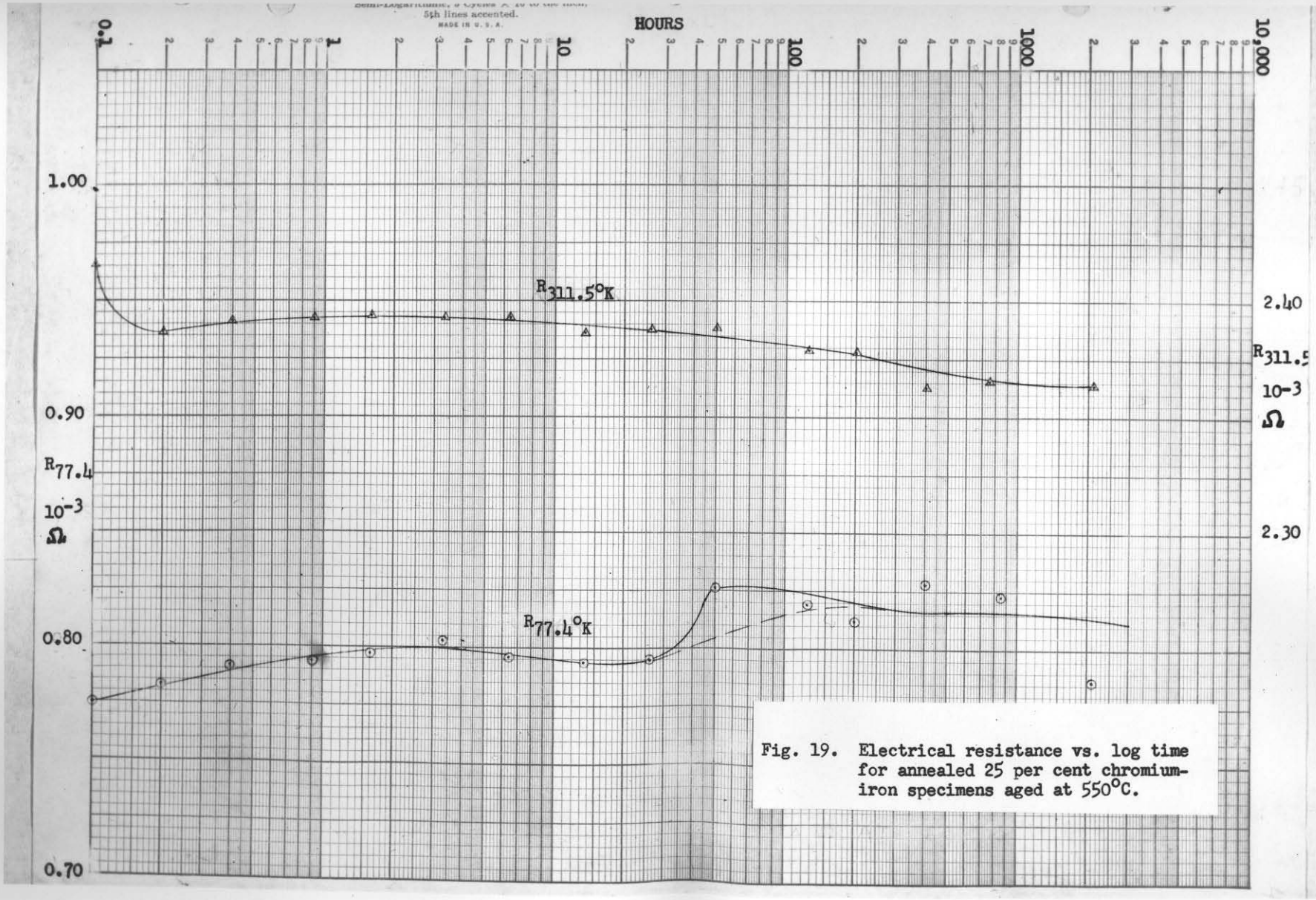

Fig. 19. Electrical resistance vs. log time for annealed 25 per cent chromium-iron specimens aged at 550°C.

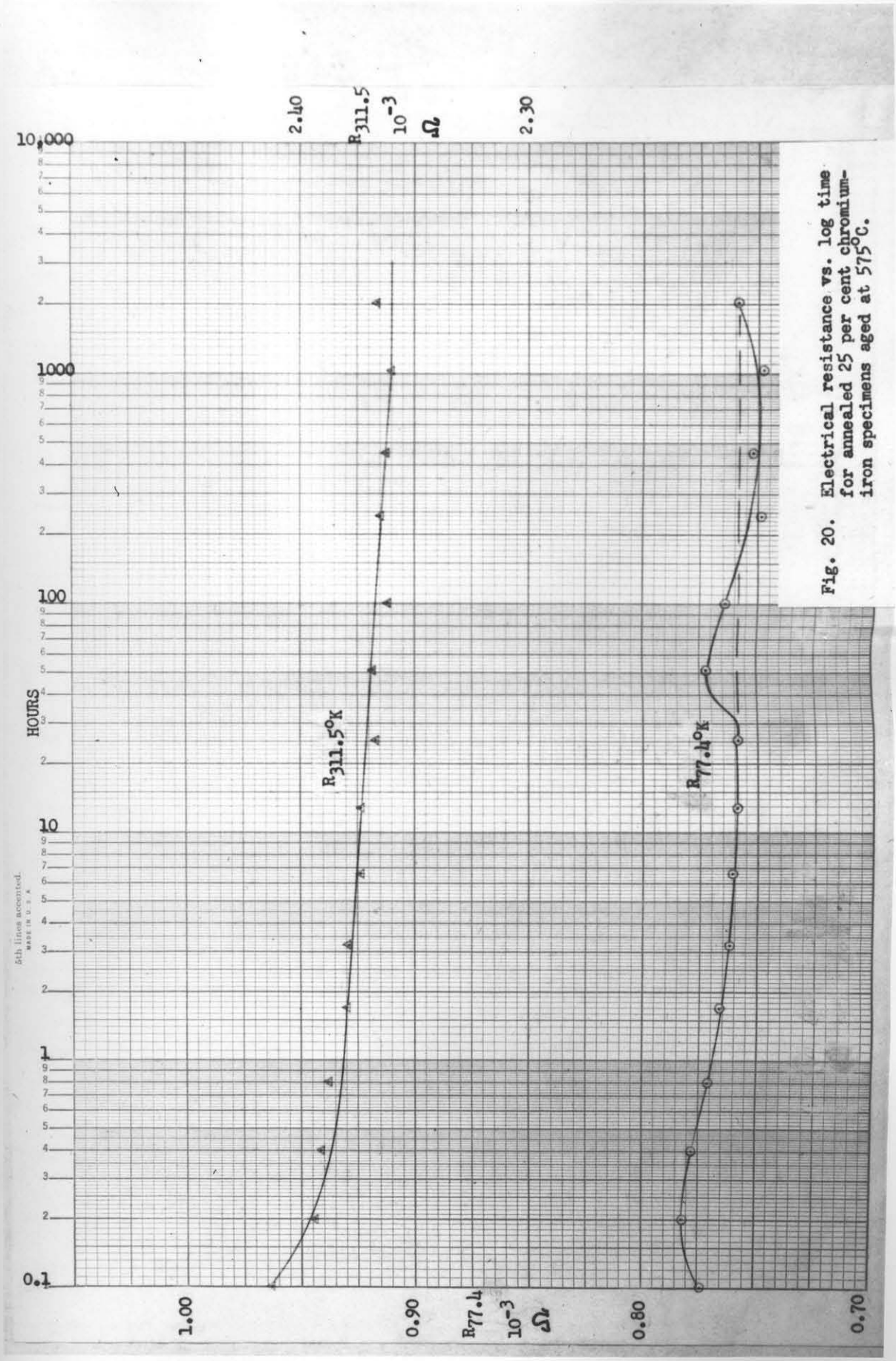

Fig. 20. Electrical resistance vs. log time for annealed 25 per cent chromium-iron specimens aged at 575°C.

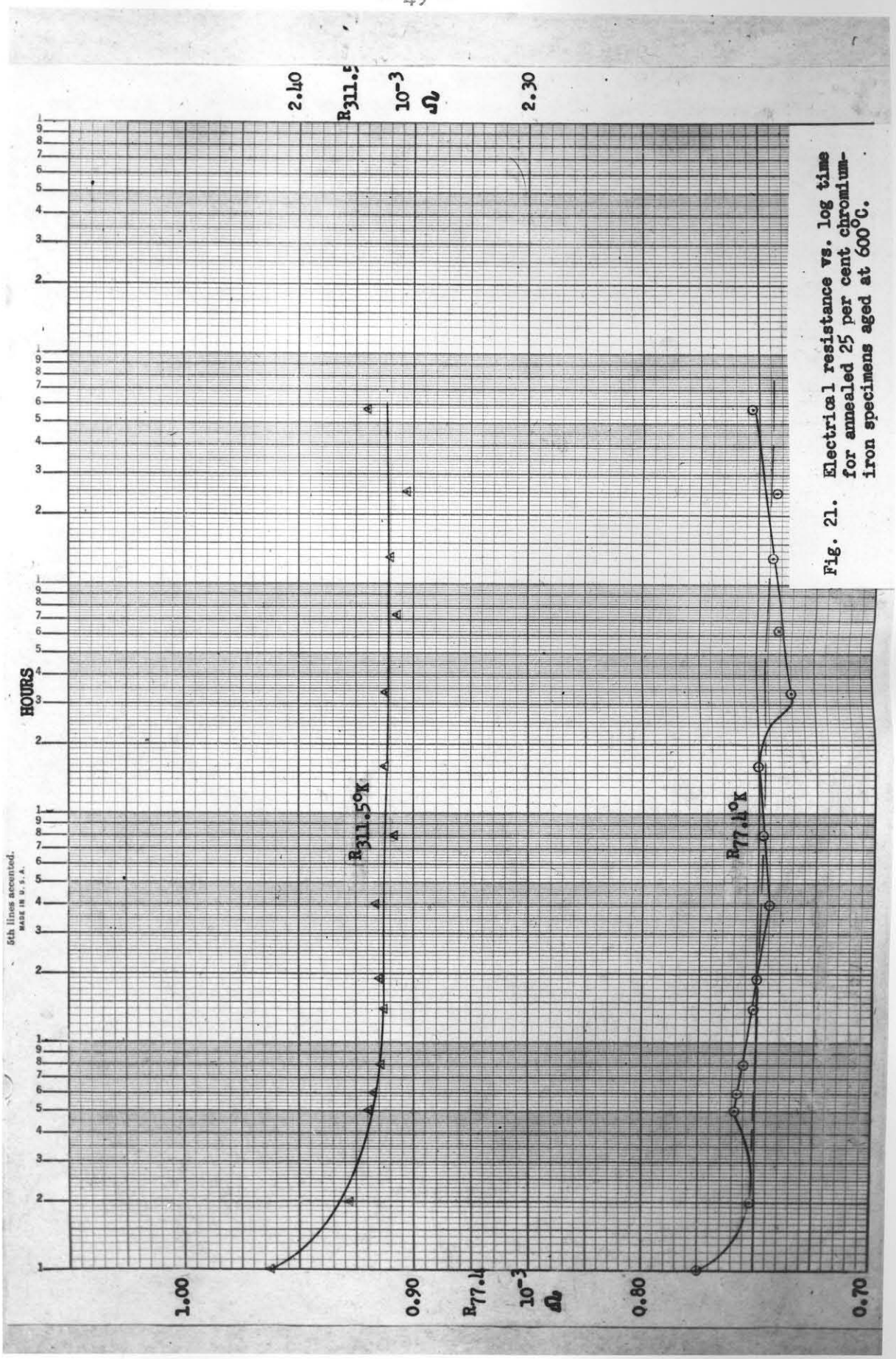

Fig. 21. Electrical resistance vs. log time for annealed 25 per cent chromium-iron specimens aged at 600°C.

explained as relief of residual strains due to quenching, and interstitial impurity effects, and these changes are generally small with respect to changes observed by aging specimens at temperatures of 460°C to 525°C. One effect which is consistent is the rapid change in electrical resistance measured at 77.4°K after 25 hours aging at 550°C, 575°C, and 600°C. This effect is strongest in the case of 550°C aging and decreases with higher aging temperature. The effect may be due to impurity reactions or to gross sigma formation. Gross sigma phase formation has been confirmed in 25 per cent chromium-iron in this investigation, as shown in Section VI. This small amount of sigma phase is formed incoherent with the alpha iron matrix so that little or no lattice strain effect is observed, and is of such small amount that little solid solution depletion occurs.

Any electrical resistance effects recognizable as precipitation embrittlement disappear between 525°C and 550°C. This is consistent with data obtained from experiments described in Section V.

V. THE EFFECT OF AGING ON HARDNESS.

Method and Procedure.

To facilitate obtaining kinetic aging information over a wide range of temperature and chromium composition the following technique was used. Specimens of nominal compositions 19 per cent, 25 per cent, 34 per cent, 42 per cent, and 49 per cent chromium (see Table 1 for exact composition) were rolled into 0.040 in. square wire. These wires were rolled from 0.5 in. diameter bar stock without intermediate annealing for all chromium compositions, resulting in 99.2 per cent reduction of area. The wire specimens were sealed in vacuum in Vycor, and heat treated from the cold worked condition, except for one specimen which was annealed at 1000°C for 1 hour and water quenched.

Specimens were then aged in a 32 in. long gradient furnace which was wound differentially on a 0.5 in. diameter tube to produce a nearly linear thermal gradient from one end of the furnace to the other. Temperature profiles for gradient furnaces 1 and 2 are plotted in Fig. 22 and 23 respectively. Specimens of each alloy were aged for approximately 1 hour, 10 hours, 100 hours, and 1000 hours from 450°C to 650°C in these furnaces. After heat treatment the specimens were marked at approximately 20°C intervals along the square wire. Three or more microhardness measurements were made over a one-quarter inch section at each interval using a Tukon Model LR Microhardness tester, and the results were averaged to give a hardness number for each section and for the corresponding furnace temperature at that section. Hardness measurements were made with a Vickers diamond

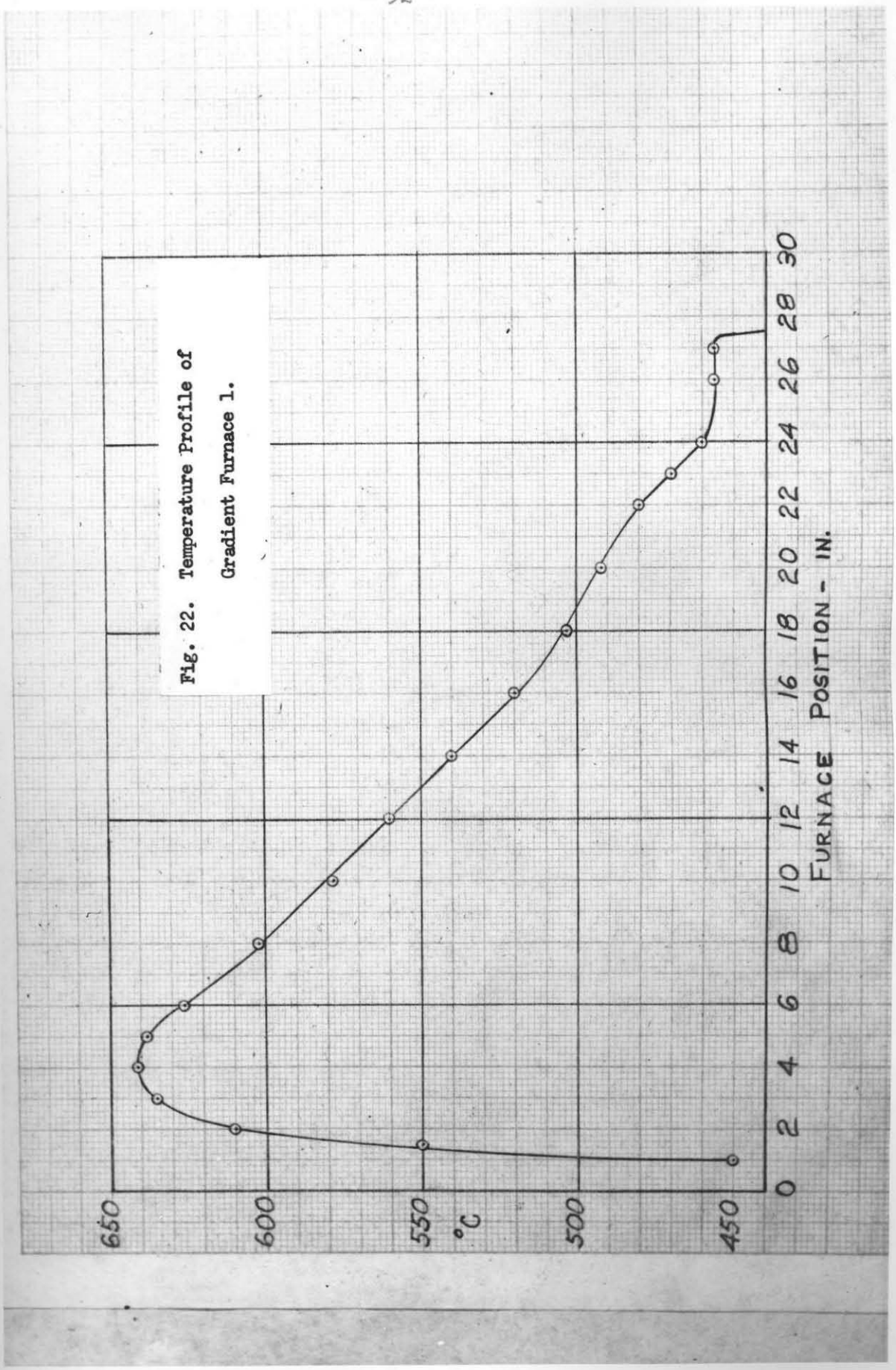

Fig. 22. Temperature Profile of Gradient Furnace 1.

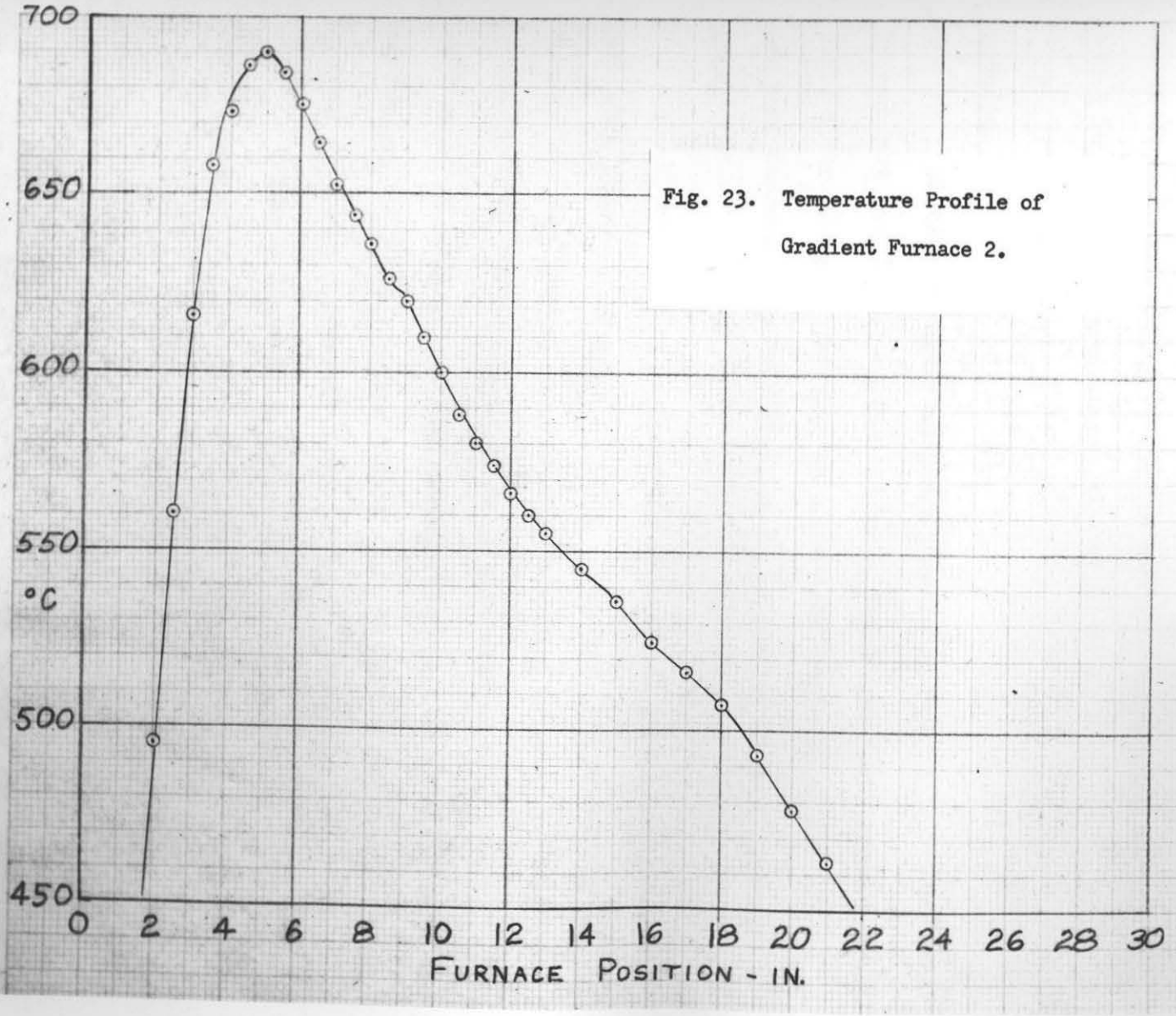

Fig. 23. Temperature Profile of Gradient Furnace 2.

pyramid indenter and a ten kilogram load except for very brittle sections (greater than 700 VHN) where a one kilogram load was necessary in some cases. The hardness results were consistent to ± 5 VHN for hardness up to 400 VHN, ± 20 VHN for hardness between 400 and 600 VHN, and ± 50 VHN for hardness above 600 VHN.

Results.

Results of these tests are plotted in Figs. 24 to 28 for 19 per cent chromium-iron, Fig. 29 to 34 for 25 per cent chromium-iron, Figs. 35 to 39 for 34 per cent chromium-iron, Figs. 40 to 44 for 42 per cent chromium-iron, and Figs. 45 to 49 for 49 per cent chromium-iron.

No increase in hardness was observed in 19 per cent chromium-iron with 1 hour or 10 hours of aging. Recovery from work hardening occurs above 500°C aging temperature. Hardening effects are observable in the 450°C to 525°C temperature range with maximum effect near 500°C with 100 hours aging. The hardness increase is small but definite (10 VHN) at 100 hours and more pronounced (30 VHN) at 900 hours aging. Recovery effects are dominant above 525°C.

Hardness increase in 25 per cent chromium-iron is observable after 10 hours aging in the 450°C to 525°C range. The maximum effect occurs near 500°C, and recovery effects are strong above 525°C. Maximum hardness increase progresses from 20 VHN at 13.2 aging hours to 35 VHN at 100 hours aging to 55 VHN at 910.5 hours. An examination of the 540°C aging curve on the plot of VHN vs. log time, Fig. 33, shows an anomaly in the usual recovery behavior at 100 hours aging time.

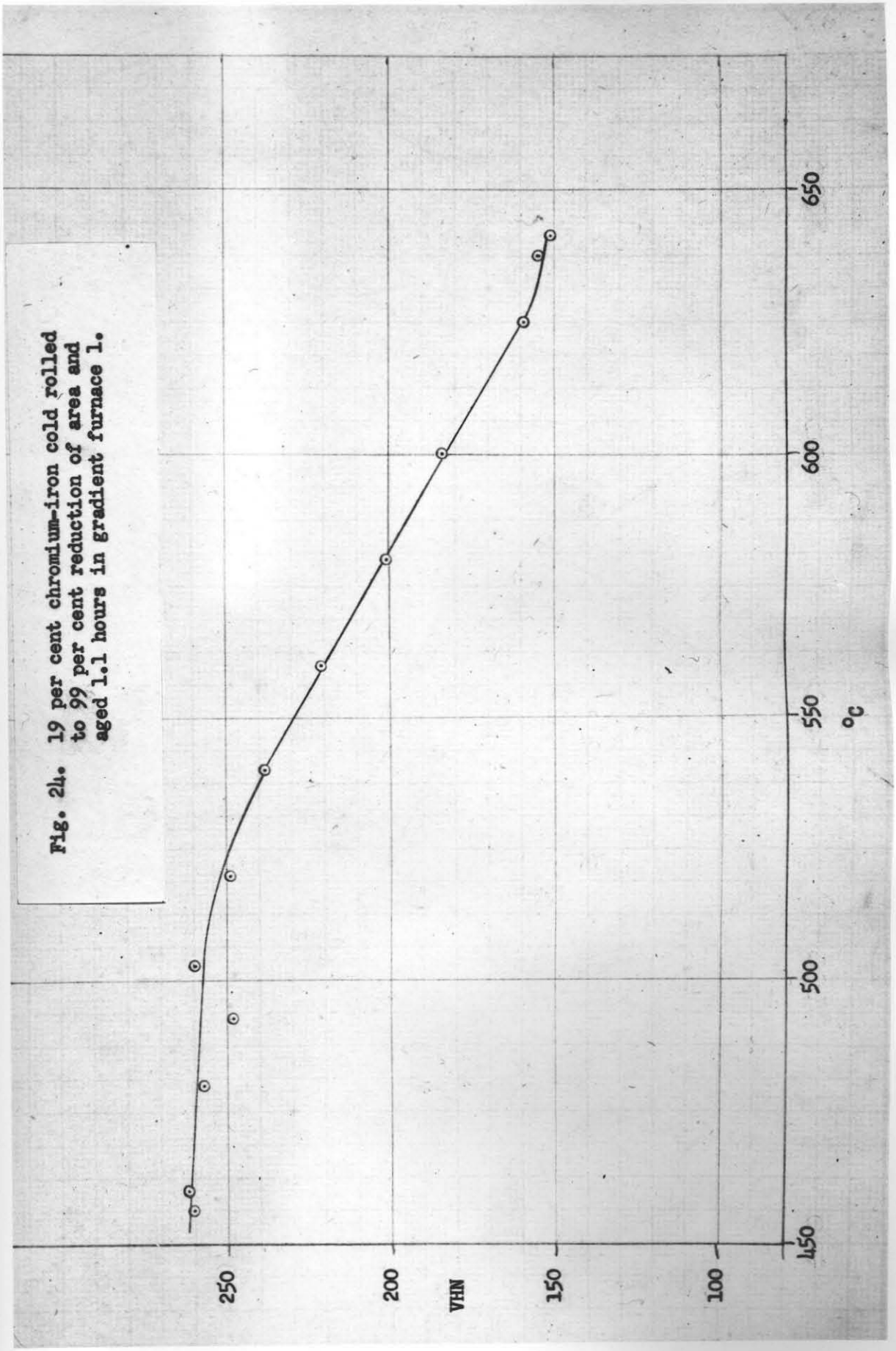

Fig. 24. 19 per cent chromium-iron cold rolled to 99 per cent reduction of area and aged 1.1 hours in gradient furnace 1.

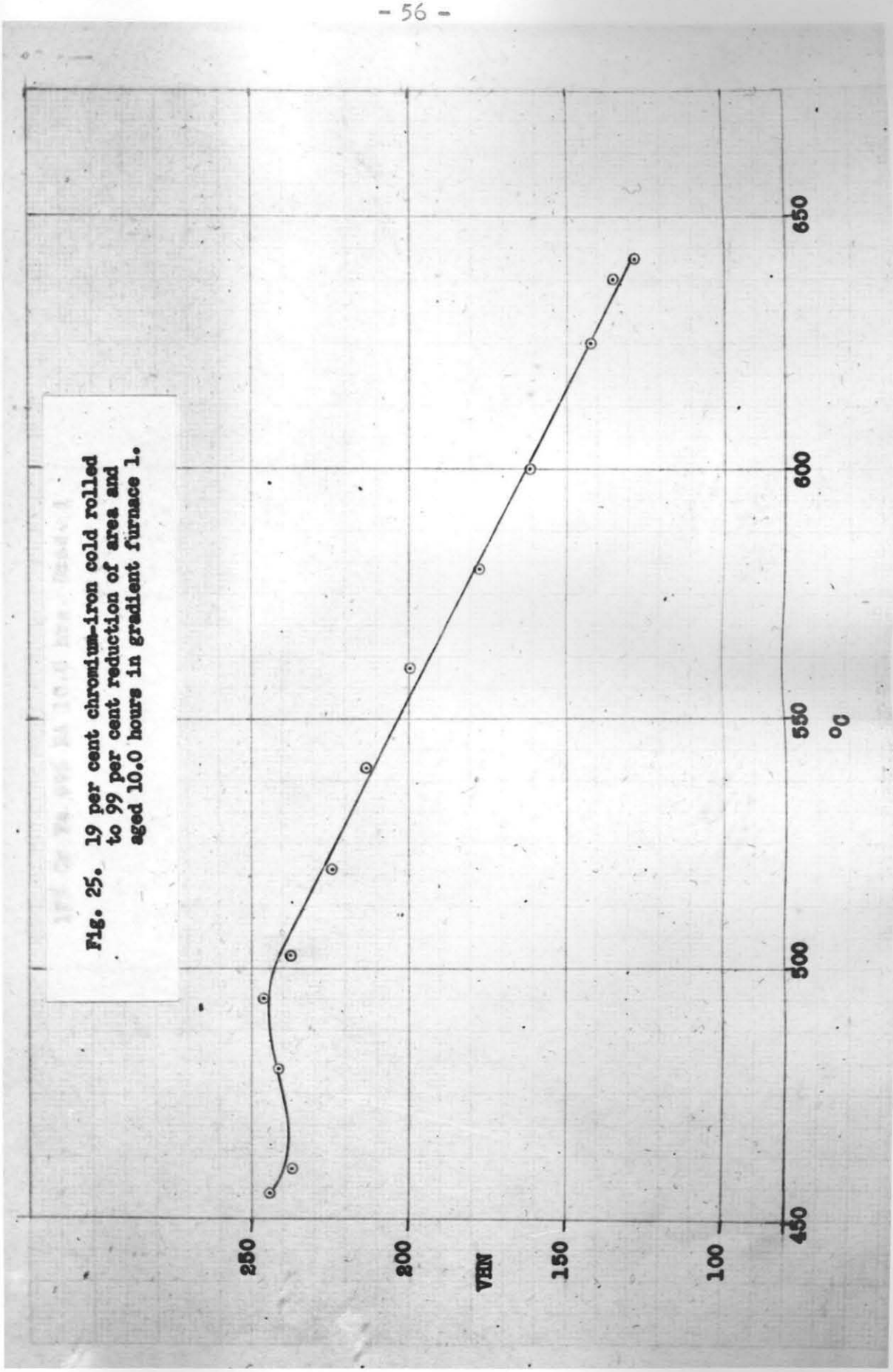

Fig. 25. 19 per cent chromium-iron cold rolled to 99 per cent reduction of area and aged 10.0 hours in gradient furnace 1.

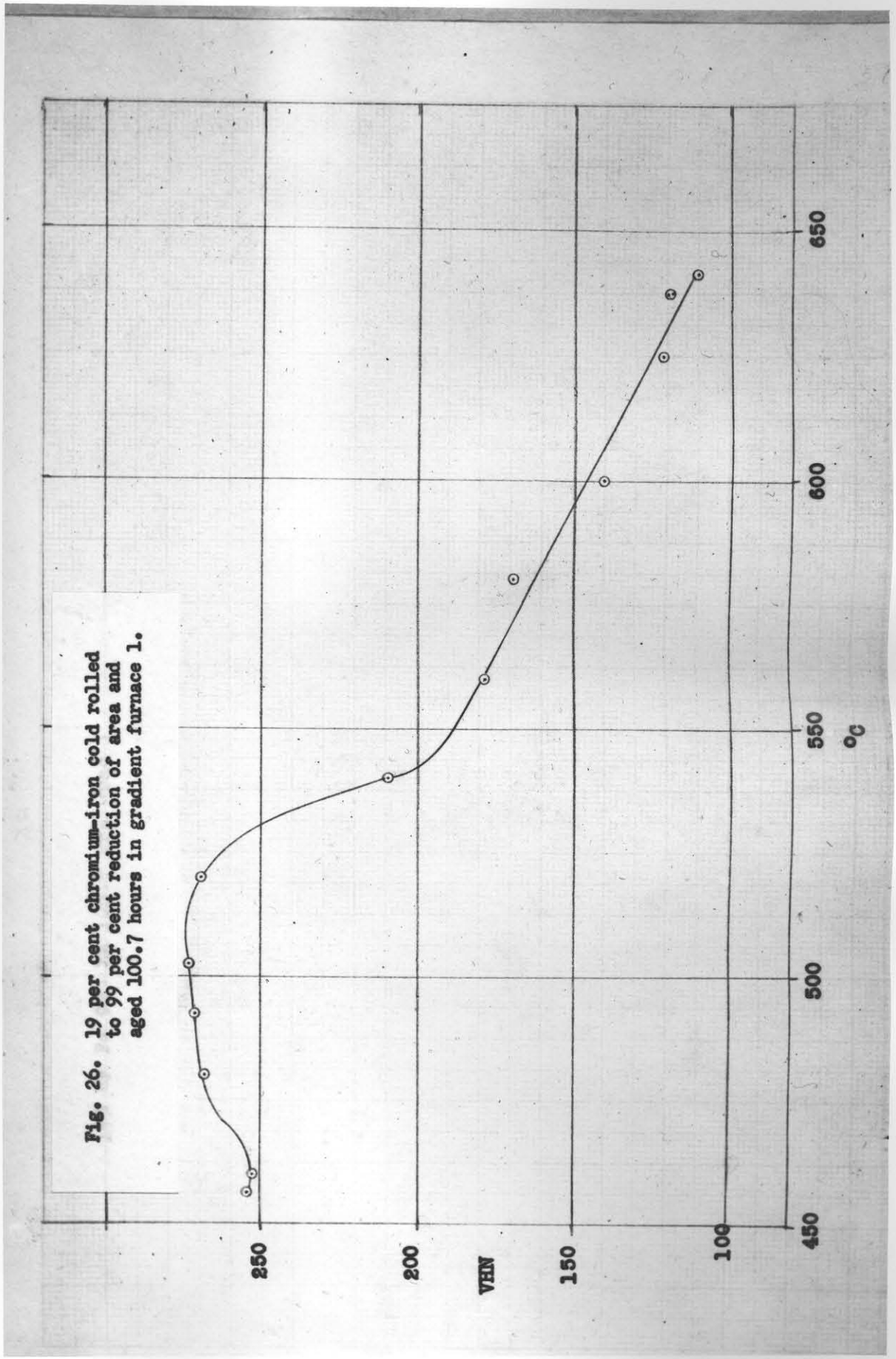

Fig. 26. 19 per cent chromium-iron cold rolled to 99 per cent reduction of area and aged 100.7 hours in gradient furnace 1.

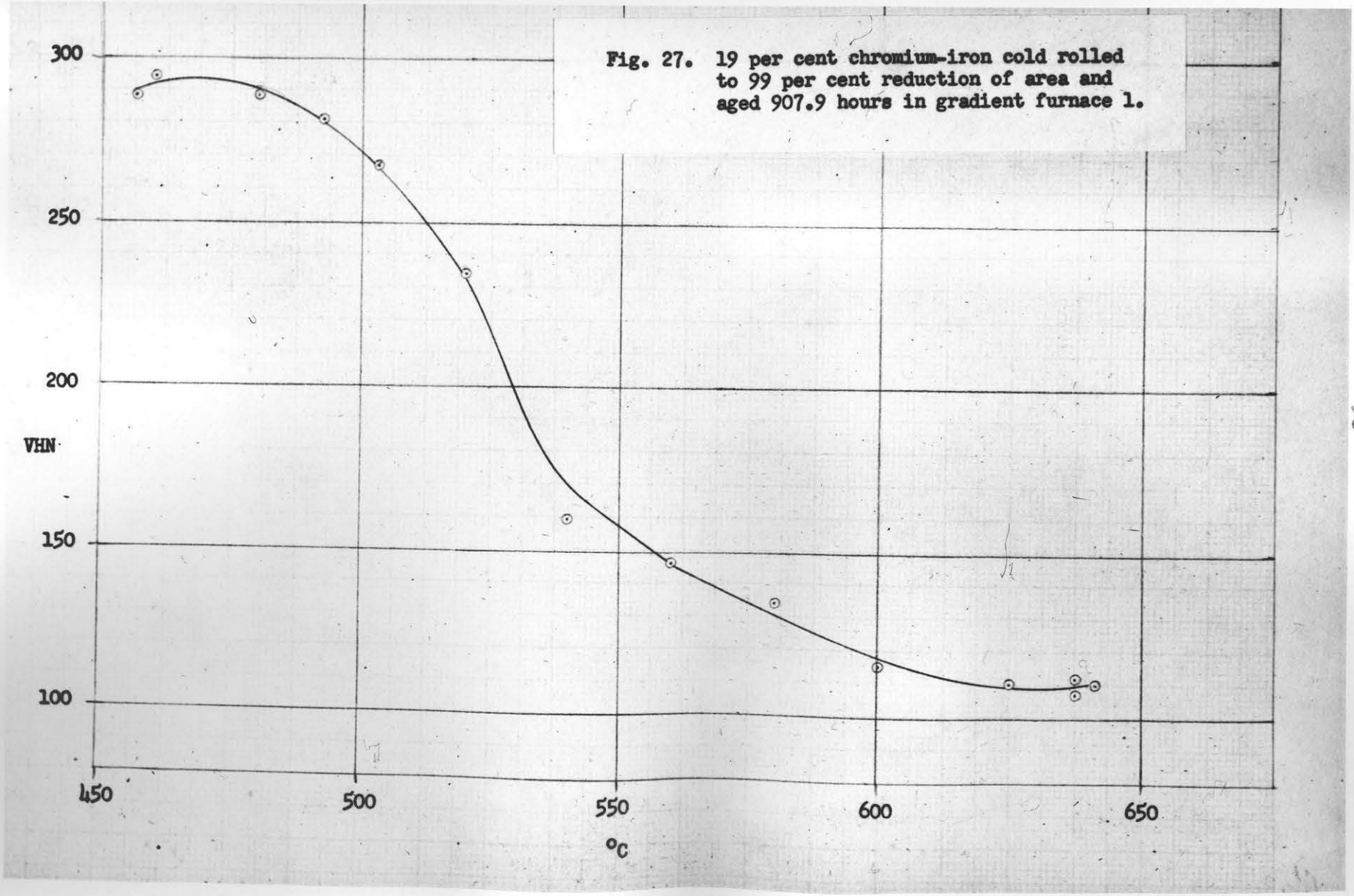

Fig. 27. 19 per cent chromium-iron cold rolled to 99 per cent reduction of area and aged 907.9 hours in gradient furnace 1.

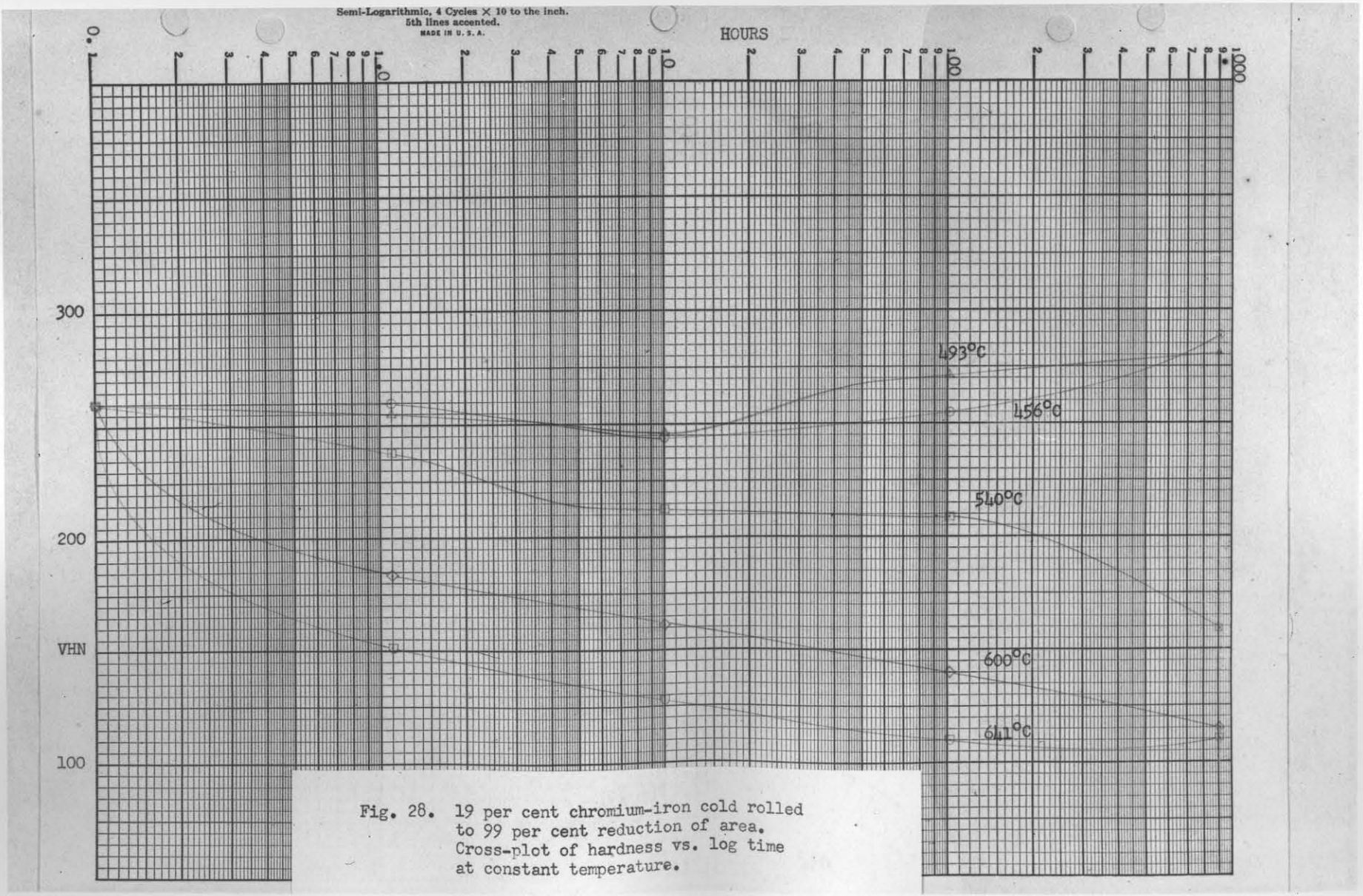

Fig. 28. 19 per cent chromium-iron cold rolled to 99 per cent reduction of area. Cross-plot of hardness vs. log time at constant temperature.

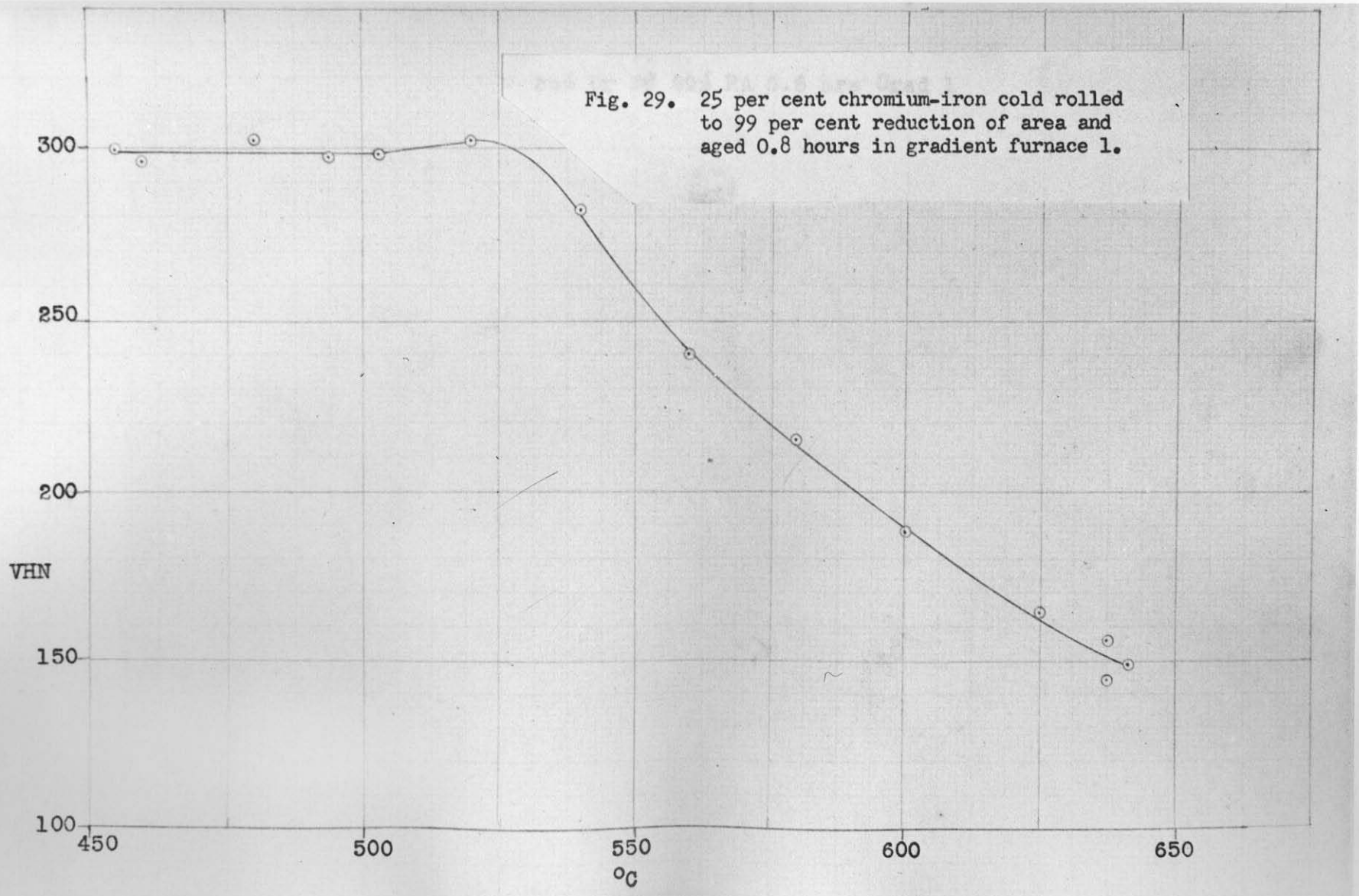

Fig. 29. 25 per cent chromium-iron cold rolled to 99 per cent reduction of area and aged 0.8 hours in gradient furnace 1.

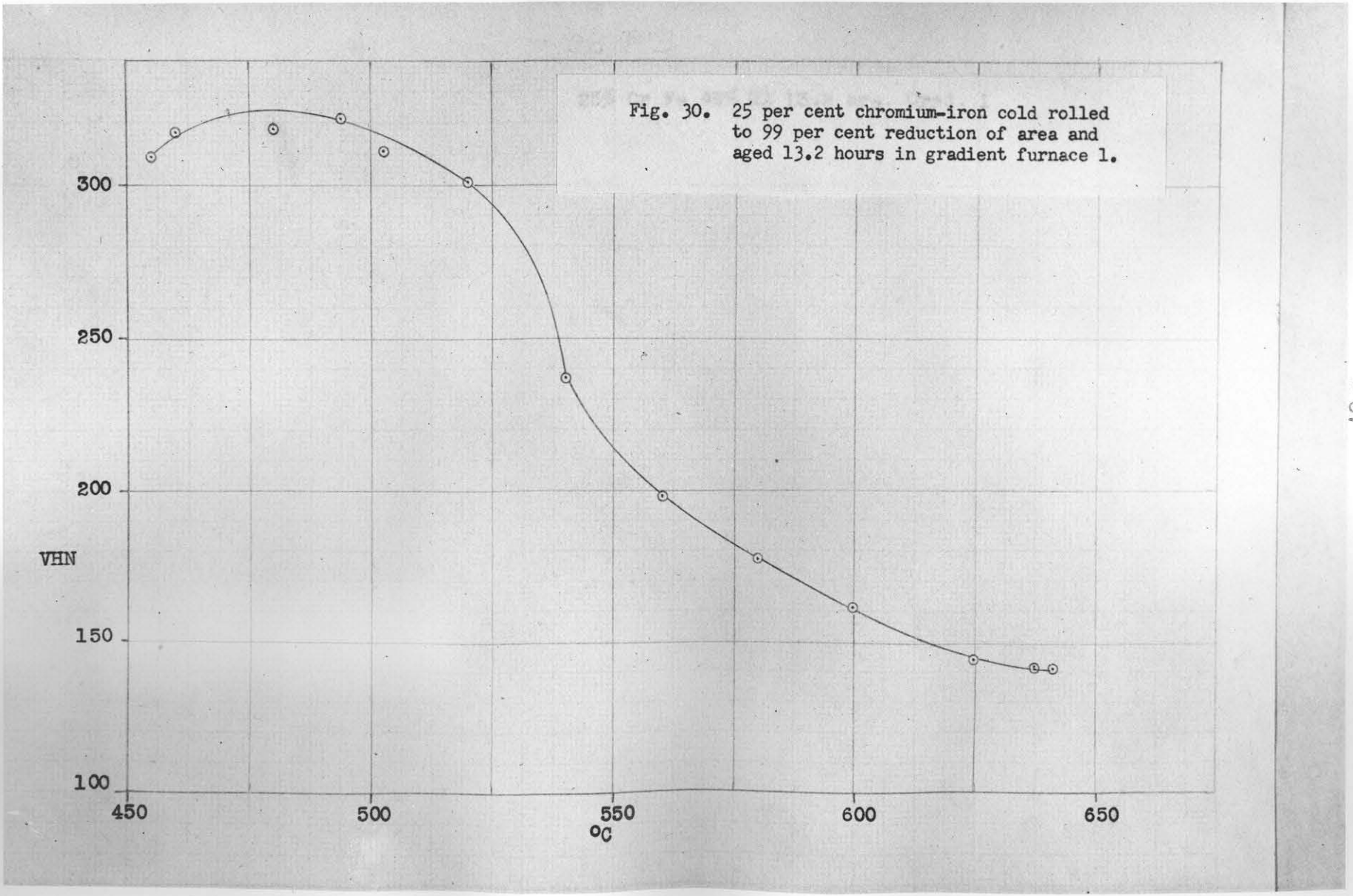

Fig. 30. 25 per cent chromium-iron cold rolled to 99 per cent reduction of area and aged 13.2 hours in gradient furnace 1.

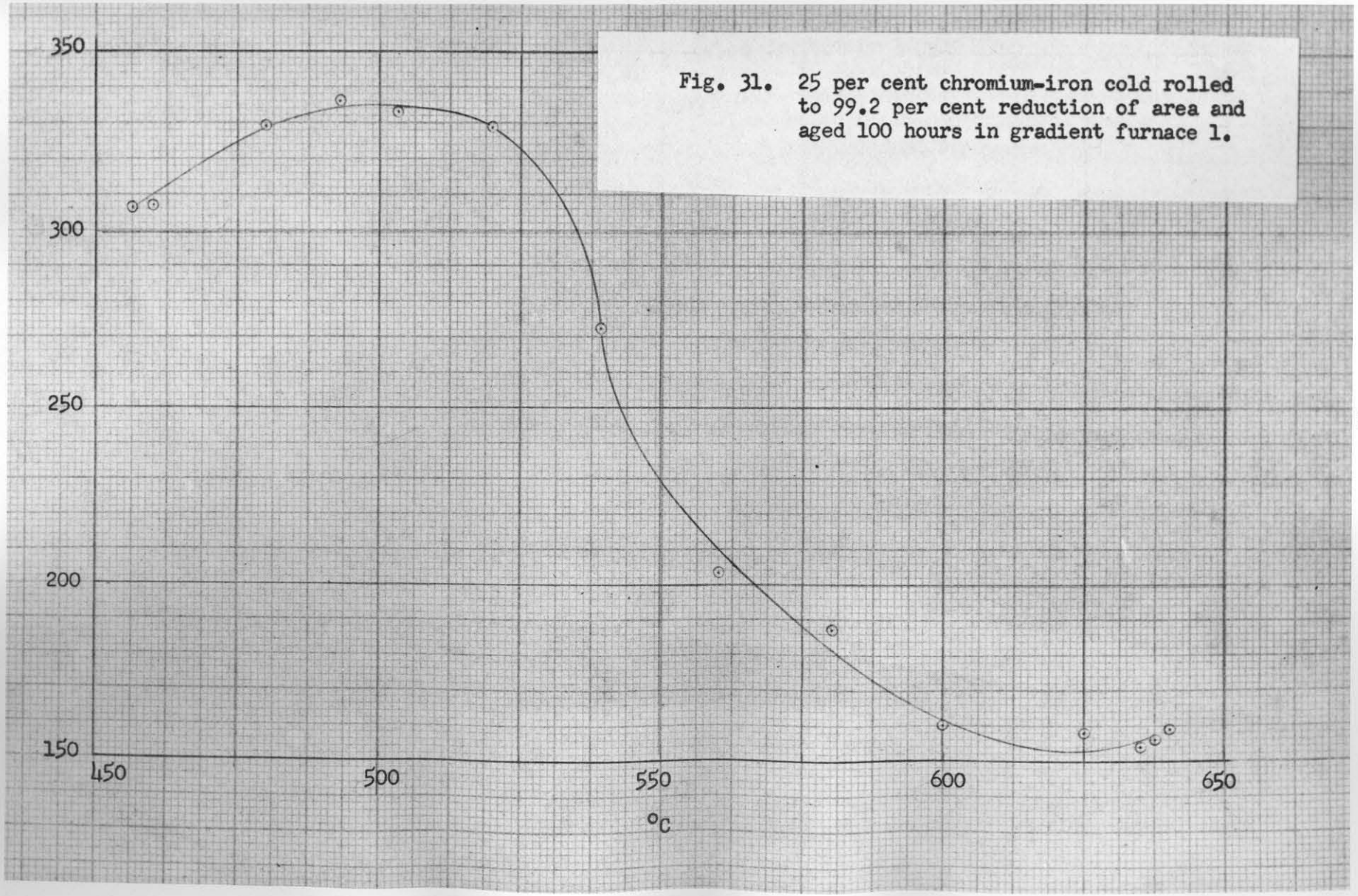

Fig. 31. 25 per cent chromium-iron cold rolled to 99.2 per cent reduction of area and aged 100 hours in gradient furnace 1.

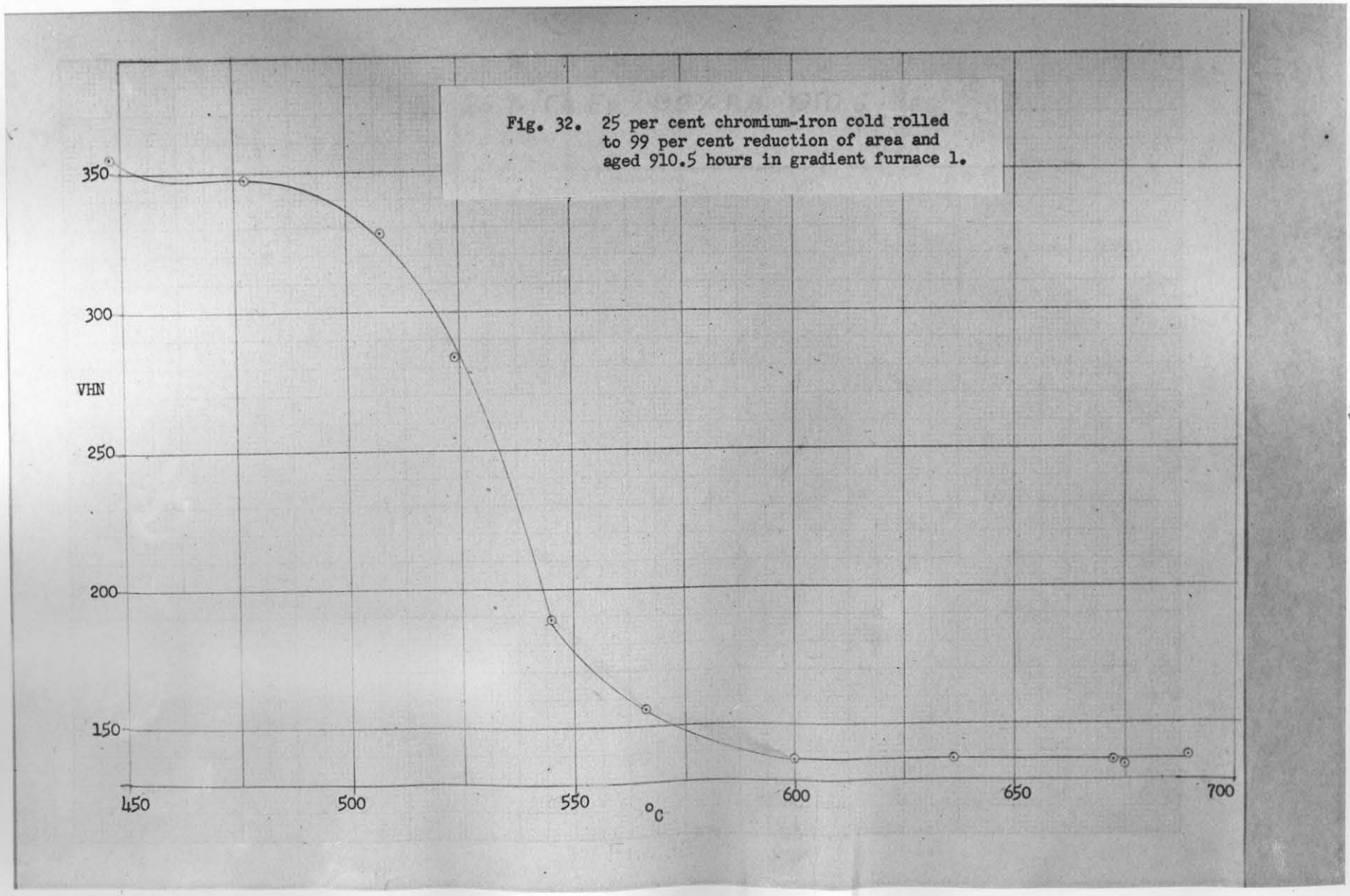

Fig. 32. 25 per cent chromium-iron cold rolled to 99 per cent reduction of area and aged 910.5 hours in gradient furnace 1.

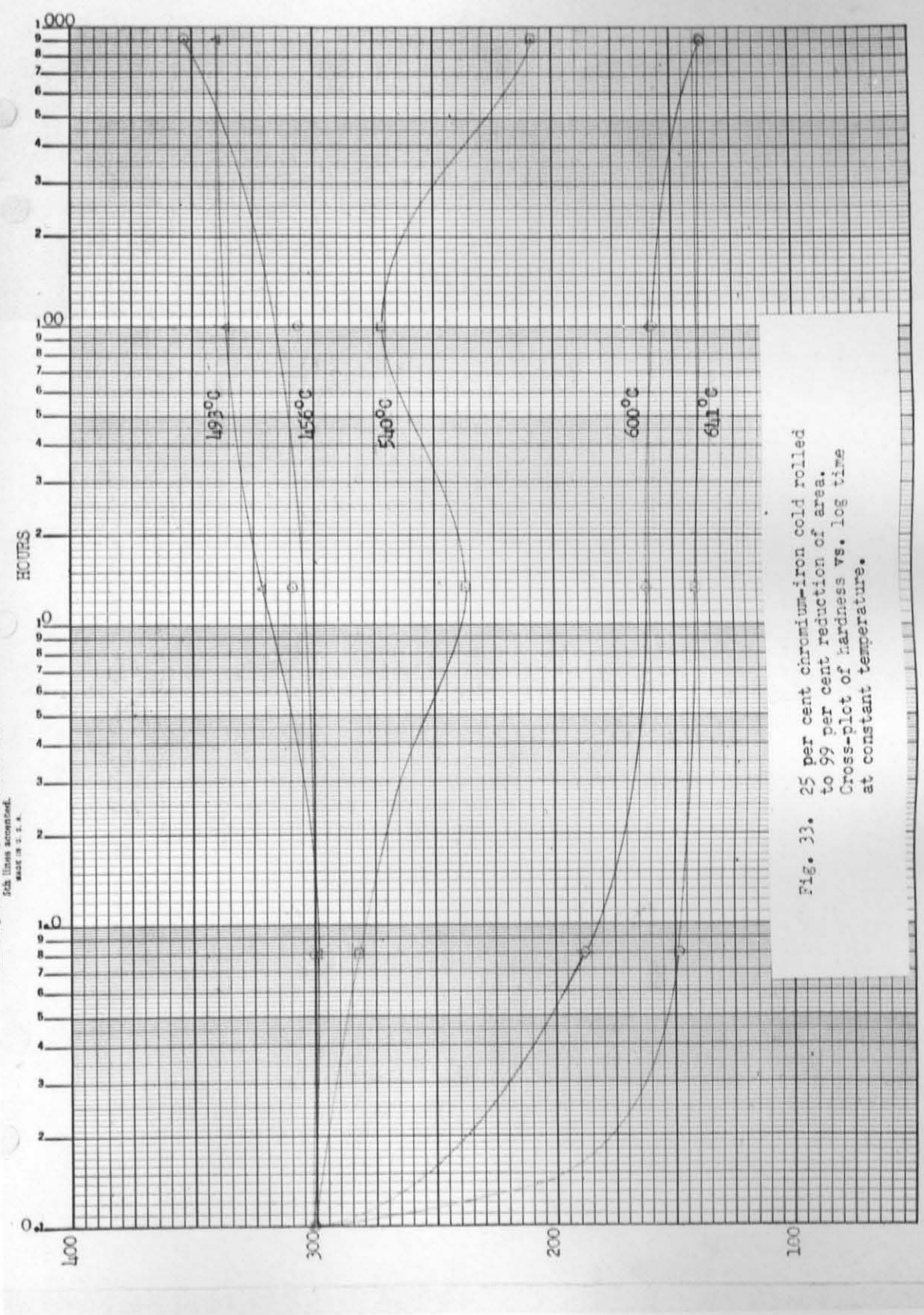

Fig. 33. 25 per cent chromium-iron cold rolled to 99 per cent reduction of area. Cross-plot of hardness vs. log time at constant temperature.

Fig. 34. 25 per cent chromium-iron annealed and then aged 97.5 hours in gradient furnace 1.

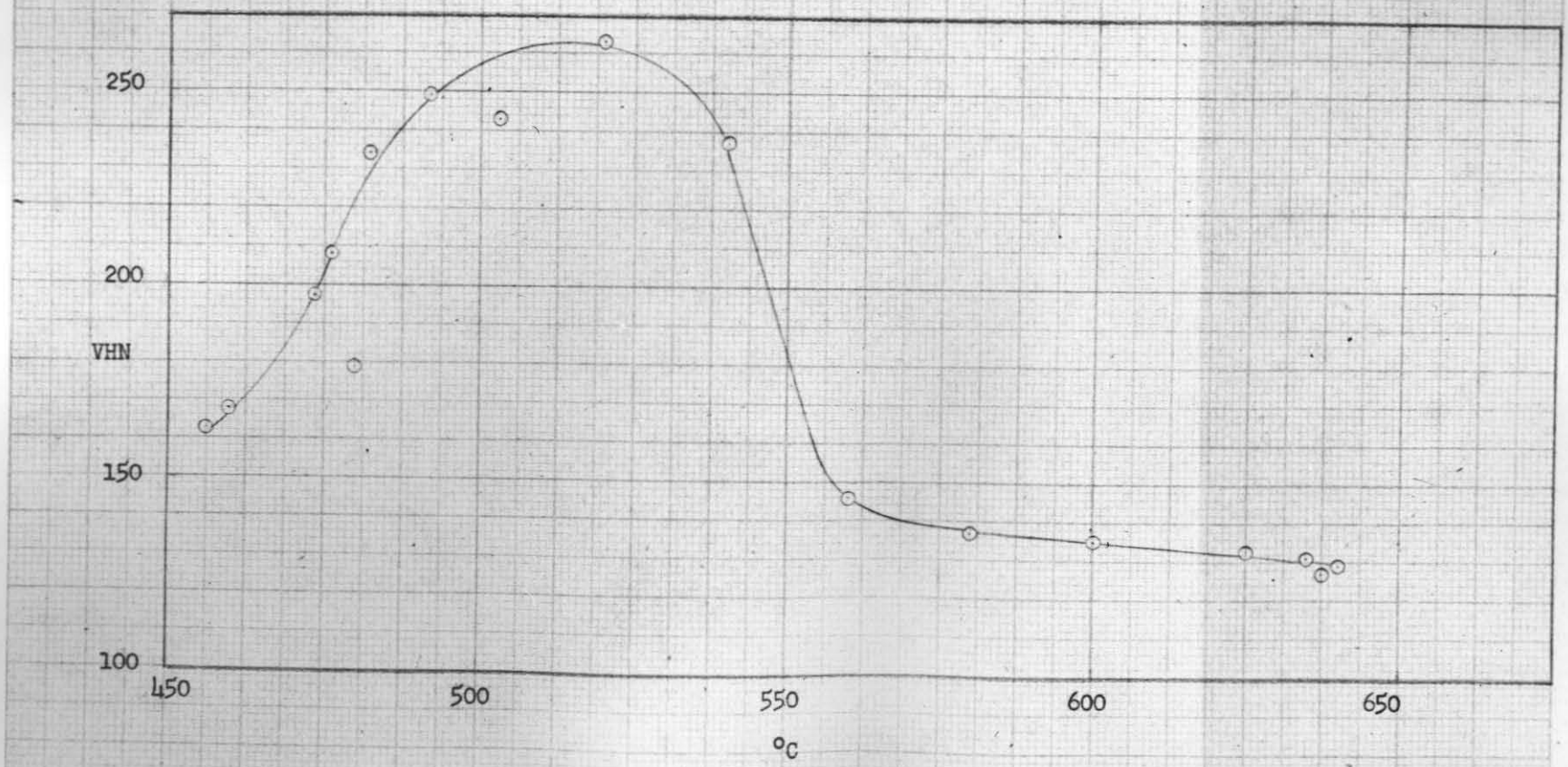

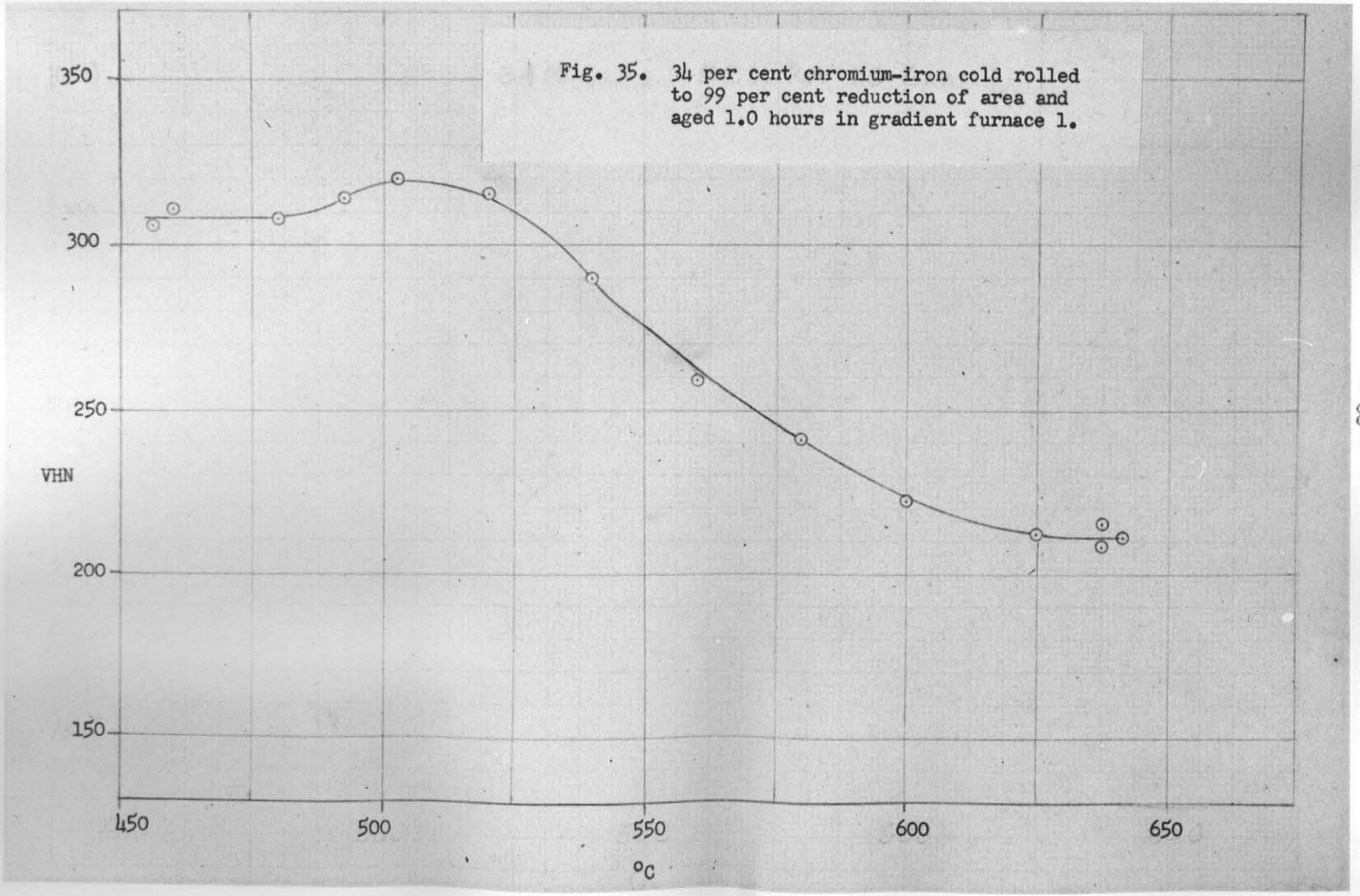

Fig. 35. 34 per cent chromium-iron cold rolled to 99 per cent reduction of area and aged 1.0 hours in gradient furnace 1.

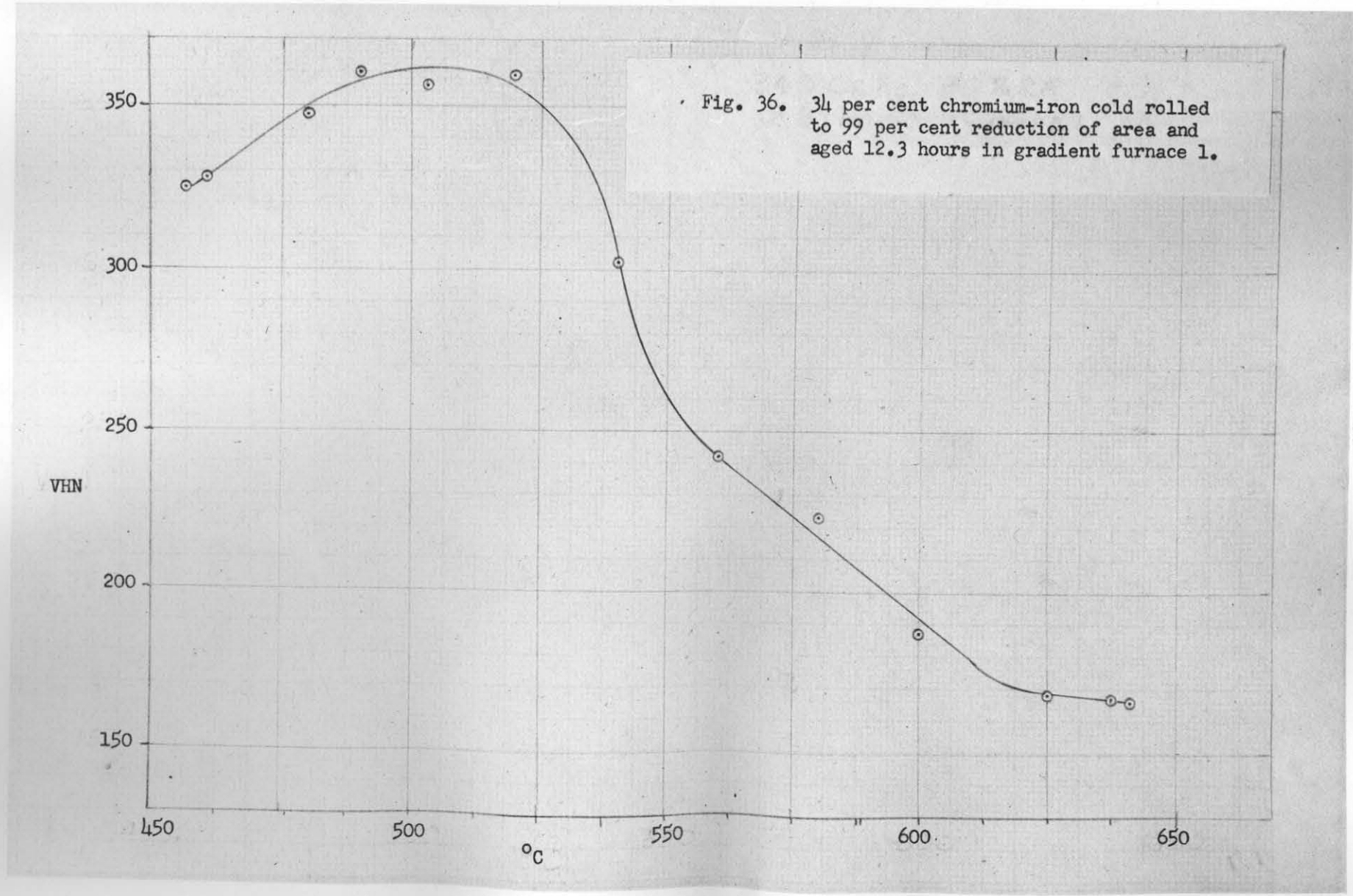

Fig. 36. 34 per cent chromium-iron cold rolled to 99 per cent reduction of area and aged 12.3 hours in gradient furnace 1.

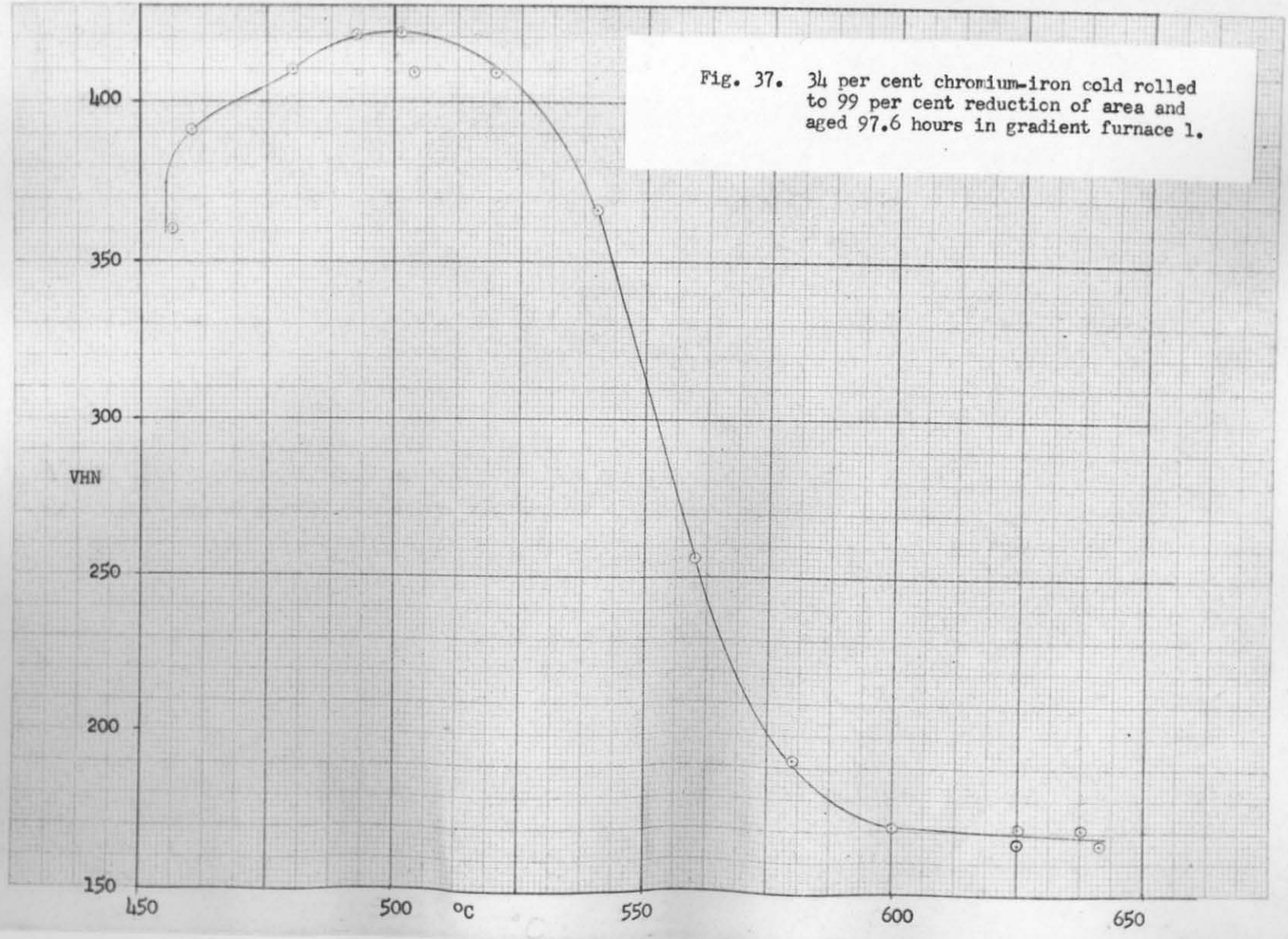

Fig. 37. 3½ per cent chromium-iron cold rolled to 99 per cent reduction of area and aged 97.6 hours in gradient furnace 1.

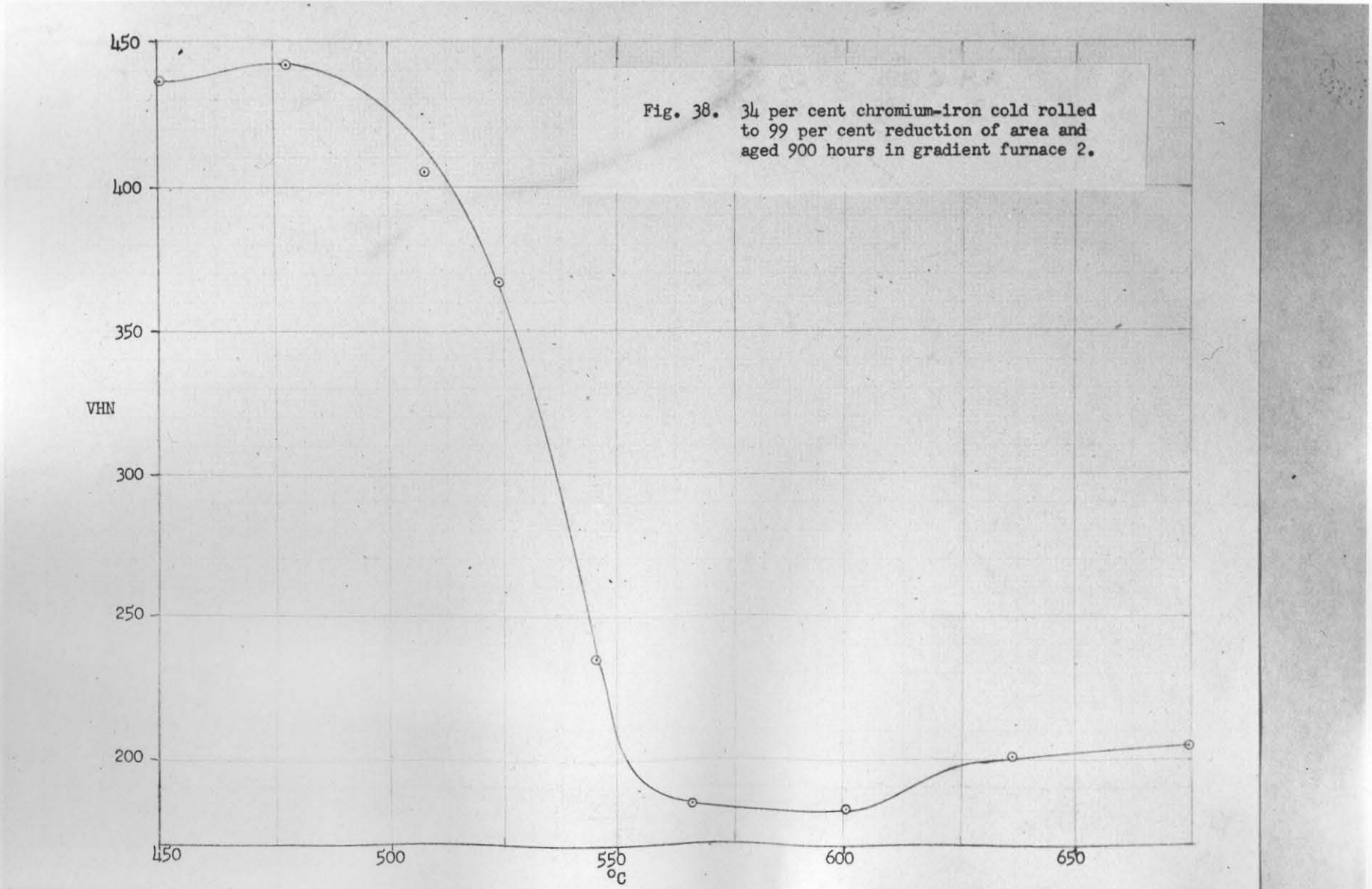

Fig. 38. 34 per cent chromium-iron cold rolled to 99 per cent reduction of area and aged 900 hours in gradient furnace 2.

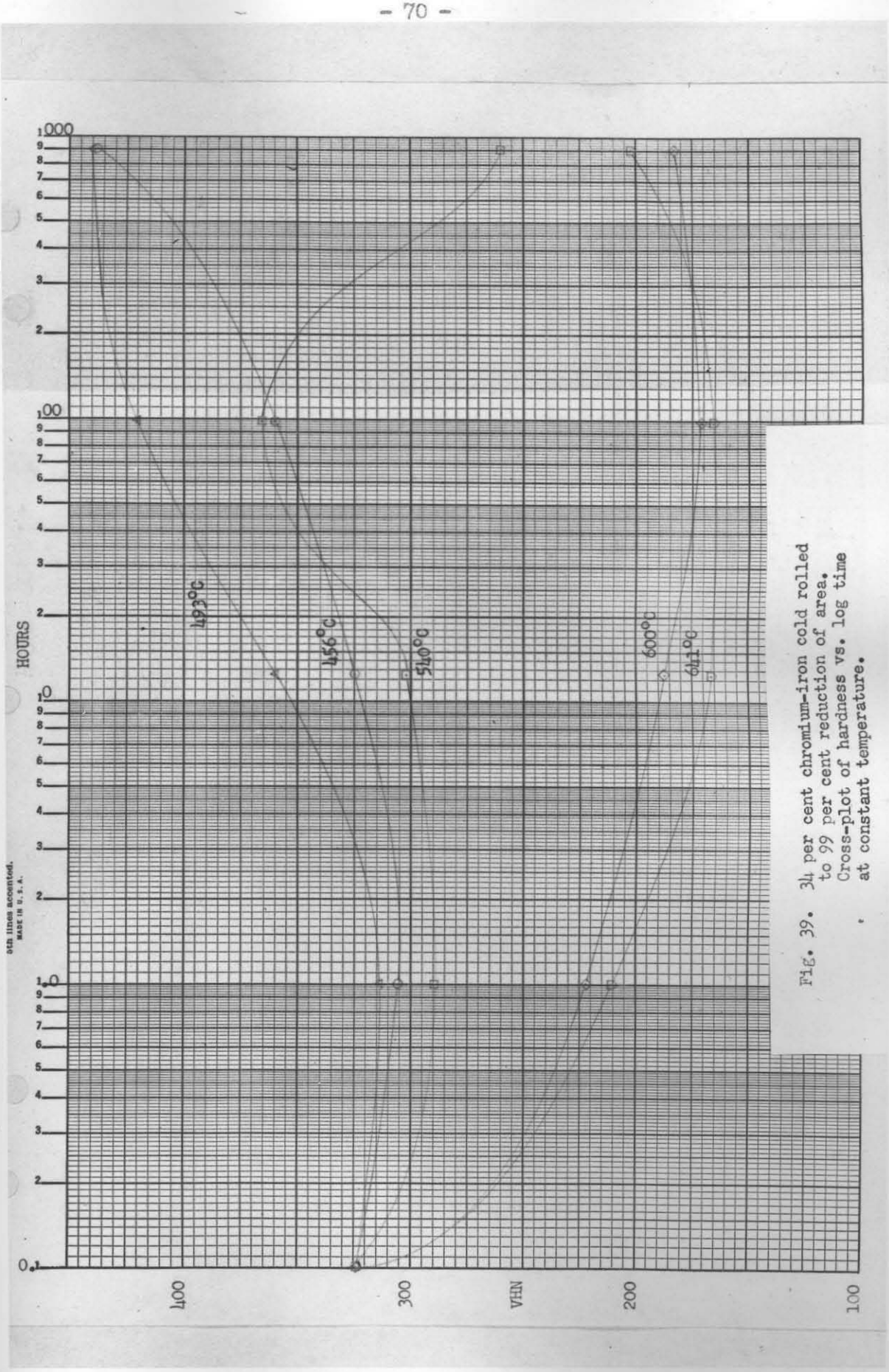

Fig. 39. 34 per cent chromium-iron cold rolled to 99 per cent reduction of area. Cross-plot of hardness vs. log time at constant temperature.

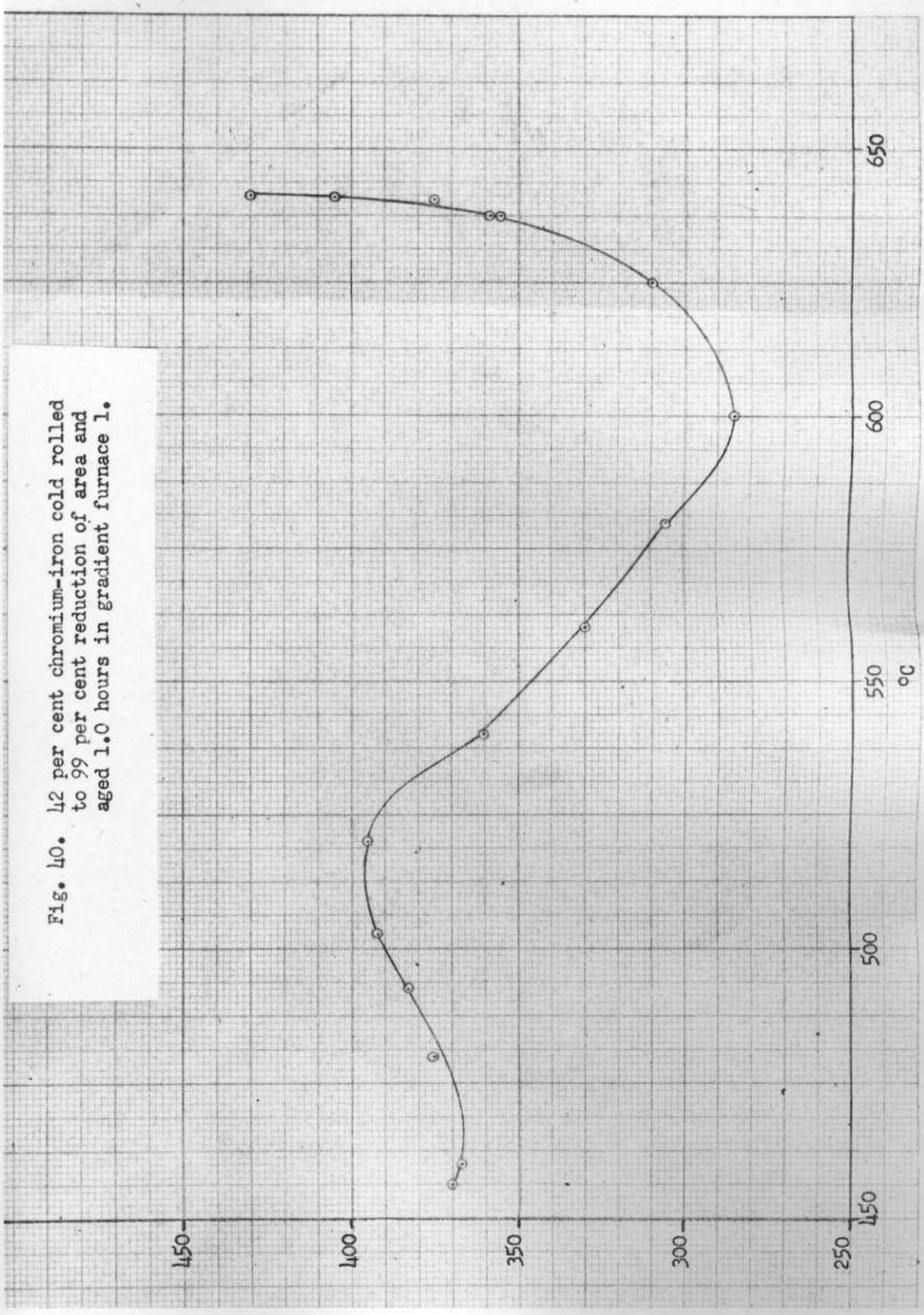

Fig. 40. 42 per cent chromium-iron cold rolled to 99 per cent reduction of area and aged 1.0 hours in gradient furnace 1.

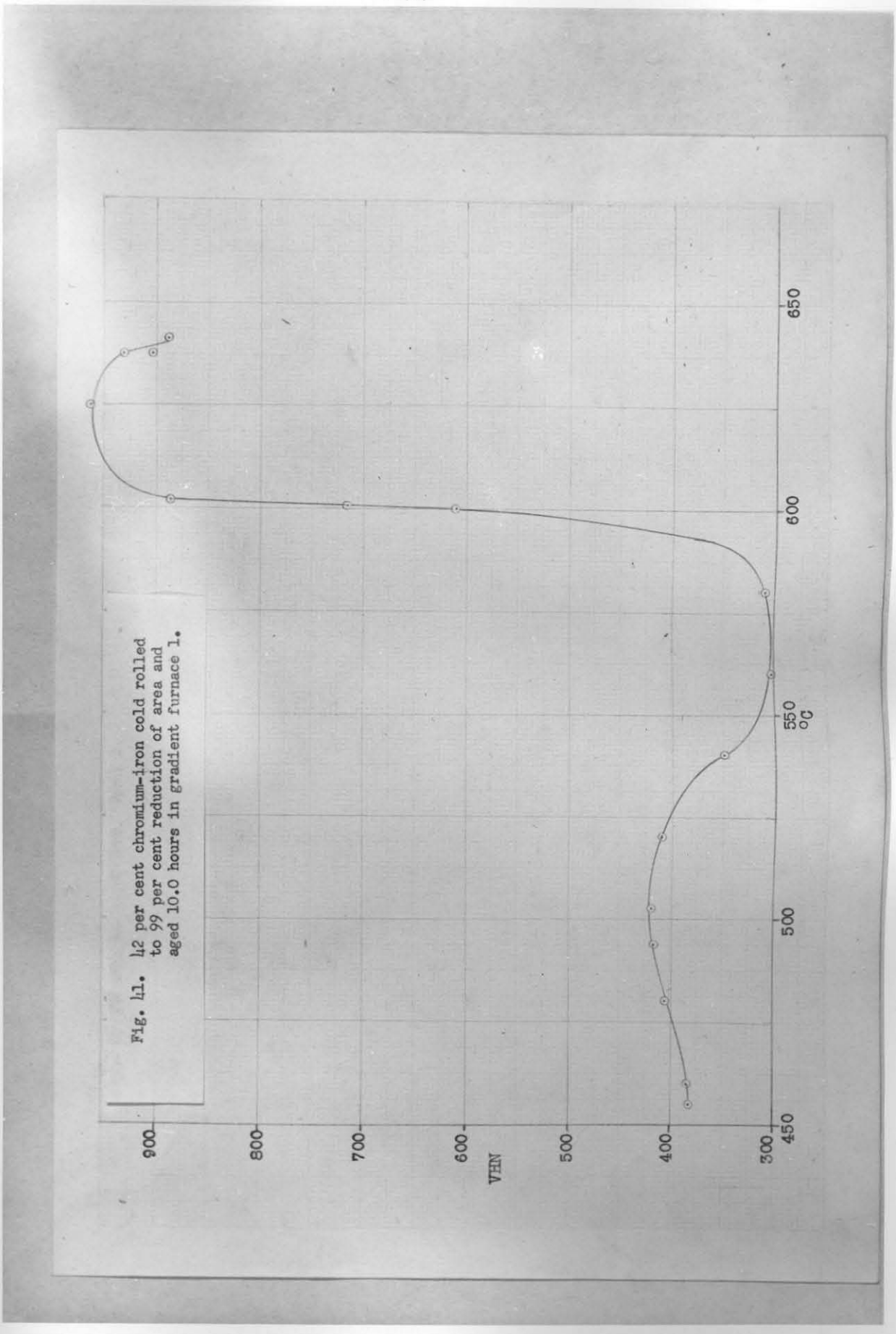

Fig. 41. 42 per cent chromium-iron cold rolled to 99 per cent reduction of area and aged 10.0 hours in gradient furnace 1.

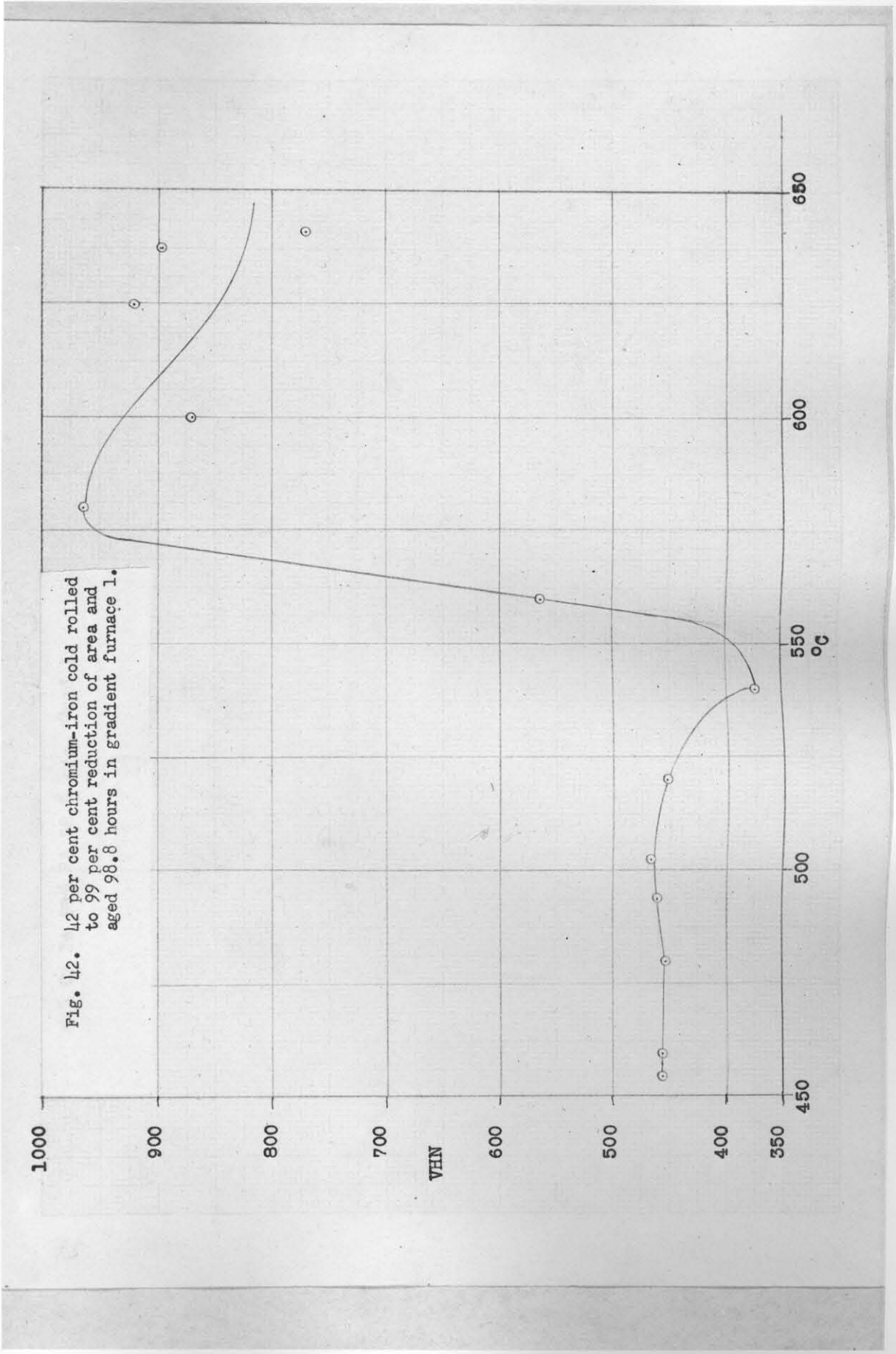

Fig. 42. 42 per cent chromium-iron cold rolled to 99 per cent reduction of area and aged 98.8 hours in gradient furnace 1.

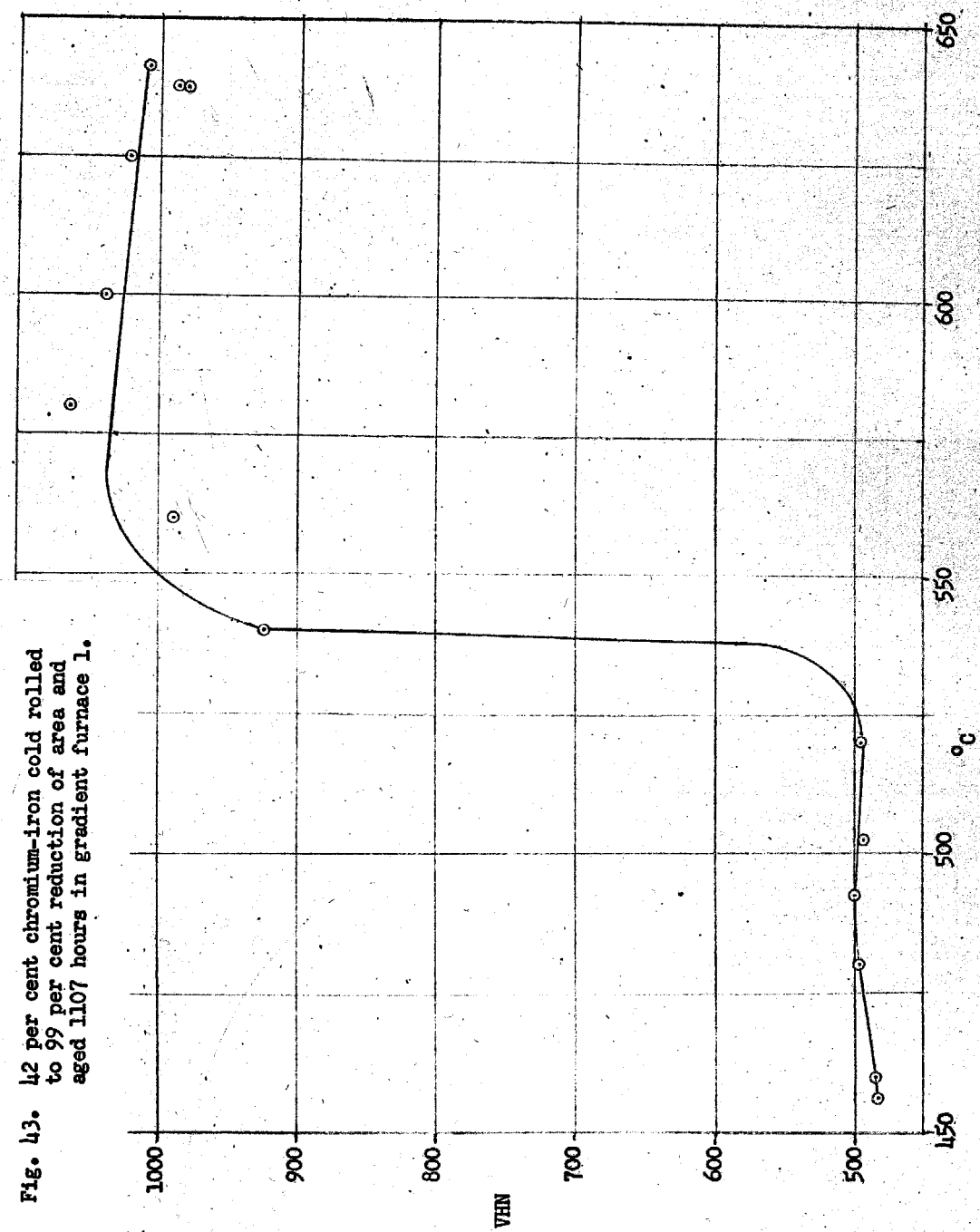

Fig. 43. 42 per cent chromium-iron cold rolled to 99 per cent reduction of area and aged 1107 hours in gradient furnace 1.

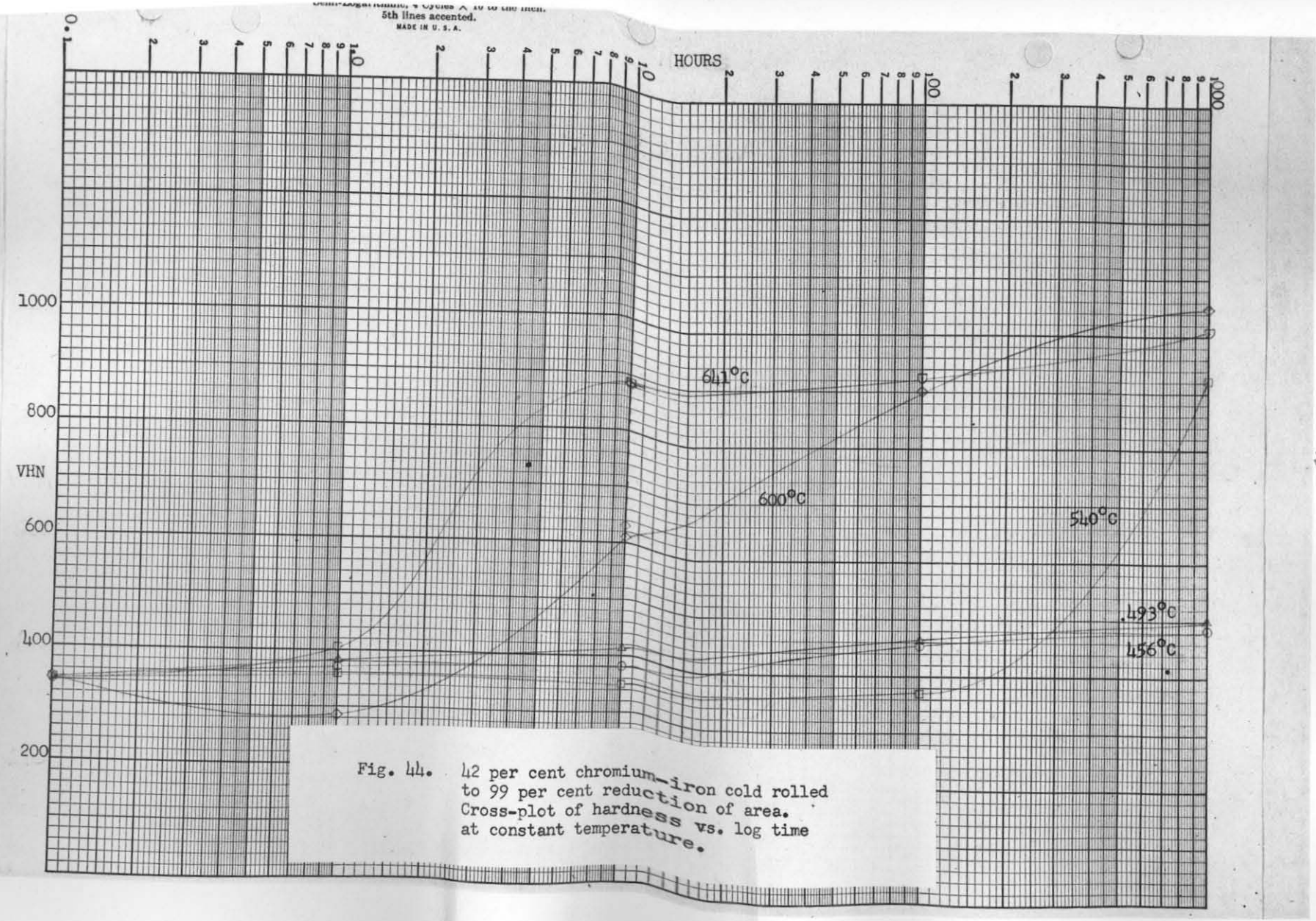

Fig. 44. 42 per cent chromium-iron cold rolled to 99 per cent reduction of area. Cross-plot of hardness vs. log time at constant temperature.

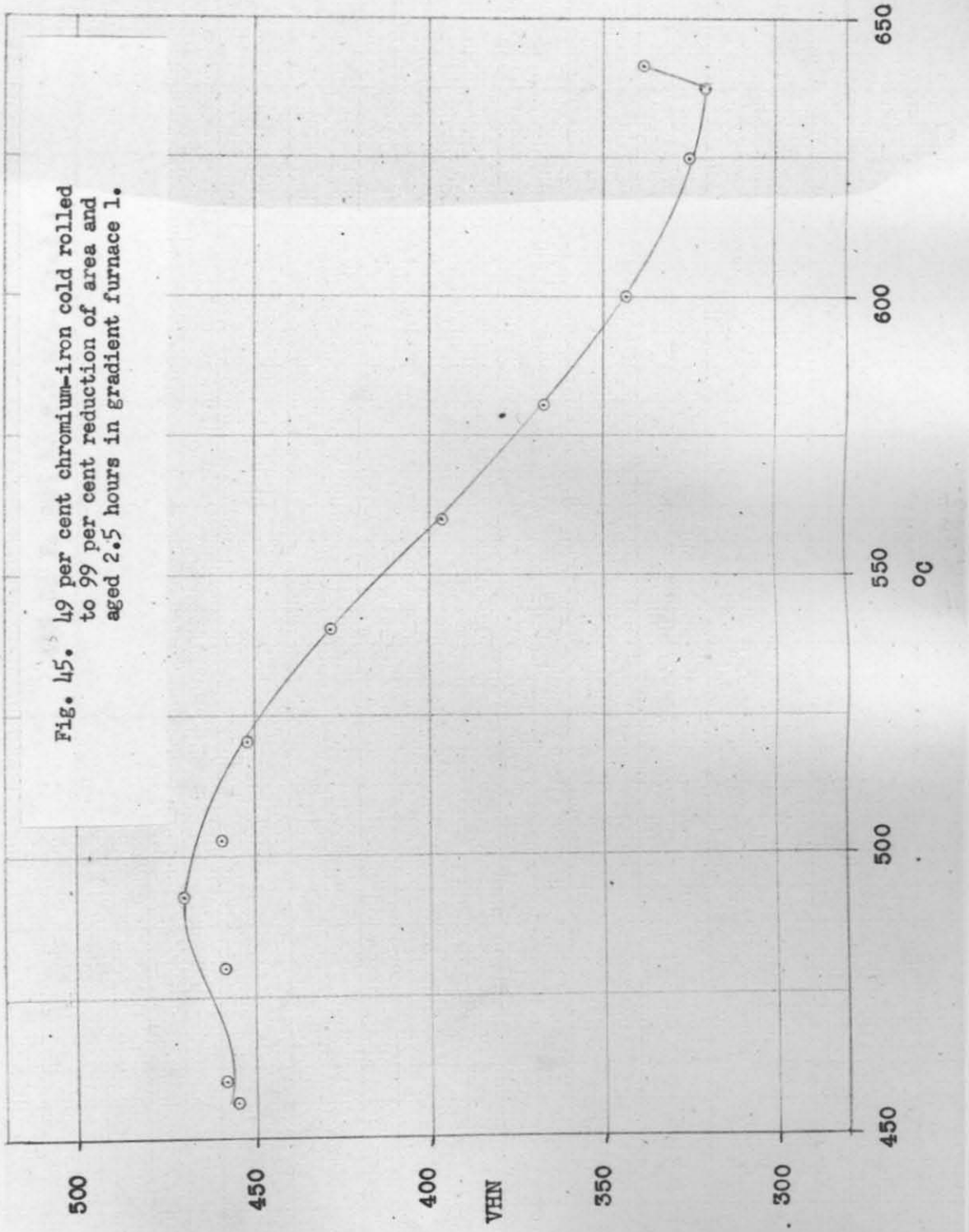

Fig. 45. 49 per cent chromium-iron cold rolled to 99 per cent reduction of area and aged 2.5 hours in gradient furnace 1.

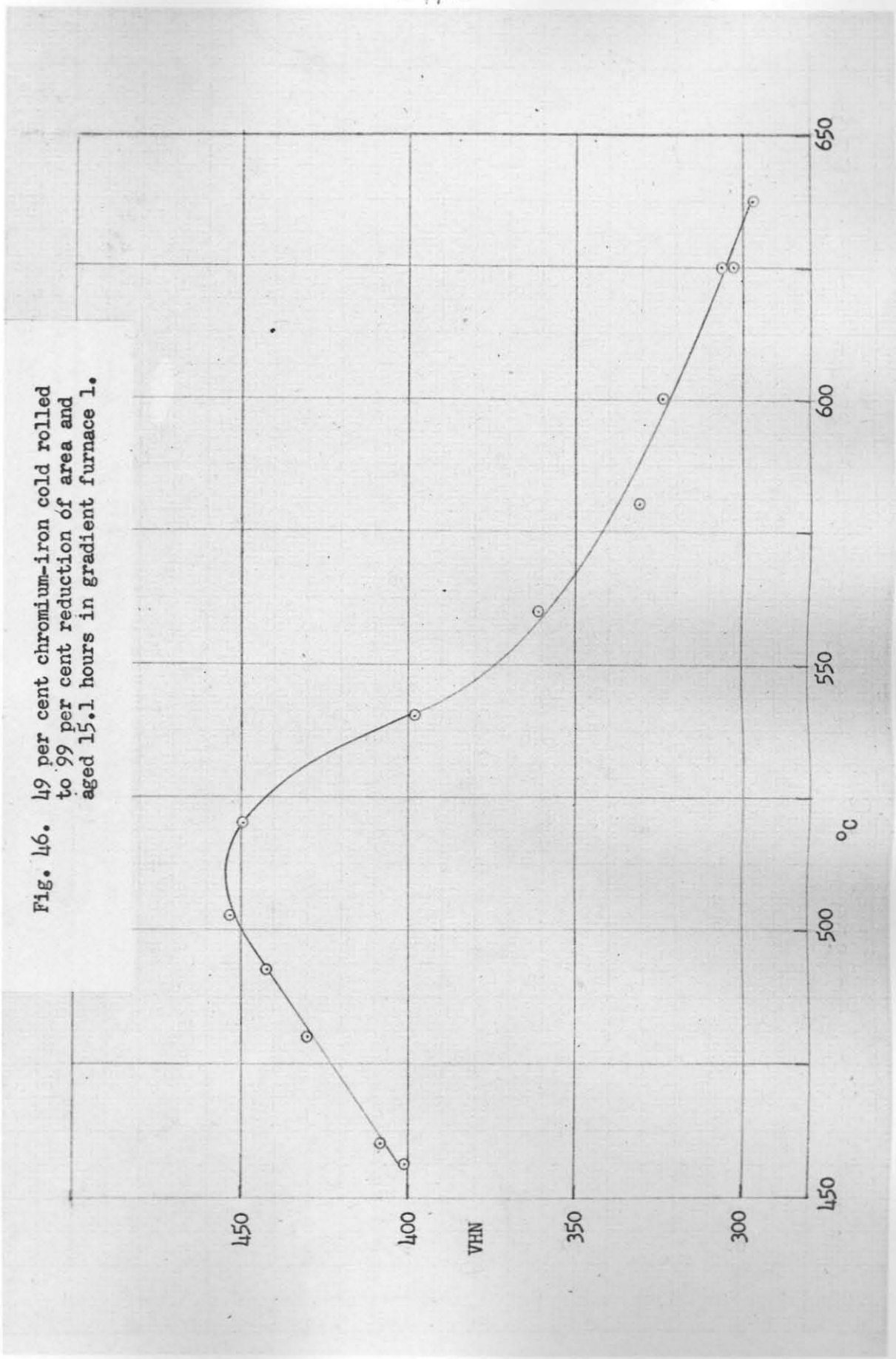

Fig. 46. 49 per cent chromium-iron cold rolled to 99 per cent reduction of area and aged 15.1 hours in gradient furnace 1.

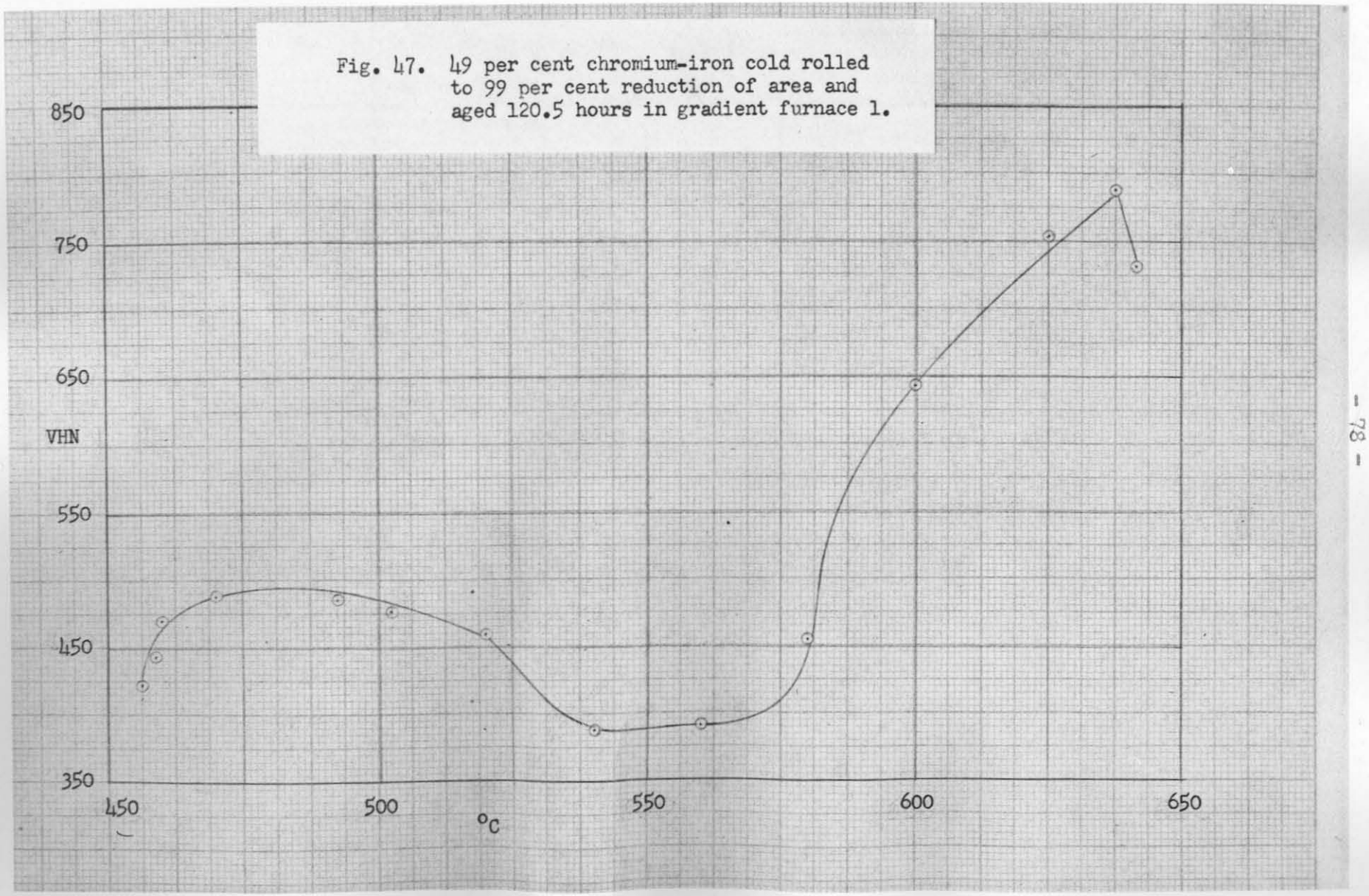

Fig. 47. 49 per cent chromium-iron cold rolled to 99 per cent reduction of area and aged 120.5 hours in gradient furnace 1.

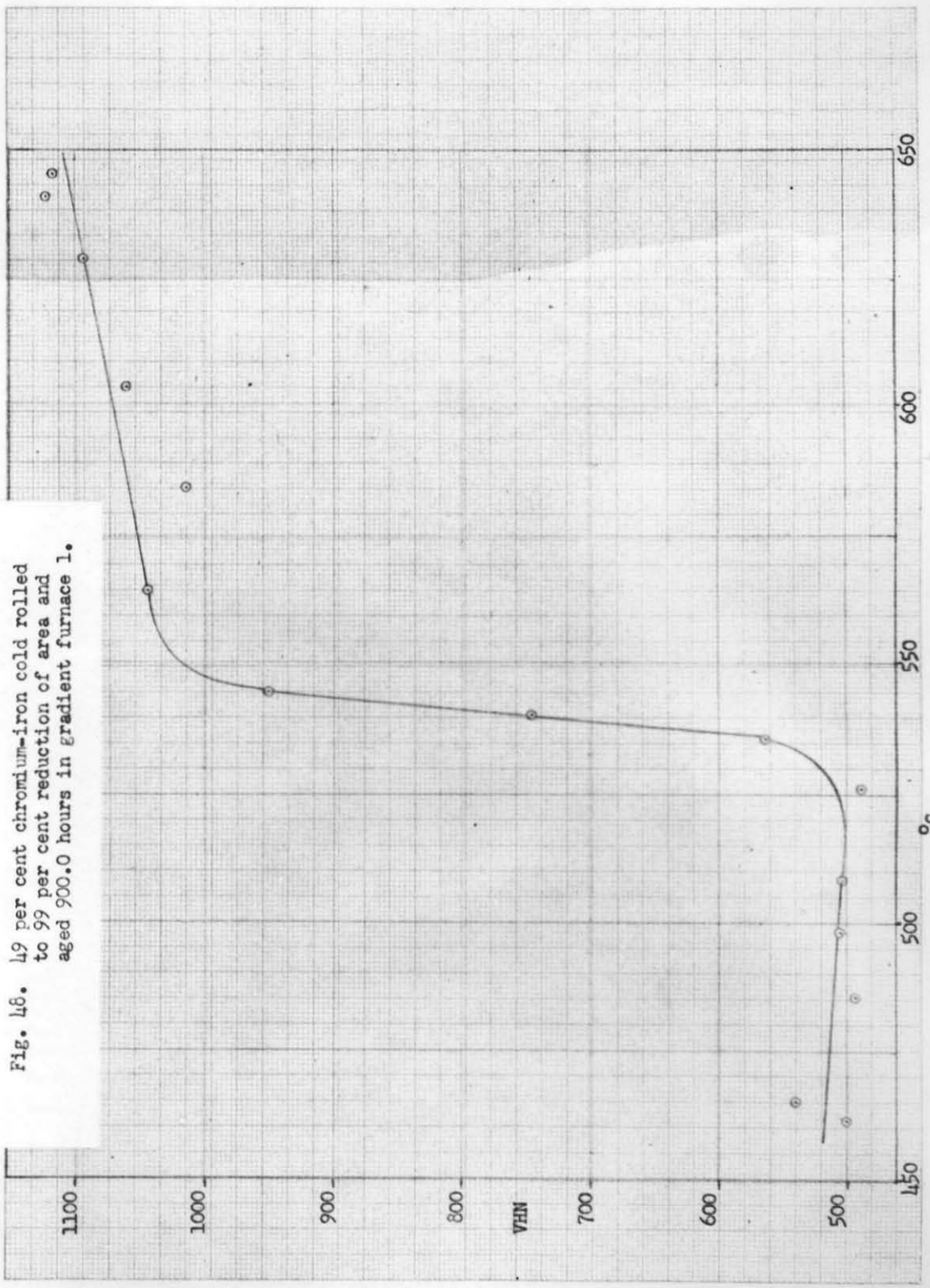

Fig. 46. 49 per cent chromium-iron cold rolled to 99 per cent reduction of area and aged 900.0 hours in gradient furnace 1.

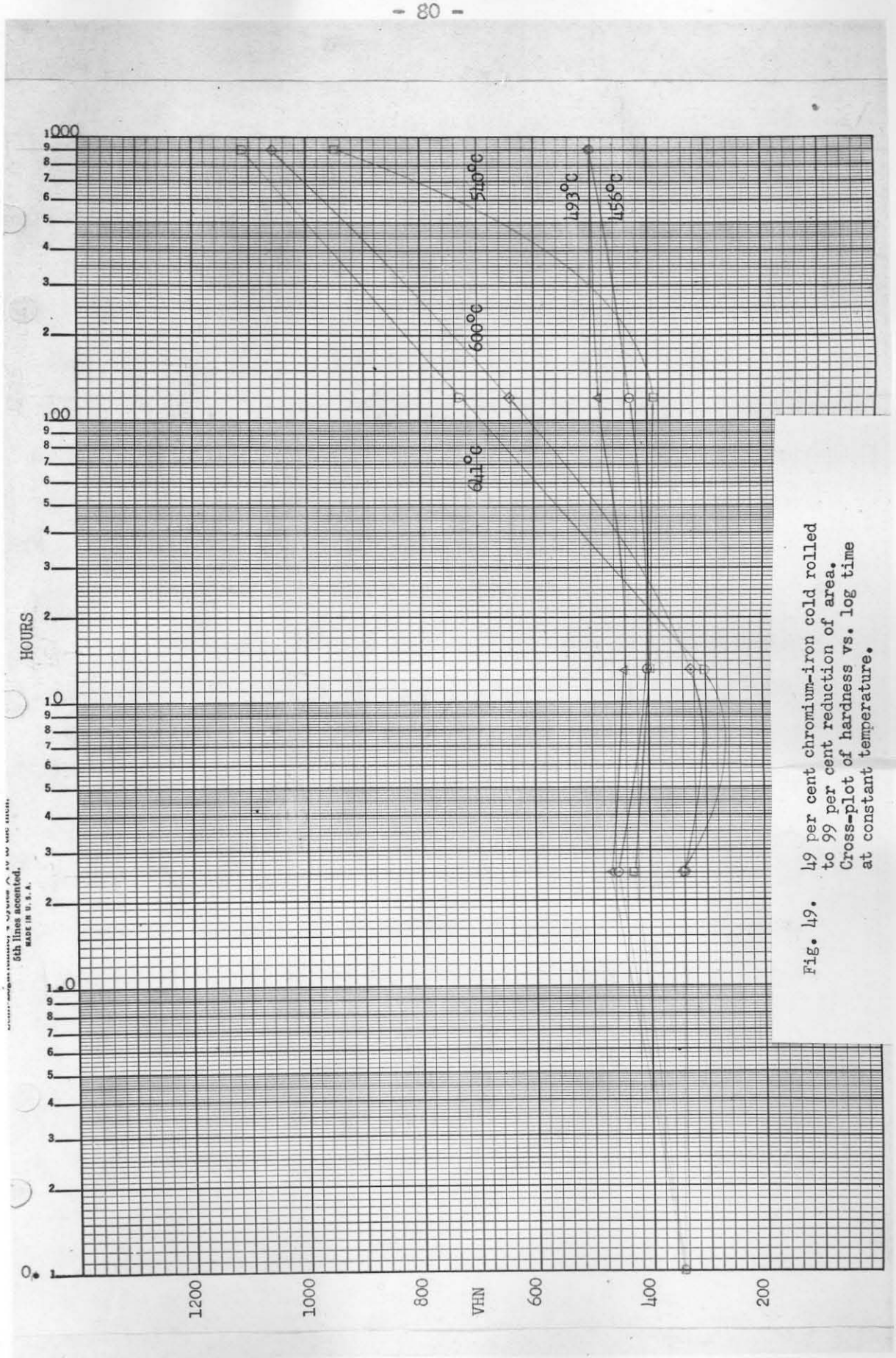

Fig. 49. 49 per cent chromium-iron cold rolled to 99 per cent reduction of area. Cross-plot of hardness vs. log time at constant temperature.

This anomaly suggests a hardening effect superimposed on the recovery process. The results of a 100 hour aging test on a 25 per cent chromium-iron sample annealed 1 hour at 1000°C before aging are plotted in Fig. 34. This curve is generally similar to that of the cold worked (99 per cent reduction of area) 25 per cent chromium-iron specimen aged 100 hours, Fig. 32, except for a larger maximum hardness increase of 105 VHN at 525°C. The maximum hardening effect appears at a higher temperature in the annealed specimen due to the absence of a recovery effect. There is a definite hardness increase at 540°C confirming the suggested reason for the anomalous effect at 540°C in the cold worked specimen.

No hardening occurs in 1 hour of aging of a cold worked 34 per cent chromium-iron specimen. After 12.3 hours aging a 30 VHN increase occurs in the 460°C to 525°C region, maximizing at about 500°C. After 97.6 hours aging a 100 VHN increase occurs with the maximum increase near 500°C. Aging 900 hours gives a 115 VHN maximum increase. As in the 25 per cent chromium-iron alloy, the plot of hardness vs. log time for 34 per cent chromium-iron Fig. 39 shows a definite hardening effect superimposed on the recovery effect at 540°C.

Hardness increases 50 VHN in the first hour of aging with 42 per cent chromium iron at 450 to 545°C. Recovery occurs from 545°C to 610°C. Hardness rises very sharply about 85 VHN from 610°C to 640°C.

After 10 hours aging a 60 VHN increase occurs in the 450°C to 540°C range. A very rapid increase occurs above 600°C, raising the hardness 600 VHN to 950 VHN.

Aging 98.8 hours increases hardness at all temperatures (450-640°C) in 40 per cent chromium-iron with the minimum increase occurring at 540°C. An increase of 120 VHN occurs in the 450°C-525°C region, and a rapid increase to 900 VHN occurs at temperatures above 550°C.

After 1107 hours a hardness increase of 150 VHN occurs from 450°C to 540°C, and a very rapid increase to 1025 VHN results above 540°C.

Referring to the plot of hardness vs. log time for 42 per cent chromium-iron (Fig. 44), it becomes obvious that a very large hardness increase occurs at temperatures above 540°C which did not occur in the lower chromium content alloys. The hardening effect in the 450 to 540°C range continues to occur as it did in the lower chromium content alloys except for a slightly larger hardness increase.

A hardness increase of 115 VHN is observed in 49 per cent chromium-iron after 205 hours of aging in the 450 to 525°C range with the maximum effect near 500°C. After 15.1 hours the maximum hardening effect is 110 VHN at 510°C. After 120.5 hours at temperature there is a 120 VHN increase in the 450-540°C range maximizing near 500°C, and a very rapid increase to 765 VHN (420 VHN rise) from 560 to 640°C. After aging 49 per cent chromium-iron for 900 hours (Fig. 48) a uniform 150 VHN increase from 450°C to 520°C is followed by a very steep increase to 1100 VHN from 530° to 640°C. Referring to the

hardness vs. log time plot for 49 per cent chromium-iron (Fig. 49), the moderate hardness increase is again observed in the 450 to 540°C range, with hardness increase to the 1000 VHN level occurring at 540°C and higher temperatures. The 540°C curve is particularly interesting in that it shows a 75 VHN increase in 2.5 hours which decreases in 120.5 hours, then rapidly rises to 950 VHN (600 VHN increase) at 900 hours.

Interpretation of Results.

The results may be summarized as follows: increasing chromium content from 19 per cent to 49 per cent decreases the time for hardening effects to appear in the 450°C to 540°C range from 30 hours to less than 1 hour, and increases the maximum hardness change from 28 VHN to 150 VHN. The hardening effect is generally most prominent near 500°C. Correlation with other experiments shows that the hardening effect in the 450°C to 540°C range is the precipitation embrittlement effect, while the very marked increase in hardness at higher temperatures in 42 per cent and 49 per cent chromium-iron alloys is clearly sigma phase formation. Observation of the hardness vs. temperature curves for 42 per cent and 49 per cent chromium-iron alloys, Fig. 40 to 43 and 45 to 48, indicate two different hardening processes above and below 540°C. Sigma phase formation is first observed after one hour aging in the 42 per cent chromium-iron alloy and after 20 hours aging in the 49 per cent chromium-iron alloy indicating more rapid formation in the 42 per cent chromium-iron alloy (see Figs. 44 and 49). The 49 per cent chromium-iron alloy reaches 1100 VHN in 900 hours

compared to 1050 VHN for the 42 per cent chromium-iron alloy. The 540°C curve in the plot of hardness vs. log time for each alloy (Figs. 28, 34, 39, 44, and 49), is quite interesting. Even in the 19 per cent chromium-iron alloy, an anomalous effect in the normal recovery process is indicated at 100 hours at 540°C. This effect becomes more pronounced in the 25 per cent chromium-iron alloy, and still more pronounced in the 34 per cent chromium-iron alloy for 540°C aging. As discussed above, this effect is associated with precipitation embrittlement in the 17, 25, and 34 per cent chromium-iron alloys. However, in the 42 and 49 per cent chromium-iron alloys, no recovery occurs at 540°C, and some precipitation embrittlement is indicated at short aging times, but a rapid increase in hardness identified with sigma formation occurs after 1000 hours aging. The temperature measurement is within $\pm$ 5°C for all specimens, and the effect is consistent with respect to increasing chromium content. Thus, there is evidence that precipitation embrittlement and sigma phase formation overlap within a very limited temperature and composition range. Finally it is interesting to note the suggestion of sigma phase formation at high temperatures in the lower chromium content alloys. Fig. 28 indicates a slight hardness increase after 900 hours at 641°C in 19 per cent chromium-iron. No such effect is observed in 25 per cent chromium-iron, Fig. 34. A definite hardening effect is observed in 34 per cent chromium-iron after 900 hours at 600°C and at 641°C, Fig. 39. These results will be considered further in Section VI.

VI. METALLOGRAPHIC AND X-RAY ANALYSIS.

Metallographic Procedure.

Metallographic sections were prepared from annealed 19, 25 34, 42, and 49 per cent chromium-iron; from annealed and embrittled 25 per cent chromium-iron microtension specimens, and from 19,25, 34, 42, and 49 per cent chromium-iron gradient furnace specimens aged 900 hours at 456, 540, and 641°C and 100 hours at 540°C. The annealed specimens were mechanically ground on wet alundum paper (180 to 400 grit) and electropolished using an electrolyte (22) composed of 2 parts perchloric acid, 7 parts ethyl alcohol, and 1 part butyl cellosolve (2-butoxyethanol). All specimens were etched in glyceregia (23) composed of 3 parts glycerine, 2 parts hydrochloric acid, and 1 part nitric acid.

Mechancial polishing of the specimens used in this study is very difficult, since there are many small hard inclusions, principally chromium carbides, in a ferritic matrix. The ferritic matrix itself is difficult to polish since it work hardens easily, and shows scratches even from 1 micron Diamet polishing compound. If any of the inclusions are pulled out of the matrix during final stages of polishing, deep scratches result. Therefore, it is desirable to electrolytically polish these specimens whenever possible. Unfortunately, all gradient furnace and microtension specimens were too small in size and unsuitable in shape to electropolish.

The following techniques have been found most suitable for mechanical polishing of these specimens:

(1) Mechanical wet grinding through 400 grit alundum paper.

(2) 500 grit alundum in soap solution on wax wheel.

(3) 6 micron Diamet on Metcloth.

(4) 1 micron Diamet on Microcloth.

(5) Etch and examine specimen.

(6) 0.1 micron Gamma Polishing Alumina on Microcloth.

(7) Etch.

The use of relatively high pressure on the specimens for short time on each polishing wheel was found desirable.

Metallographic Results.

Photomicrographs of annealed (0.5 hours at 1000°C) 19, 25, 34, 42, and 49 per cent chromium-iron structures are shown at a magnification of 100 diameters in Figs. 50, 51, 52, 53, and 54 respectively. These structures are typical coarse grained ferritic stainless steel structures with numerous inclusions. The nature of these inclusions will become apparent in subsequent structures. Grain sizes for the annealed structures are ASTM grain size 1 for 19 per cent chromium-iron, 1 for 25 per cent chromium-iron, 1-2 for 34 per cent chromium-iron, 2 for 42 per cent chromium-iron, and 3-4 for 49 per cent chromium-iron.

Photomicrographs of the gradient furnace specimens are shown at a magnification of 500 diameters in Figs. 55 to 72. Fig. 55 shows a 19 per cent chromium-iron specimen, cold rolled to 99 per cent

reduction of area, and aged 908 hours at 456°C. The structure is cold rolled ferrite with several inclusions. Fig. 56 shows that the same material aged 908 hours at 641°C has recrystallized. Several inclusions are present and there is some suggestion of small crystallites of a second phase in the structure.

A 25 per cent chromium-iron structure cold rolled to 99 per cent reduction of area aged 911 hours at 456°C is shown in Fig. 57. The structure is cold rolled ferrite with a few inclusions. After 100 hours at 540°C, Fig. 58, several small areas of a dark etching constituent appear in the structure. This constituent has been identified as sigma phase by Link and Marshall (6) and others (24), (25). After 911 hours at 540°C, Fig. 59, the sigma phase structure develops further and partial recrystallization of the ferrite has occurred. After 911 hours at 641°C, Fig. 60, complete recrystallization of the ferrite has occurred with grains elongated in the same direction as the initial cold rolling. Small amounts of sigma phase appear in the structure.

In the case of 34 per cent chromium-iron alloys, several inclusions are present in the cold rolled ferrite structure after aging 900 hours at 456°C, Fig. 61, and 97.6 hours at 540°C, Fig. 62, while small amounts of sigma phase appear in the cold rolled ferrite structure after aging 900 hours at 540°C, Fig. 63. After 900 hours at 641°C, Fig. 64, ferrite recrystallization has occurred and substantial amounts of sigma phase appear in the structure outlining ferrite grains.

Aging 42 per cent chromium-iron 1107 hours at 456°C produces the cold rolled ferritic structure with inclusions shown in Fig. 65. After aging 98.8 hours at 540°C, Fig. 66, sigma phase appears in the structure and some refinement of the cold rolled ferritic matrix has taken place. The structure resulting from aging 1107 hours at 540°C is shown in Fig. 67. This structure looks like partially recrystallized ferrite with many inclusions; however, the partial iron-chromium phase diagram, Fig. 3, shows the equilibrium structure of a 42 per cent chromium-iron alloy at 540°C is sigma phase and the 923 VHN hardness of this structure indicates sigma phase rather than ferrite. The structure will be assumed to be sigma phase, and will be discussed further in interpretation of these results. After aging 1107 hours at 641°C, Fig. 68, a single phase structure with inclusions is obtained.

Fig. 69 shows the cold rolled ferritic structure of 49 per cent chromium-iron aged 900 hours at 456°C. After 120.5 hours at 540°C, Fig. 70, some sigma phase appears, and matrix refinement has started. After 900 hours aging at 540°C, Fig. 71, a structure of approximately 50 per cent sigma phase and 50 per cent partially recrystallized ferrite appears. After 900 hours aging at 641°C, Fig. 72, a 90 per cent sigma phase structure has formed.

The microstructures of several strain aged specimens are shown in Figs. 73 to 79. Figs. 73 and 74 show the structure obtained by straining a specimen to 2.8 per cent elongation, aging 168 hours at 490°C and retesting to failure, Fig. 5. Neumann bands are clearly visible in the structure, while no gross precipitate is visible. Fracture is clearly transcrystalline and follows a definite fracture plane.

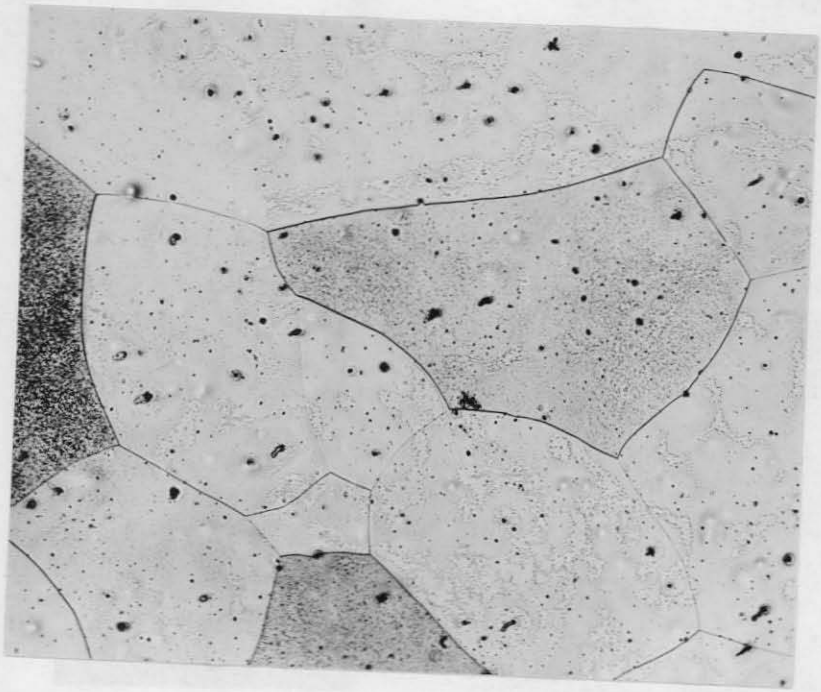

Fig. 50. 19 per cent chromium-iron annealed 0.5 hours at 1000°C. 116 VHN. ASTM grain size 1. Electrolytic polish. Glyceregia etch. 100X.

Fig. 51. 25 per cent chromium-iron annealed 0.5 hours at 1000°C. 162 VHN. ASTM grain size 1. Electrolytic polish. Glyceregia etch. 100X.

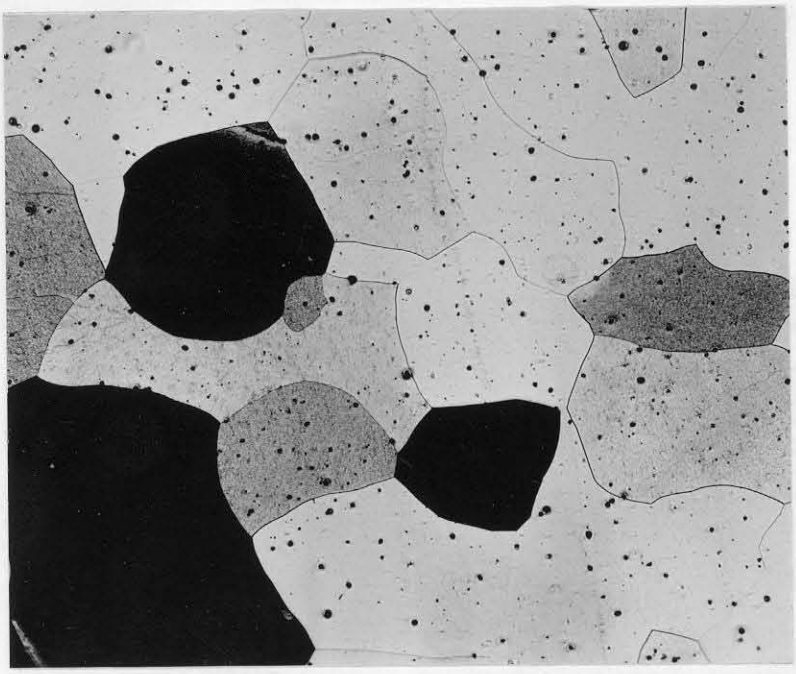

Fig. 52. 34 per cent chromium-iron annealed 0.5 hours at 1000°C. 159 VHN. ASTM grain size 1-2. Electrolytic polish. Glyceregia etch. 100X.

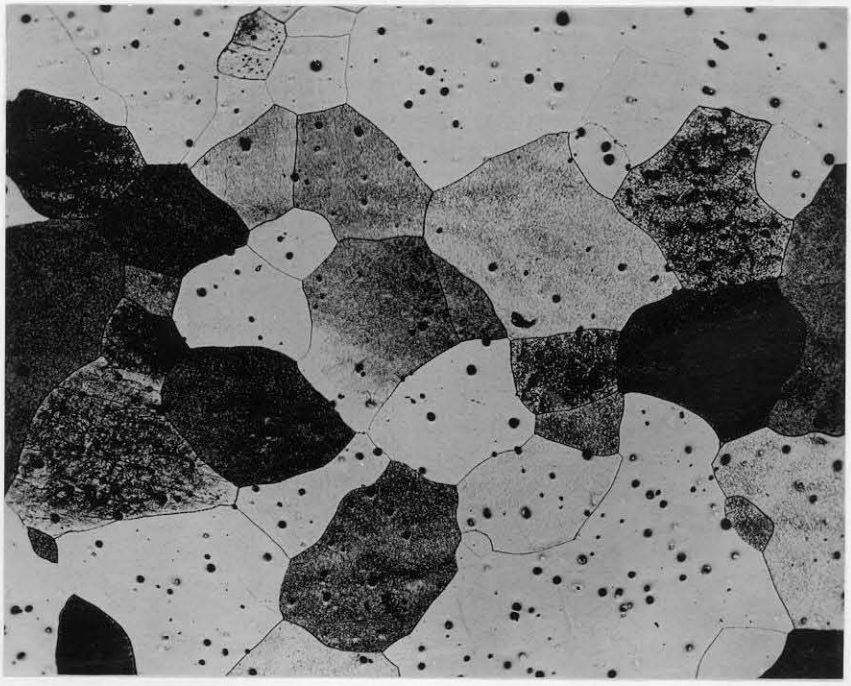

Fig. 53. 42 per cent chromium-iron annealed 0.5 hours at 1000°C. 195 VHN. ASTM grain size 2. Electrolytic polish. Glyceregia etch. 100X.

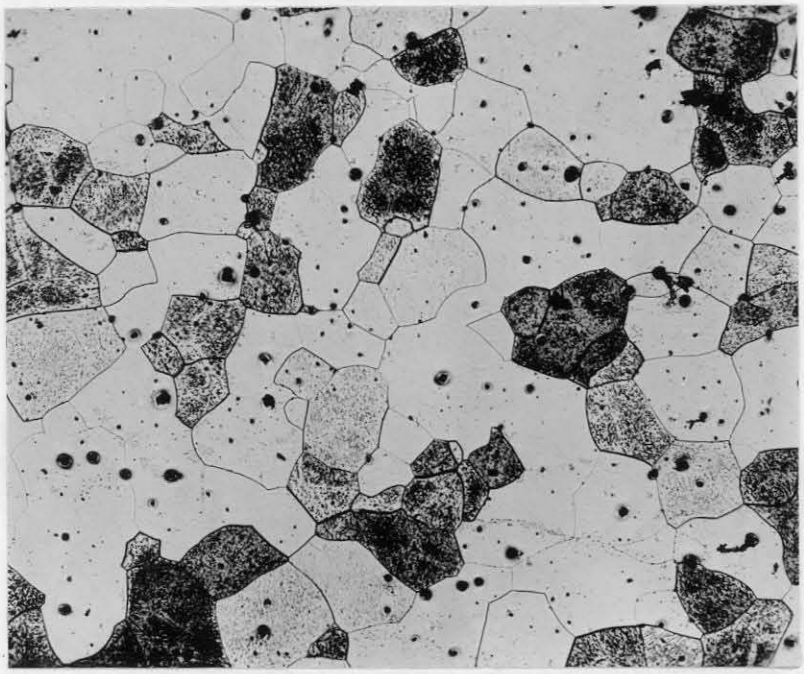

Fig. 54. 49 per cent chromium-iron annealed 0.5 hours at 1000°C. 234 VHN. ASTM grain size 3-4. Electrolytic polish. Glyceregia etch. 100X.

Fig. 55. 19 per cent chromium-iron, cold rolled 99 per cent, aged 907.9 hours at 456°C. 288 VHN. Mechanical polish. Glyceregia etch. 500X.

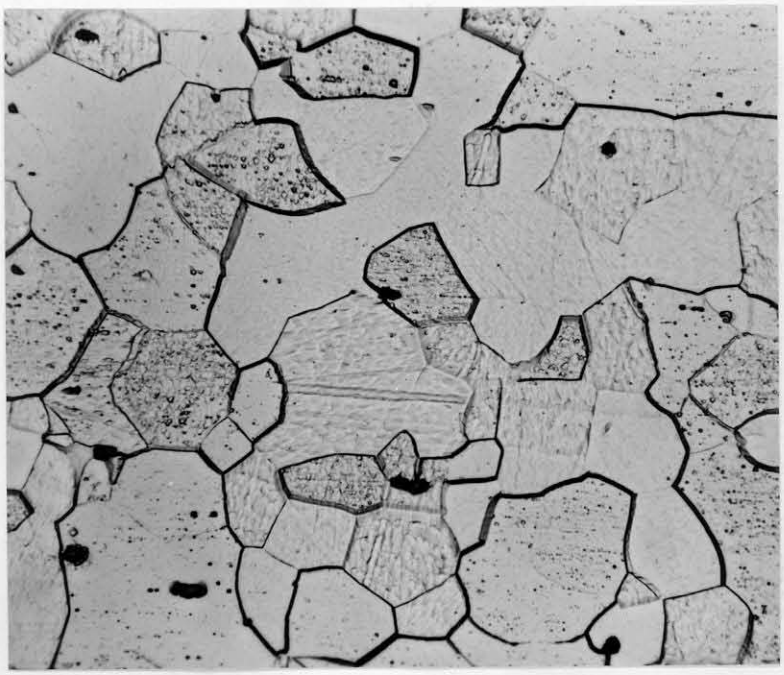

Fig. 56. 19 per cent chromium-iron, cold rolled 99 per cent, aged 907.9 hours at 641°C. 110 VHN. Mechanical polish. Glyceregia etch. 500X.

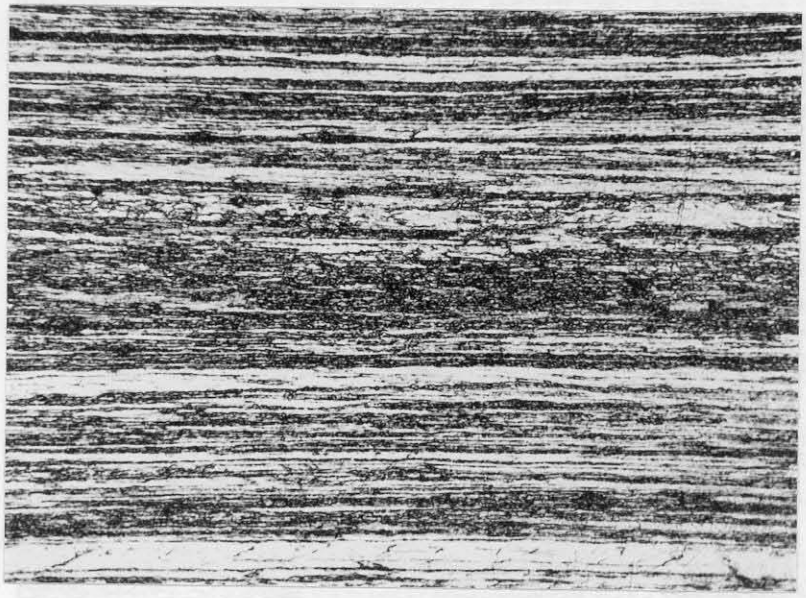

Fig. 57. 25 per cent chromium-iron, cold rolled 99 per cent, aged 910.5 hours at 456°C. 352 VHN. Mechanical polish. Glyceregia etch. 500X.

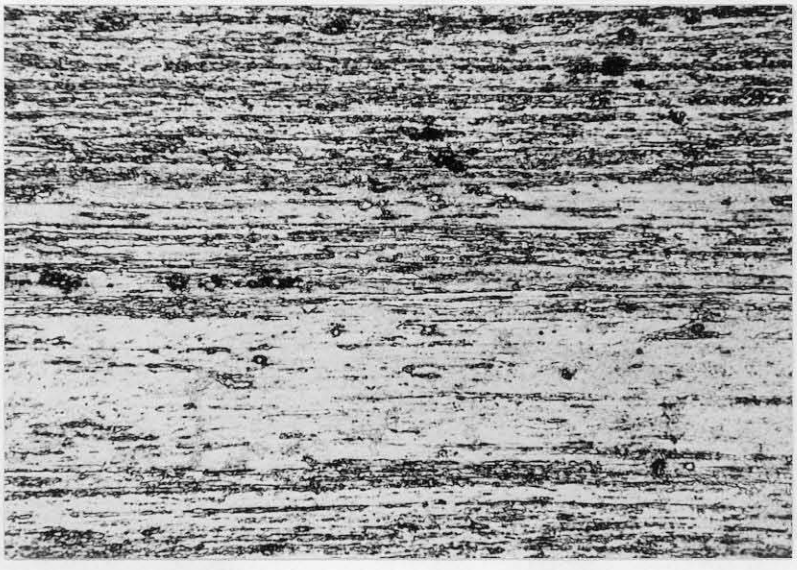

Fig. 58. 25 per cent chromium-iron, cold rolled 99 per cent, aged 100 hours at 540°C. 272 VHN. Mechanical polish. Glyceregia etch. 500X.

Fig. 59. 25 per cent chromium-iron, cold rolled 99 per cent, aged 910.5 hours at 540°C. 195 VHN. Mechanical polish. Glyceregia etch. 500X.

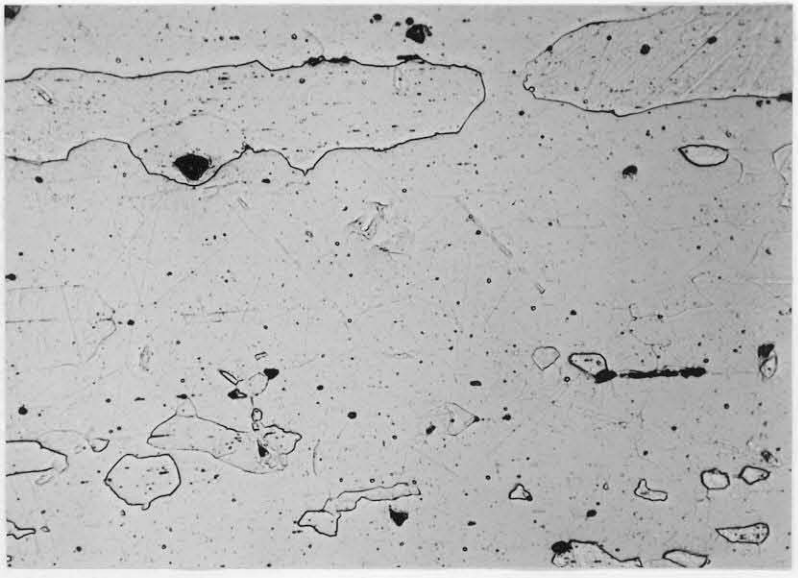

Fig. 60. 25 per cent chromium-iron, cold rolled 99 per cent, aged 910.5 hours at 641°C. 137 VHN. Mechanical polish. Glyceregia etch. 500X.

Fig. 61. 34 per cent chromium-iron, cold rolled 99 per cent, aged 900 hours at 456°C. 438 VHN. Mechanical polish. Glyceregia etch. 500X.

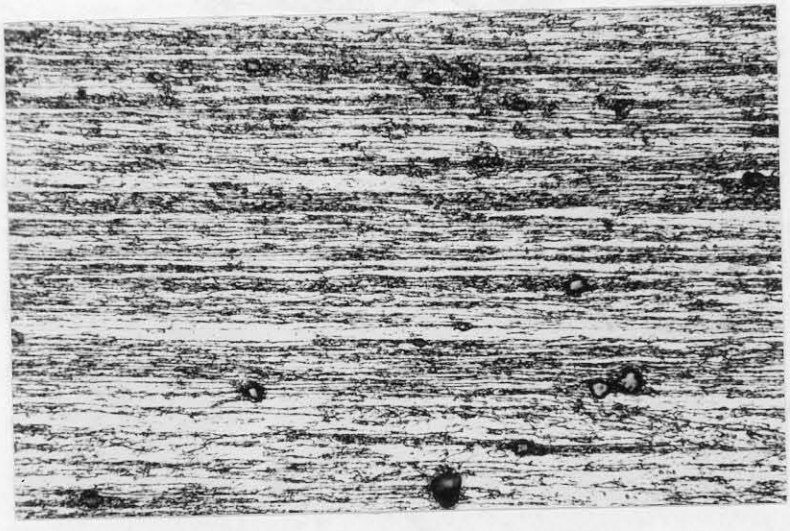

Fig. 62. 34 per cent chromium-iron, cold rolled 99 per cent, aged 97.6 hours at 540°C. 366 VHN. Mechanical polish. Glyceregia etch. 500X.

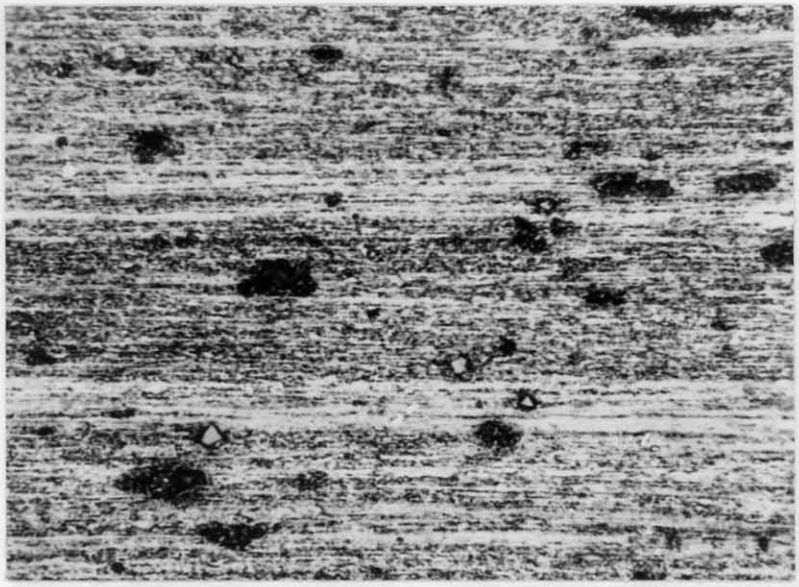

Fig. 63. 34 per cent chromium-iron, cold rolled 99 per cent, aged 900 hours at 540°C. 240 VHN. Mechanical polish. Glyceregia etch. 500X.

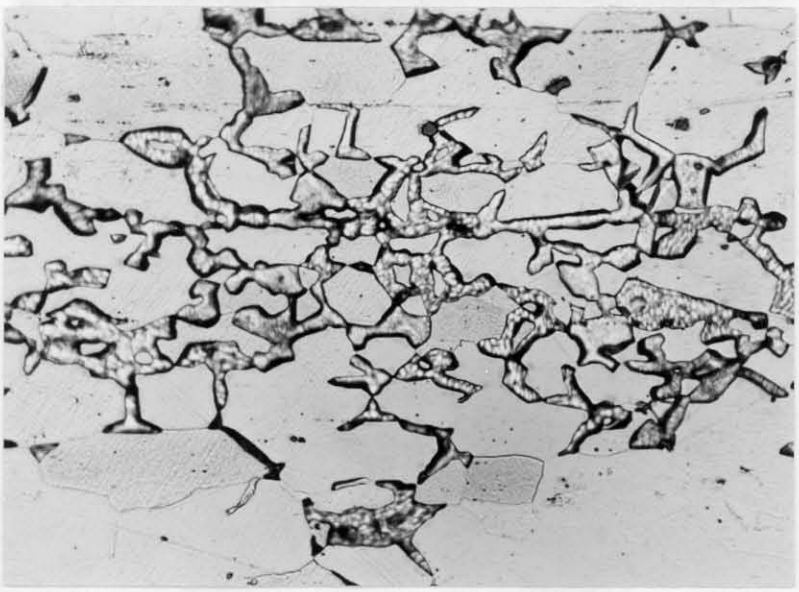

Fig. 64. 34 per cent chromium-iron, cold rolled 99 per cent, aged 900 hours at 641°C. 202 VHN. Mechanical polish. Glyceregia etch. 500X.

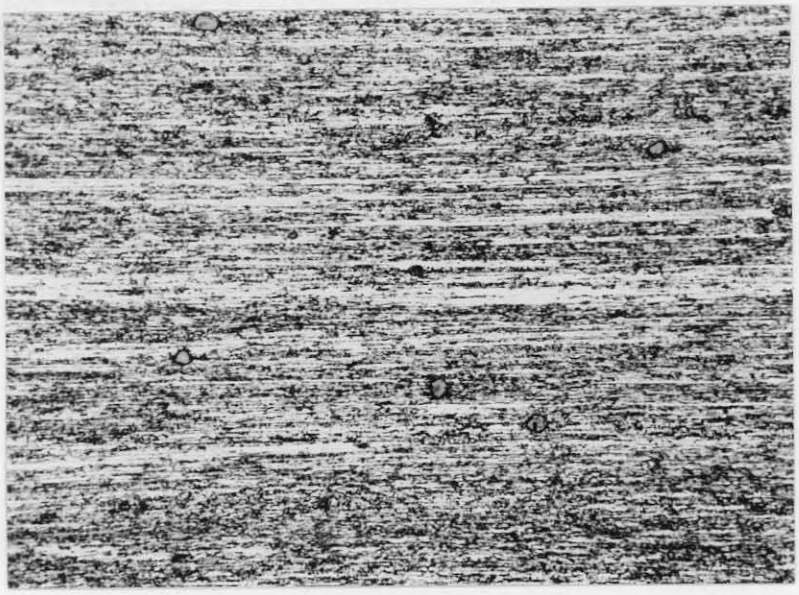

Fig. 65. 42 per cent chromium-iron, cold rolled 99 per cent, aged 1107 hours at 456°C. 482 VHN. Mechanical polish. Glyceregia etch. 500X.

Fig. 66. 42 per cent chromium-iron, cold rolled 99 per cent, aged 98.8 hours at 540°C. 373 VHN. Mechanical polish. Glyceregia etch. 500X.

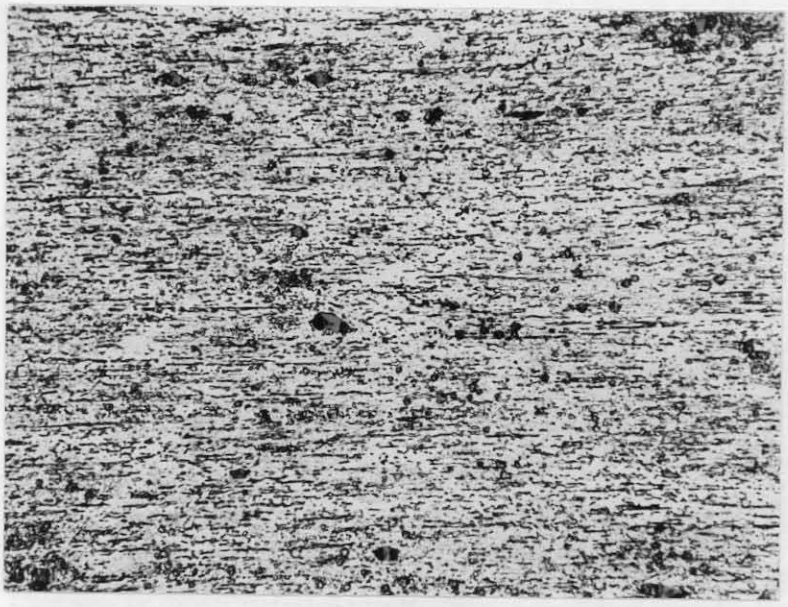

Fig. 67. 42 per cent chromium-iron, cold rolled 99 per cent, aged 1107 hours at 540°C. 923 VHN. Mechanical polish. Glyceregia etch. 500X.

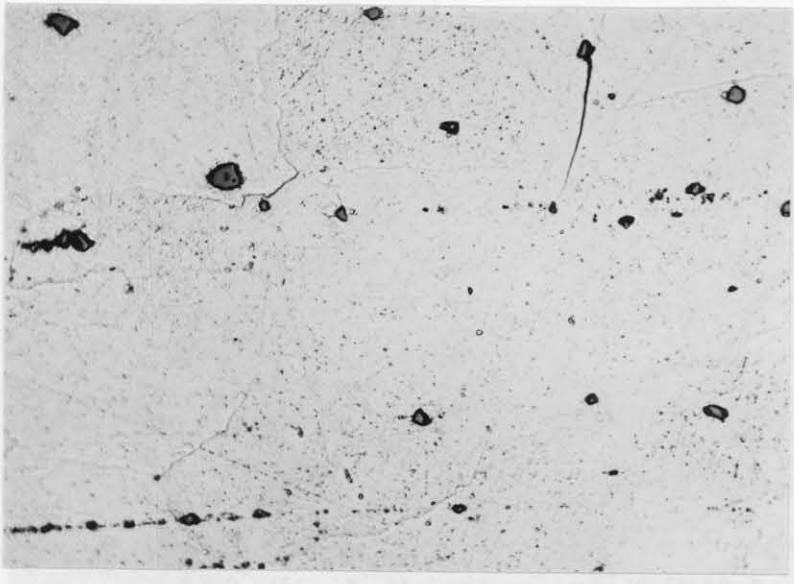

Fig. 68. 42 per cent chromium-iron, cold rolled 99 per cent, aged 1107 hours at 641°C. 1008 VHN. Mechanical polish. Glyceregia etch. 500X.

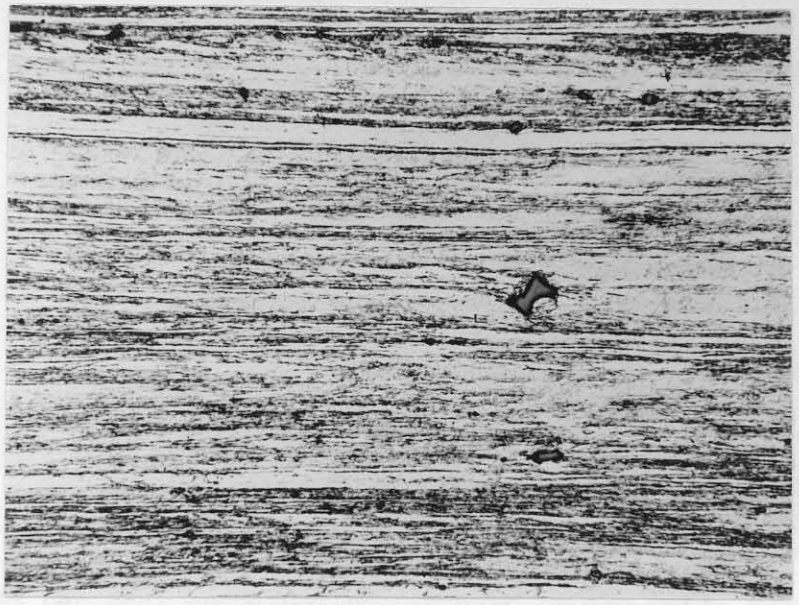

Fig. 69. 49 per cent chromium-iron, cold rolled 99 per cent, aged 900 hours at 456°C. 502 VHN. Mechanical polish. Glyceregia etch. 500X.

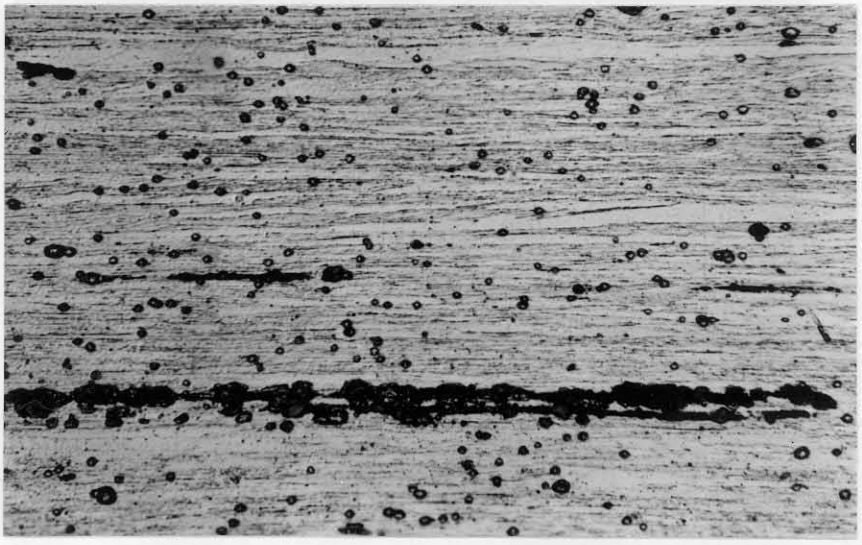

Fig. 70. 49 per cent chromium-iron, cold rolled 99 per cent, aged 120.5 hours at 540°C. 387 VHN. Mechanical polish. Glyceregia etch. 500X.

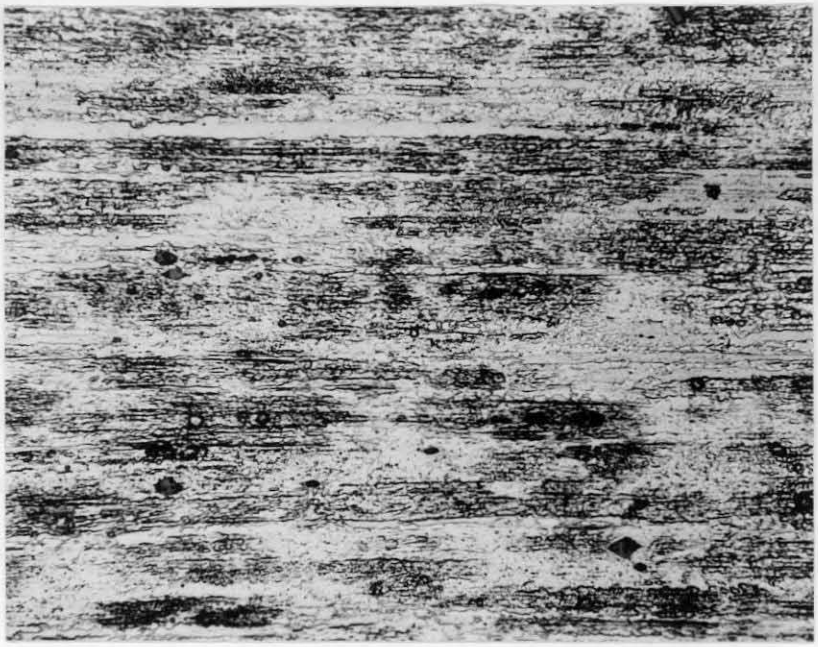

Fig. 71. 49 per cent chromium, cold rolled 99 per cent, aged 900 hours at 540°C. 952 VHN. Mechanical polish. Glyceregia etch. 500X.

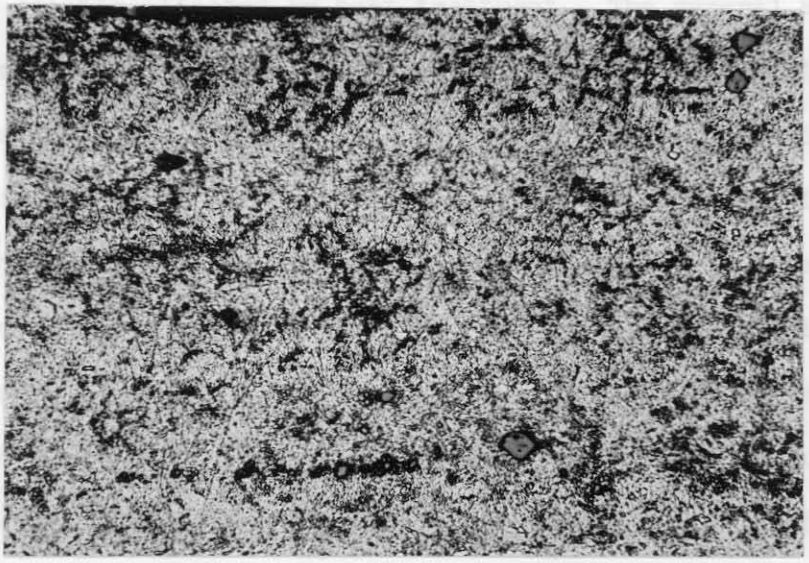

Fig. 72. 49 per cent chromium-iron, cold rolled 99 per cent, aged 900 hours at 641°C. 1116 VHN. Mechanical polish. Glyceregia etch. 500X.

Brittle fracture is shown in a photomicrograph, Fig. 75, of a broken 25 per cent chromium-iron microtension specimen which was annealed and then aged 534.3 hours at 490°C. A higher magnification of this structure, Fig. 76, shows grain boundary precipitate and the nitride needles observed by Lena (10). A 25 per cent chromium-iron microtension specimen strained to 3.86 per cent elongation and then aged 418.2 hours at 490°C has the structures shown in Figs. 77 to 79. Angular transcrystalline fracture, carbide inclusions, Neumann bands, grain boundary widening, and nitride precipitation are observed.

Interpretation of Metallographic Results.

The small angular inclusion particles which are found to some extent in all the structures shown above, e.g. Figs. 61, 72, and 77, are not greatly affected by heat treatment. The general appearance and behavior of these inclusions identify them as chromium carbides; see (1) and (25). These carbides may provide initial lattice strain which affects the rate of sigma phase formation and aging kinetics in these alloys, and carbon in solid solution may be responsible for the yield point effects observed in the strain aging experiments, Section III. Nitride precipitation was also observed in a few strain aging specimens, and is assumed to be responsible for anomalous electrical resistance effects observed in Section IV.

Sigma phase precipitate is observed after 100 hours aging at 540°C, with a greater amount formed in 910.5 hours aging at 540°C, while a very small amount of sigma phase appears after 910.5 hours aging at 641°C, Figs. 58 to 60. Thus, sigma phase is observed at a

higher temperature than reported by Cook and Jones (3) for 25 per cent chromium-iron. Sigma phase appears after 900 hours aging at 540°C and 641°C in 34 per cent chromium-iron, after 100 hours aging at 540°C in 42 per cent chromium-iron, and after 100 hours at 540°C in 49 per cent chromium-iron. No sigma phase was observed in any specimens aged at 456°C.

As expected from equilibrium diagram considerations, sigma phase formation at 540°C is accelerated by increasing chromium content from 25 to 49 per cent. Sigma phase formation is correlated with the large hardness increases at aging temperatures of 540°C and above which were described in Section V. The structures obtained from 456°C aging, and from strain aging 25 per cent chromium-iron at 490°C show no indications of gross sigma phase formation or other precipitation except for interstitial impurities.

Fracture is transcrystalline and angular. Zappfe (26) has shown fracture occurs on (100) planes in embrittled 25 per cent chromium-iron, and the 90° angles between fracture planes in Fig. 77 is consistent with this hypothesis.

Neumann bands are narrow twinned regions commonly found in structures deformed by impact or low temperature strain (27). The existence of such twinned regions indicates impediment of normal slip processes due to a high rate of deformation, low temperature of deformation, or structure changes which impede slip. In this study Neumann bands are observed only after deformation of embrittled material and may be considered as additional evidence of a precipitation hardening reaction where normal slip processes are restrained due to

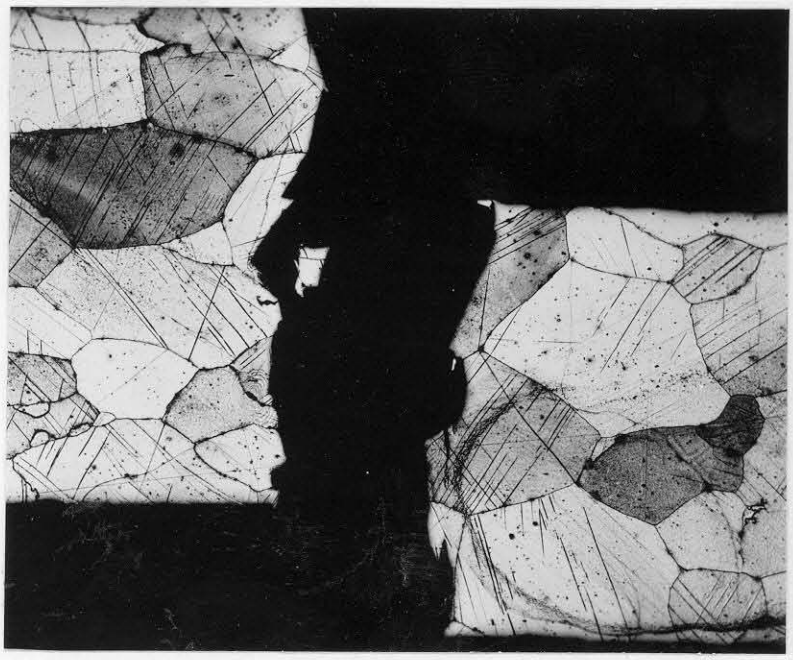

Fig. 73. 25 per cent chromium-iron, 2.8 per cent elongation, 168 hours at 490°C (Fig. 5). Mechanical polish. Glyceregia etch. 50X.

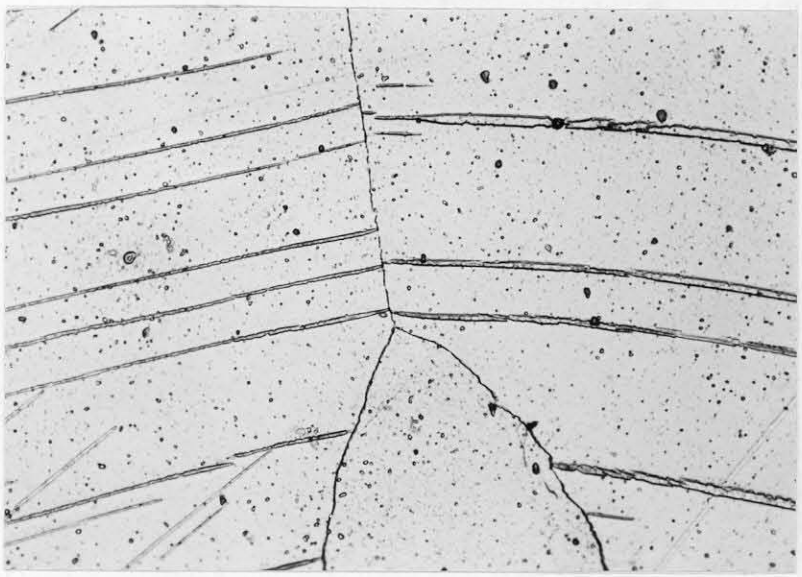

Fig. 74. 25 per cent chromium-iron, 2.8 per cent elongation, 168 hours at 490°C (Fig. 5). Mechanical polish. Glyceregia etch. 500X.

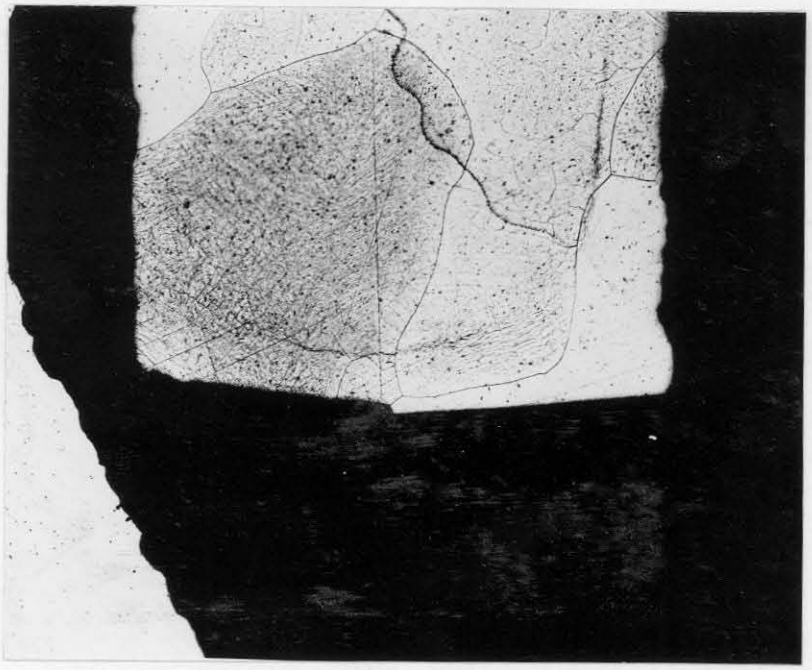

Fig. 75. 25 per cent chromium-iron, annealed, aged 534.3 hours at 490°C. Mechanical polish. Glyceregia etch. 50X.

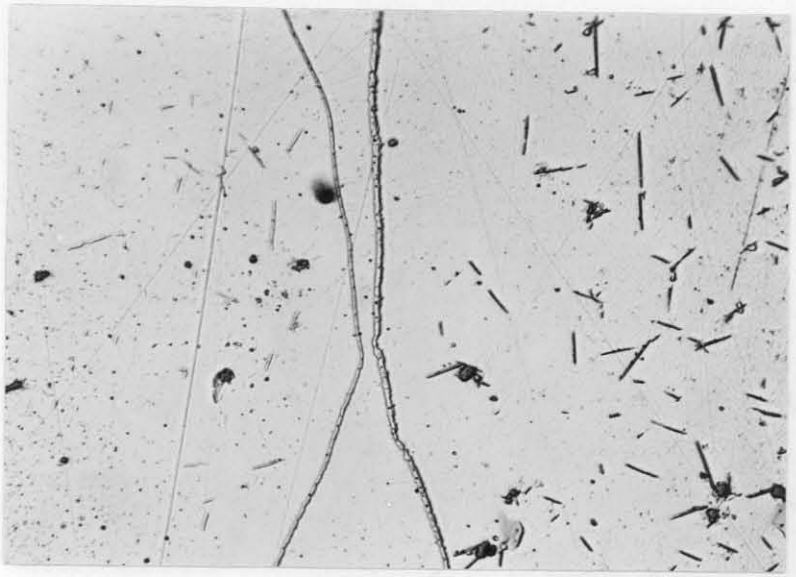

Fig. 76. 25 per cent chromium-iron, annealed, aged 534.3 hours at 490°C. Mechanical polish. Glyceregia etch. 500X.

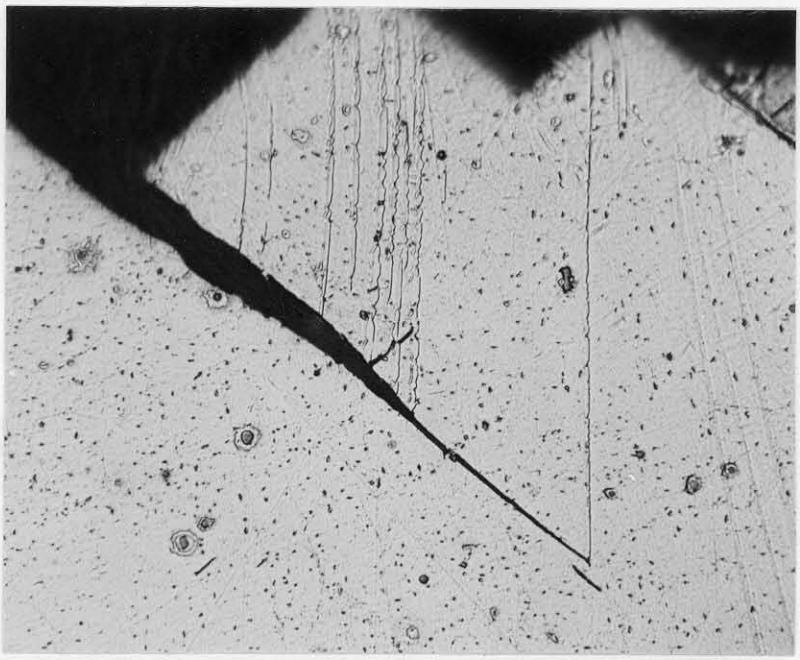

Fig. 77. 25 per cent chromium-iron, 3.86 per cent elongation, 418.2 hours at 490°C. Mechanical polish. Glyceregia etch. 500X.

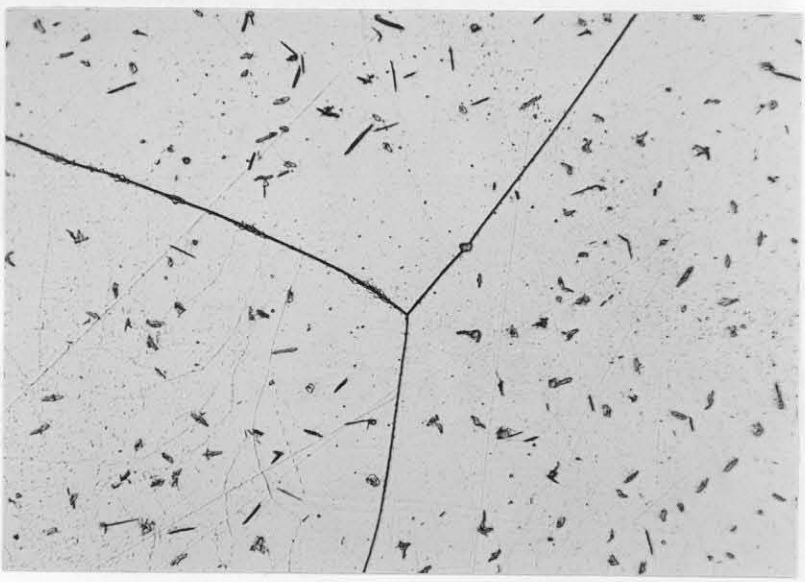

Fig. 78. 25 per cent chromium-iron, 3.86 per cent elongation, 418.2 hours at 490°C. Mechanical polish. Glyceregia etch. 500X.

Fig. 79. 25 per cent chromium-iron, 3.86 per cent elongation, 418.2 hours at 490°C. Mechanical polish. Glyceregia etch. 500X.

lattice strain and other precipitation effects. Newell (7) reported Neumann bands in Type 446 stainless steel (27 per cent chromium) after 13,000 hours aging at 475°C. Newell suggests the Neumann bands were formed directly by lattice strain caused by precipitation.

In summary, metallographic results show that gross sigma phase formation in 25 to 49 per cent chromium-iron alloys occurs at temperatures of 540°C to 641°C. No gross precipitate was observed at 490°C or 456°C, although Neumann bands and fracture patterns observed after aging show severe embrittlement has occurred without a microscopically visible precipitate.

X-Ray Procedure.

A specimen of the 25 per cent chromium-iron alloy was cold drawn to 0.020 in. wire which was then strain annealed (2 per cent elongation, one-half to 24 hours at 1000°C) repeatedly until several large grains 0.040 in. to 0.125 in. long were grown in the wire. This specimen was mounted in a single crystal universal goniometer and oriented by the Greninger back reflection Laue technique (28), (29). Laue transmission exposures were then made using tungsten white radiation with the incident beam parallel to the (100) or (111) axis of the crystal being studied. Transmission Laue photgraphs were taken of the annealed specimen and after aging the specimen 10, 100, and 1000 hours at 490°C. Typical exposures are shown in Figs. 80 to 82. No precipitation hardening effects of the type first reported by Guinier (30) and Preston (31) which cause asterism in Laue transmission photographs, were observed. Results from this part of the investigation are completely negative.

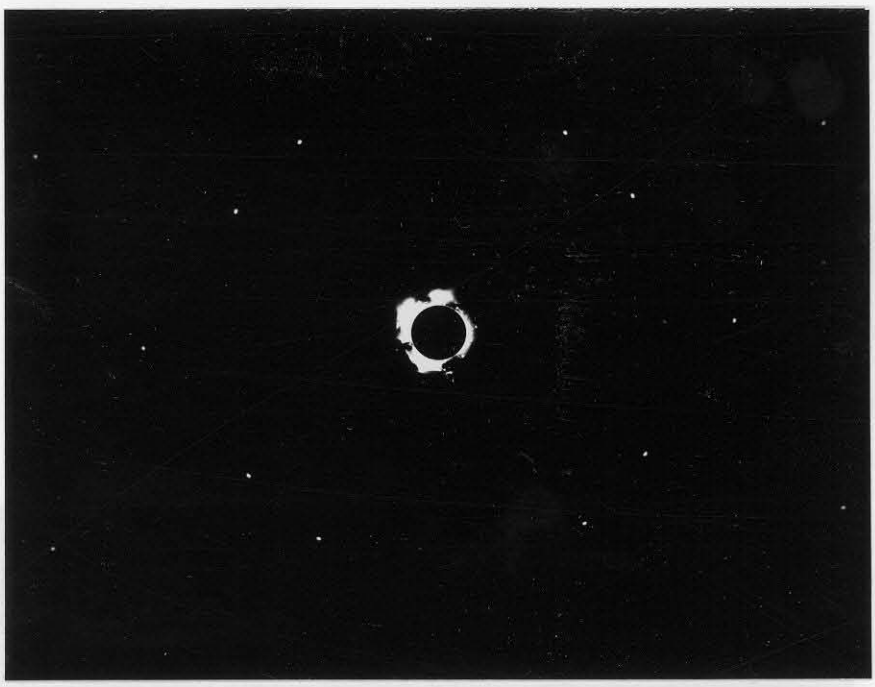

Fig. 80. Annealed 25 per cent chromium-iron. Laue transmission (100) orientation.

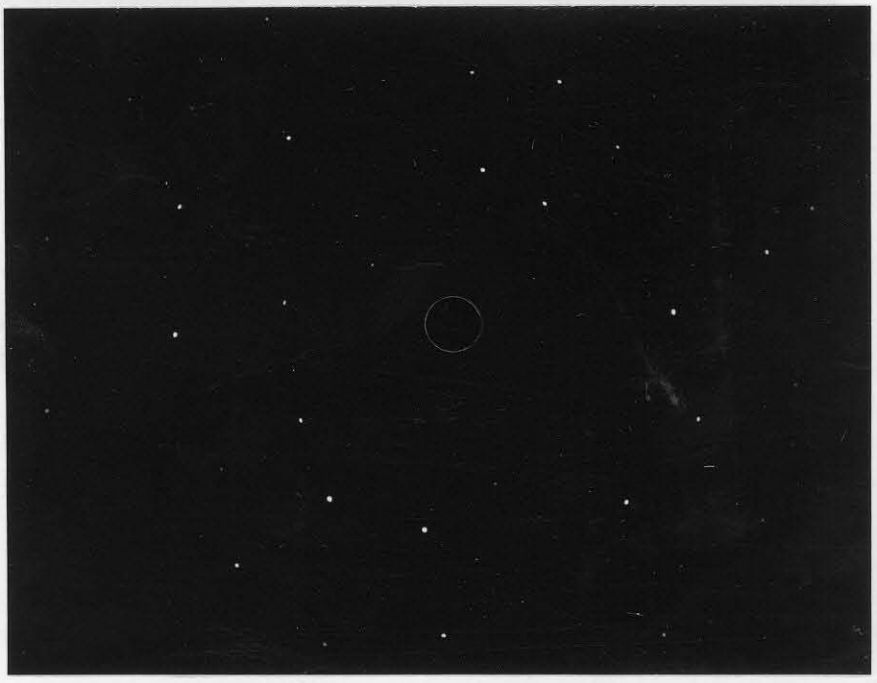

Fig. 81. 25 per cent chromium-iron, aged 10 hours at 490°C. Laue transmission (111) orientation.

Fig. 82. 25 per cent chromium-iron, aged 100 hours at 490°C. Laue transmission (100) orientation.

Powder Studies.

Powder samples were prepared by filing 25 and 49 per cent chromium-iron alloys and sieving the powder through 200 mesh screen. The powder was then sealed in a quartz capillary tube and annealed at 1000°C for 10 minutes. The 25 per cent chromium-iron powder specimen was aged in its sealed capillary tube for 0.2 hours, 0.6 hours and progressively up to 446 hours at 490°C. Debye-Sherrer powder pictures were made during each interrupted step of the aging with a Norelco 11 cm camera and Cobalt K radiation. No change was observed in relative line intensity, line width, or lattice parameter (2.8737 ± 0.0005 Å) of the 25 per cent chromium-iron material, nor did any new lines appear during this aging process.

Aging 49 per cent chromium iron powder at 490°C produced no change in line intensity or line width, but apparently changed the lattice parameter as follows:

annealed	$a = 2.8767 \pm 0.0005$ Å
aged 13 hours 490°C	$a = 2.8754 \pm 0.0005$ Å
aged 100 hours 490°C	$a = 2.8758 \pm 0.0005$ Å
aged 1000 hours 490°C	$a = 2.8780 \pm 0.0005$ Å.

Lattice parameters were determined by plotting a vs. $\cos^2 \theta$ for each film and extrapolating linearly to $\cos^2 \theta = 0$.

After aging 49 per cent chromium-iron at 600°C no change in line intensity, line width, or lattice parameter were observed up to 1000 hours aging. However, several extra lines were present after 13 hours aging at 600°C. The spacing and intensity of these lines did

not change during aging. The spacings are:

intensity	d, Å
vw	1.810
w	1.664
w	2.465
w	2.645

These spacings cannot be fitted to published values for sigma phase (32), and have not yet been otherwise identified.

Acid Extraction Techniques.

Several 25 per cent chromium-iron specimens were cold worked (99 per cent reduction of area) and aged 500 hours at 490°C, then dissolved by two different acid extraction techniques in an attempt to obtain an identifiable second phase. The first extraction technique has proven useful in extracting sigma phase from known sigma structures and consists of partially dissolving the specimen in a boiling 5 per cent HF, 65 per cent HNO_3 solution, then dissolving the remainder in a boiling solution of 10 per cent HCl, 30 per cent ($Cu\ Cl_2 \cdot KCl \cdot 2H_2O$). This technique requires a reflux condenser apparatus to maintain constant acid concentration. The residue was then washed, dried, and analyzed by X-Ray diffraction and chemical analysis. No sigma phase or residue other than 25 per cent chromium-iron matrix has been obtained from embrittled 25 per cent chromium-iron by this process. This technique has successfully extracted sigma

phase from higher chromium alloys aged at 600 to 850°C where sigma is known to form (15).

The second acid extraction technique was first reported by Fisher, Dullis, and Carroll (11), and consists of dissolving the embrittled specimen in a solution composed of hydrochloric acid and picric acid in alcohol, or Vilella's etch. This process progresses satisfactorily at room temperature and requires no special apparatus. The residue was washed, dried, and analyzed by X-Ray diffraction and chemical analysis. In this investigation two extracts were obtained. The first was mechanically removed from the specimen after some residue had accumulated on the surface, and was found to have the same lattice parameter and chromium composition as the initial matrix. The second residue was obtained after the specimen was completely dissolved. This residue was determined to have a body centered cubic structure with lattice parameter a = 2.8794 $\pm$ 0.0005 Å and with a chemical composition of approximately 75 per cent chromium-iron. The X-Ray powder pattern of this residue had lines broad enough to indicate very small powder particles (< 100 Å) or other line broadening effects, such as the existence of two BCC lattices with nearly the same lattice parameter (33). The chemical analysis was semi-quantitative spectroscopic and indicated a 3 to 1 chromium to iron ratio. These results are consistent with those of Fisher, Dullis and Carroll, op. cit.; who found 78 to 82 per cent chromium-iron extracts with a body centered cubic structure with lattice parameter, a, equal to 2.878 Å in 27 per cent chromium steels aged 5000 to 30,000 hours at 475°C.

As discussed in Section IV, the type of aging curves obtained in this investigation suggest the formation of a coherent precipitate with little lattice disregistry. The results indicated above suggest this coherent precipitate may be a high chromium ferrite with a lattice constant approximately 0.2 per cent larger than that of the 25 per cent chromium-iron matrix. The existence of such a precipitate could account for the negative results obtained in X-Ray powder studies. The scattering factors for iron and chromium are nearly equal and their crystal structures are identical, thus it is difficult to detect phase changes in iron-chromium solid solutions not involving mass formation of a new phase, such as sigma phase, with a different crystal structure. Long range order could not be detected in iron-chromium solid solutions by ordinary X-Ray diffraction techniques.

On the other hand, it is not immediately obvious why severe lattice strain effects indicated by electrical resistance aging effects and hardness aging effects, are not apparent in the transmission Laue studies or even in the powder studies. It might be reasonable to assume that a coherent platelet of a chromium-rich ferrite forming in an iron-rich ferrite would not give Guinier type asterism in a Laue transmission photograph due to the similarity in lattice structure and in the iron and chromium scattering factors. However, strains causing lattice distortion should produce some observable effect in X-Ray analysis. In 49 per cent chromium-iron powder aged at 490°C, the lattice parameter change which was observed may be due to lattice strain. The hardness data described in Section IV shows a stronger aging effect

at 490°C in the 49 per cent chromium-iron alloy than in the 25 per cent chromium-iron alloy. This greater change of hardness in the 49 per cent chromium-iron alloy is consistent with the fact that an increase in lattice parameter was observed in the 49 per cent chromium-iron alloy but not in the 25 per cent chromium-iron alloy.

VII. SUMMARY AND CONCLUSIONS

Precipitation embrittlement occurs at temperatures of less than 450°C to about 540°C with the rate of embrittlement increasing with increasing temperature. The maximum embrittlement effect occurs nearer 500°C than 475°C. Embrittlement effects begin after 0.5 hour aging and may, in general, continue after 2000 hours aging of the alloys used in this study. An activation energy of approximately 60,000 cal/mol was established for the precipitation embrittlement process in 25 per cent chromium-iron.

The rate and magnitude of precipitation embrittlement is increased with increasing chromium content from 19 to 49 per cent chromium. Precipitation embrittlement is sensitive to strain and plastic deformation, and the rate of embrittlement increases with increasing strain or plastic deformation applied prior to aging.

The results of this study support the hypotheses of Heger (8); Fisher, Dullis, and Carroll (11); and Lena and Hawkes (10), that precipitation embrittlement is due to the formation of a metastable coherent precipitate which eventually leads to the formation of sigma phase. Further, this study establishes that aging phenomena are encountered in precipitation embrittlement which are analogous to precipitation hardening in alloys such as aluminum-copper, and that aging characteristics are exhibited which indicate embrittlement is due to formation of a coherent precipitate with little lattice disregistry. Such extensive aging studies have not been previously reported.

This study also supports the hypothesis that the coherent precipitate is a chromium rich body centered cubic ferrite. However, the lattice parameter of this precipitate was found to be slightly larger than the iron rich matrix in the present study, while Fisher, Dullis, and Carroll found a chromium rich ferrite with slightly smaller lattice parameter than the iron rich matrix. The Fisher, Dullis, and Carroll result was based on the measurement of one strong forward reflection line in a Debye-Scherrer powder photograph, whereas the result reported here included several forward and back reflection lines and may be more accurate.

Experimental results of this study establish that the coherent precipitate leads to formation of sigma phase, and this transition may be observed in reasonable aging times in a limited temperature and chromium composition range.

Precipitation embrittlement is not independent of sigma phase formation, since the coherent precipitate which causes embrittlement is a transition step in sigma phase formation below 540°C. Thus, precipitation embrittlement occurs more rapidly and with greater effect in alloys which have a greater tendency to form sigma phase.

It has not been established in this study that external strain is necessary to induce precipitation embrittlement in vacuum melted iron-chromium alloys, although external strain does markedly affect the rate of precipitation embrittlement. However, these alloys were not sufficiently free of interstitial impurities to eliminate lattice strain from interstitial precipitates.

REFERENCES

1) E.E. MacQuigg, Book of Stainless Steels, ASM, 1933, Trans. AIME, 69, 831-847 (1923).

2) F.M. Becket, Trans. AIME, 131, 15 (1938).

3) A.J. Cook and F.W. Jones, J. of Iron and Steel Inst., 148, 217 (1943).

4) J.J. Heger, Symposium on the Nature, Occurrence, and Effects of Sigma Phase, ASTM, 75 (1950).

5) F.J. Shortsleeve and M.E. Nicholson, Trans. ASM, 43, 549 (1951).

6) H.S. Link and P.W. Marshall, Trans. ASM, 44, 549 (1952).

7) H.D. Newell, Metal Progress, 49, 977 (1946).

8) J.J. Heger, Metal Progress, 60, 55 (1951).

9) G. Bandel and W. Tofante, Archiv f.d. Eisenhuttenwesen, 15, 307 (1942).

10) A.J. Lena and M.F. Hawkes, J. of Metals, 6, 607 (1954).

11) R.M. Fisher, E.J. Dullis, and K.G. Carroll, J. of Metals, 5, 690 (1953).

12) Catalog E, Leeds and Northrup Co., 41 (1939).

13) Standard Conversion Tables, Leeds and Northrup Co., 14

14) J.D. Lubahn, Trans. ASM, 44, 643-666 (1952).

15) H. Martens, private communication, Jet Propulsion Laboratory.

16) Catalog E, Leeds and Northrup Co., 16 (1939).

17) W.O. Alexander and D. Hanson, J. Inst. Metals, 61, 83-99 (1937).

18) W.L. Fink and D.W. Smith, Trans. AIME, 128, 238-240, 244-248 (1938).

19) R.F. Mehl and L.K. Jetter, Age Hardening of Metals, ASM, 342-417 (1940).

20) A.H. Geisler, Trans. AIME, 180, 230-254 (1949).

REFERENCES

21) A.H. Geisler, Phase Transformations in Solids, Wiley, 387-544 (1951).

22) E. Knuth-Winterfeldt, Mikroskopie, 5, 184 (1950).

23) G.L. Kehl, The Principles of Metallographic Laboratory Practice, 3rd edition, McGraw-Hill, 413 (1949).

24) A. Lena, Metal Progress, 6, 122 (1954).

25) E.J. Dullis and G.V. Smith, Symposium on the Nature, Occurrence and Effects of Sigma Phase, ASTM, 3 (1951).

26) C. Zappfe, Stahl und Eisen, 71, 109-119 (1951).

27) C.S. Barrett, Structure of Metals, 2nd edition, McGraw-Hill, 376 (1952).

28) C.S. Barrett, Structure of Metals, 2nd edition, McGraw-Hill, 185-190 (1952).

29) A.B. Greninger, Trans. AIME, 117, 61 (1935).

30) A. Guinier, Compt. Rend., 206, 1641-1643 (1938).

31) G.O. Preston, Proc. Roy. Soc. London, A167, 526-538 (1938).

32) P. Duwez and S.R. Baen, Symposium on Nature, Occurrence, and Effect of Sigma Phase, ASTM, 48-54 (1951).

33) A. Taylor, X-Ray Metallography, Wiley, 14 (1952).